EFFECTS OF BACTERIAL ENDOTOXIN ON LIVER MASS AND HEPATOCYTE VOLUME

DALONG QIAN

EFFECTS OF BACTERIAL ENDOTOXIN ON LIVER MASS AND HEPATOCYTE VOLUME

by

© Dalong Qian, B. Med.

A thesis submitted to
the School of Graduate Studies
in partial fulfilment of the requirements for
the degree of Master of Science

Department of Biochemistry
Memorial University of Newfoundland
Canada

1993

St. John's Newfoundland

ISBN 0-315-91593-5

Dedicated to my beloved wife, Jane, and parents.

Memorial
University of Newfoundland

Department of Biochemistry

BIOCHEMISTRY SEMINAR

"Effects of Bacterial Endotoxin on Liver Mass and Hepatocyte Volume"

Mr. Dalong Qian
Department of Biochemistry
Memorial University of Newfoundland

Tuesday, April 5, 1994

L.A.W. Feltham Room, S-4015
3:30 p.m.

ABSTRACT

Hepatomegaly is common in infections. An increase in liver mass, which cannot be accounted for by the net increase of hepatic protein and lipid contents, has been reported to be a common tumour necrosis factor α (TNFα)-mediated host response after such stress stimuli as endotoxemia, sepsis, trauma and chronic inflammation in either fasted or fed rats. The increase of hepatocyte volume has also been associated with, in experiments *in vitro*, alterations in hepatic metabolic functions such as protein and carbohydrate metabolism. There are, however, no previous studies carried out on alterations in liver mass and hepatocyte volume *in vivo* as a host response of endotoxic animals which undergo profound metabolic changes in liver.

In this study, a single intraperitoneal injection of *E. coli* lipopolysaccharide (LPS, 0127:B8) at a sublethal dose (3 mg/kg, LD_5) was found to introduce a generally time- and dose-dependent increase in hepatic mass and water content of fasted rats compared to corresponding saline-injected controls. Twenty-four hr after LPS treatment, the absolute and relative weight of livers removed by complete hepatectomy remain unaltered in fasted endotoxic rats but they decrease by 20% in the fasted saline-controls, compared

to that in the normal rats fed ad libitum. The difference in the mean liver weight between the endotoxin- and saline-treated animals is 2.0-2.5 g, i.e. 20-25% of the total liver mass of 300-350 g rats. The hepatic wet/dry weight ratio is significantly higher in endotoxic livers than that in the other two groups. The hepatic water content increases by almost the same extent (27%) as the increase (26%) in the total liver mass 24 hr after treatment, indicating that the effect of E. coli LPS is mainly on the hepatic water content, rather than on the dry mass components.

Analyses of hepatic dry mass components and hepatic cellular spaces show that only one third (0.79 g) of the increase (2.18 g) in the total liver mass can be accounted for by the net increase of the dry mass components (0.38 g) plus the blood/plasma and/or interstitial fluid (0.41 ml) in the extrahepatocellular space; and hepatic K^+ content, the predominant intracellular cation, increases by 25%, 24 hr after LPS injection. These suggest that an expansion of the hepatocellular space is mainly responsible for the increase in the liver mass of endotoxic rats. This hypothesis is also supported by morphometric data from an image analysis system demonstrating that the mean transsectional area and the mean volume is 8% and 12% larger, respectively, in the mononucleate hepatocytes from the endotoxic livers.

The phenomenon of increases in the hepatic mass, water

content and wet/dry weight ratio after LPS treatment can be reproduced by a single intravenous administration of rhTNF-α (25 μg/250 g B.W.) and prevented by the pretreatment of endotoxic rats with an intraperitoneal injection of goat anti-mTNFα serum (20 mg/300 g B.W.). The mean transsectional area and mean volume is 11% and 17% larger, respectively, in mononucleate hepatocytes from the livers of endotoxic rats treated with goat non-immune IgG compared to the anti-mTNFα serum-treated rats. These data suggest that effects of E. coli LPS on the increase in hepatic mass and hepatocyte volume are mediated by cytokine TNF-α.

Twenty-four hr after E. coli LPS injection, the concentrations of hepatic adenine nucleotides in the endotoxic rats are not significantly different from either the saline-controls or the normal fed rats. There are no significant changes in the activity of SGPT or in the plasma ratio of lactate/pyruvate and ß-hydroxybutyrate/acetoacetate during the 24 hr after LPS injection. These observations argue against "compensatory hyperplasia" resulting from acute liver damage due to direct endotoxin toxicity or hepatocyte swelling due to tissue hypoxia and impaired energy status in the liver. Metabolic changes mediated by insulin, TNF-α and/or other "hepatotrophic factors" may be responsible for the increase of liver mass after E. coli LPS administration.

ACKNOWLEDGEMENTS

I wish to express sincere appreciation to my supervisor, Dr. John Brosnan, for his excellent guidance and continued encouragement throughout my graduate study. I am also grateful to Dr. Margaret Brosnan for being the co-supervisor during this study. Dr. Markendeya Jois was the member of my supervisor committee during the preliminary study of this project. Special thanks are due to Dr. Gene Herzberg, the head of our department, for his advice on the statitstical analysis of experimental data.

I would like to thank Drs. Thomas Scott and John McLean in Faculty of Medicine for their meaningful discussion on the morphometric study of hepatocytes and generous permission to use Bioquant™ image analysis system. During the morphometric study of hepatocytes, Ms. Judy Foote of Electron Microscope Lab processed liver specimens; Mrs. Andrea Darby-King of Cell Biology Group was the "blind" investigator who performed morphometric measurements. During other experiments, Mr. Douglas Hall and Mrs. Sonia Banfield of Biochemistry carried out the assay of blood and hepatic free amino acids; Mrs. Marleen Hooper of Chemistry determined hepatic potassium and sodium content. I acknowledge the quality of their professional cooperation.

I would also like to thank Mrs. Beatrice Hall for her instruction and technical assistance in many experiments of this project. Thanks are also due to Stephen Ewart, Stephen Squires and Dr. Srinivas Dhanakoti for creating a friendly working atmosphere in our lab.

This study is financially supported by Dr. John Brosnan's grant from Medical Research Council of Canada. My graduate student bursary awarded by School of Graduate Studies, Memorial University of Newfoundland is also acknowledged. I would like to thank Dr. Kelvin Keough, the former head of our department, for my opportunity of being a teaching assistant.

I am deeply grateful to my parents in China for their support and encouragement while I pursue my graduate study abroad.

I feel greatly indebted to my wife, Jane (Zheng) Wang, who has been undertaking the majority of household duties and taking care of our daughter and me. She also participated in some experiments of this study while she was working in our lab as a technician. Without her constant support, perseverence, understanding, and love, I would not be able to bring this study to completion.

TABLE OF CONTENTS

List of Tables

List of Figures

CHAPTER 1

INTRODUCTION

CHAPTER 1 INTRODUCTION

General Introduction

Infection and Host Response

Infection is the presence of pathogenic microorganisms or their toxins in the blood and tissues of the host (**Hensyl**, 1990). It occurs as a primary pathologic process or a complication with other disease states, such as trauma (surgical or accidental injury). Severe bacterial infection of the mammalian bloodstream can lead to sepsis (**Wichterman** et al., 1980). The most common bacteria among those with important clinical significance are the gram-negative bacteria, such as Escherichia coli (E. coli), which contain endotoxins /lipopolysaccharides (LPS). The toxicity of gram-negative bacteremia was originally attibuted to the effect of endotoxin, but endogenous cytokines, cachectin/tumour necrosis factor-α (TNF-α) (**Beutler** et **Cerami**, 1988; **Old**, 1987), interleukin-1 (IL-1) (**Fong** et al., 1989) and IL-6 particularly (**Evans** et al., 1989), rather than LPS itself are now known to mediate the pathogenesis during endotoxemia (**Tracey** et al., 1987; **Warren** et al.,

1988). In normal animals or healthy human subjects, the acute inflammatory responses, induced by the administration of either endotoxin/LPS or recombinant TNF-α that is virtually endotoxin-free, are often indistinguishable from each other (**Tracey** et al., 1986; 1989).

Infection causes a variety of defensive reactions of the affected host. The host response consists of metabolic and hormonal alterations that maintain and restore physiological homeostasis. They have been collectively termed the "acute phase response" (**Kushner**, 1986), including fever, leukocytosis, increased hepatic gluconeogenesis and plasma protein synthesis, enhanced release of amino acids, mainly alanine and glutamine, from skeletal muscle, and redistribution of serum divalent cations. The accelerated net breakdown of peripheral tissue with concomitant enhancement of hepatic anabolism represents altered priorities in carbon and energy utilization as an adaptation of the host for survival (**Warren** et al., 1987). These metabolic adaptations have been attributed, in part, to the elevation in the plasma levels of glucagon, insulin, glucocorticoids and the catecholamines (**Wilmore**, 1976; **Warren** et al., 1988).

Although the host responses after infection vary with the type and severity of the insults, they are usually very similar, suggesting a systemic response regulated by a

common mechanism. This mechanism, however, is not yet fully understood (**Beisel**, 1975; **Goldstein**, 1989). It is for this reason that clinical manifestations, metabolic changes and their interrelationships have continued to be the focus of studies on trauma and/or infection.

Animal Models for Experimental Study of Bacterial Infection

The diversity of diseases, organisms and other variables in clinical infection makes it very difficult to perform controlled studies. Over the past few decades, the following animal models have been used to simulate the clinical infection and septic situation (**Wichterman** et al., 1980).

1. The intravenous infusion of concentrated live organisms to produce bacteremia (**Postel** et **Scholoerb**, 1977);

2. The placement of infected foreign materials into soft tissues (e.g. muscle, skin) or abdominal cavity to introduce prolonged abscess (**Thal** et al., 1976; **Bartlett** et al., 1978);

3. The implantation of fecal materials or live organisms into the abdominal cavity to produce peritonitis (**Perkash** et al., 1970; **Browne** et **Leslie**, 1976);

4. Surgical operations that partially destroy the normal barriers of the gastrointestinal tract to cause peritonitis, such as bowel infarction or perforation, caecal ligation plus punctures (**Perbellini** et al., 1978; **Wichterman**

et al., 1980)

5. The administration of purified LPS and/or recombinant cytokines (cachectin/TNF-α, IL-1) (**Evans** et al., 1989; **Fong** et al., 1989; **Levin** et al., 1988; **Michie** et al., 1988; **Tracey** et al., 1987; 1988; 1989; **Warren** et al., 1987; 1988).

Although none of these animal models can precisely mimic the features of clinical infection, the administration of LPS has been a widely-used reproducible model, comparatively convenient, economical and less biologically hazardous, especially suitable for acute experiments studying tissue and cell metabolism in small animals (**Waisbren**, 1964; **MacNicol** et **Clowers**, 1972). Among the variety of bacterial, viral and parasitic products which are capable of causing macrophages to release TNF-α, bacterial LPS appears to be the most potent stimulus to induce in the host widespread alterations of the acute phase response comparable to those resulting from TNF-α (**Michie** et al., 1988; **Tracey** et al., 1988).

Origin of This Study

Since the pioneering work of **Cuthbertson** (1930), a great amount of information from experimental animals including the bacterial endotoxin-treated rat has become available and has added to our understanding of the physiological and the biochemical changes in bacterial

infection. Alterations of liver mass and hepatocyte volume, however, have not been reported as a host response to endotoxemia. Although liver and spleen are known to be the major organs for the distribution and degradation of bacterial endotoxin (**Freudenberg** et **Galanos**, 1988), and hepatomegaly is common in gram-negative bacteria infections (**Holdstock** et al., 1985), the mechanism which causes the enlargement of liver at the cellular level has not been elucidated.

A few studies have described significant increase in the liver mass in experiments on animal models of sepsis (**Pedersen** et al., 1986), endotoxemia (**Jepson** et al., 1986), trauma (**Wusteman** et al., 1990), chronic inflammation (**Vary** et **Kimball**, 1992) or recombinant human tumor necrosis factor-α (rhTNF-α) (**Feingold** et **Grunfeld**, 1987), but the focus of those studies was largely on changes in protein synthesis or lipid metabolism, and the net increase of hepatic protein or lipid content reported could not account for the increase in the liver mass. In a preliminary experiment originally conducted to study interorgan fuel metabolism, we found a similar increase in rat liver mass, as compared to the saline-control group, after administration of E. coli endotoxin. These observations coincided with a number of recent studies implicating altered liver cell volume and/or volume regulatory responses

in the regulation of metabolism in the liver. In experiments in vitro, the increase of hepatocyte volume has been associated with inhibition of hepatic glycogenolysis, glycolysis and proteolysis, and stimulation of hepatic glycogen synthesis, amino acid uptake, ureogenesis from amino acids and protein synthesis (**Haussinger et Lang**, 1991). There are, however, few published studies on altered hepatocyte volume in vivo and no information is available for the endotoxic animal which undergoes profound metabolic change in the liver.

The present study was designed to examine the phenomenon of an increase in hepatic mass, as compared with corresponding saline-controls, in fasted rats treated with E. coli LPS.

Endotoxins (Lipopolysaccharides, LPS)

History

One hundred years ago, Richard Pfeiffer found, in his pioneering study, that the lysates of heat-inactivated gram-negative bacteria exhibited toxicity and caused fever, hypotension, shock, disseminated intravascular coagulation and death. He postulated that the toxic principle was present within the bacterial cells and therefore termed it

endotoxin (**Pfeiffer**, 1892). In subsequent studies, however, endotoxins were shown to be localized on the surface of bacteria cells and to form, together with phospholipids and proteins, the outer membrane of gram-negative bacteria. Andre Boivin first isolated endotoxin and discovered that bacteria which produce endotoxin were all of the gram-negative type (**Boivin** et **Mesrobeanu**, 1935). This led to numerous studies of endotoxin administration to laboratory animals and human subjects.

Relationship of LPS Structure to Biological Activity

The extraction by a phenol-water or phenol-chloroform-petroleum ether procedure combined with other purification steps yields endotoxin preparation free of nucleic acids, proteins, phospholipids and other bacterial cell components. Highly-purified endotoxin chemically consists of lipopolysaccharide (LPS) (**Boivin** et **Mesrobeanu**, 1935; **Westphal** et al., 1952). Various endotoxins share a common architecture of a polysaccharide component and a lipid portion (Lipid A) (**Figure. 1.1.**).

The polysaccharide component consists of an oligosaccharide core linked with O-specific chain. The O-specific chain is made up of many repeating oligo-saccharide units. As the surface antigen, it is unique for a given LPS and its parental bacterial strain. There exists as many serotypes of LPS as the diversities of individual

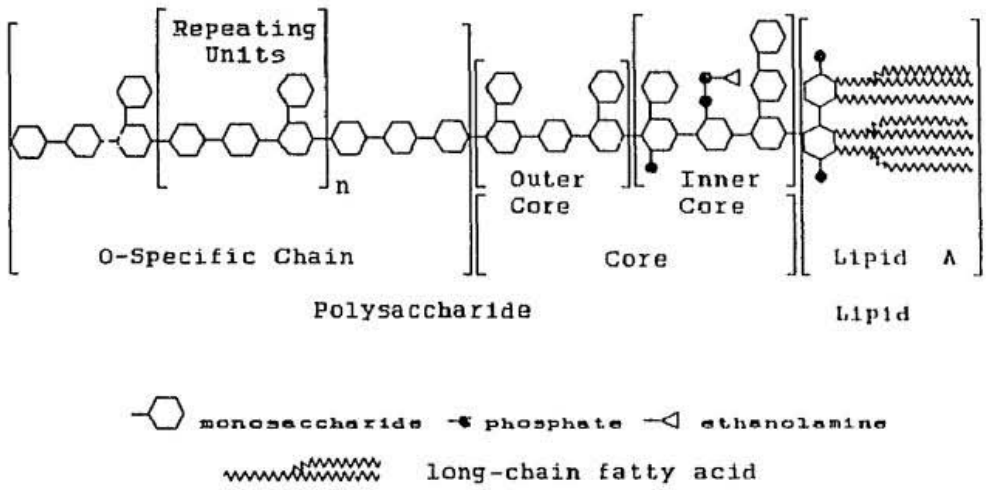

Figure 1.1 Schematic structure of an enterobacterial lipopolysaccharide (Modified from **Brade** et al.,1988)

monosaccharides within a repeating unit (**Brade** et al., 1988). The core region consists of a hetero-oligosaccharide and has very little structure variability compared with the O-specific chain. In E. coli and Salmonella, only six and one core type, respectively, have been described so far for more than one hundred different serotypes (**Brade** et al., 1988). The oligosaccharide core is also related to the antigenicity of LPS. The lipid A-proximal inner core region is now known to trigger the production of TNF-α and IL-1 (**Levin** et al., 1988).

Lipid A is a complex molecule which harbours a hydrophilic region containing bisphosphorylated D-glucosamine disaccharide and a lipophilic region containing fatty acids. Studies using chemically synthetic E. coli LPS revealed that the lipid A portion is the essence of the LPS effect, i.e. the minimal structural requirement for the full expression of endotoxicity of LPS (**Brade** et al., 1988).

Metabolic Fate of LPS

The release of LPS from the outer membrane of gram-negative bacteria may occur with or without the killing of bacteria by natural death and/or bacteriolysis mediated via antibiotics, complement or phagocytosis (**Levin** et al., 1988). The clearance, distribution, degradation and elimination of endotoxins have been investigated on rats in

vivo using biosynthetic LPS uniformly labeled by ^{14}C (**Mathison et Ulevitch**, 1979) or double-labelled by ^{3}H (fatty acids) and ^{14}C (sugars) (**Freudenberg et Galanos**, 1988).

1. Clearance. The rate of LPS clearance is independent of the dose, but dependent on the chemical and physiological properties of the LPS injected (**Freudenberg et al.**, 1984). LPS present in the plasma compartment is partially bound to high-density lipoproteins (HDL) and remains in this form until it is cleared from the circulation. Since the free LPS is incorporated into cells much more effectively, the LPS ($t_{1/2}$ = minutes) in unbound form is cleared from the circulation much faster than the LPS in bound form ($t_{1/2}$ = hours) (**Freudenberg et Galanos**, 1988).

2. Distribution. The highest tissue concentration of unbound LPS was found in the liver and spleen. In the rat, 80% of the unbound LPS is found in the liver after 5 hr. The LPS associated with HDL accumulates in the liver more slowly and to a significantly lower extent (about 43% on after 3 days). The highest concentration of bound LPS is found in the spleen followed by the liver and adrenal glands. The unbound LPS in the liver is first taken up by sinusoidal cells, hepatocytes and granulocytes, whereas bound LPS only by sinusoidal cells and granulocytes. Both bound and unbound LPS pass ultimately from sinusoidal cells

to hepatocytes (**Freudenberg** et al., 1982).

3. Degradation. Although LPS may circulate in experimental animals for a long time, no evidence for chemical degradation or detoxification in plasma was found. Despite the differences in distribution, liver, by virtue of its mass, is the main clearance organ for both bound and unbound LPS. Experiments with double labeled LPS showed the vast majority of injected LPS was found in liver macrophages and granulocytes, and the cleavage of fatty acids in vivo occurs in all LPS-containing organs. It is not known at present whether hepatocytes contribute to the chemical degradation of LPS (**Freudenberg** et **Galanos**, 1988).

4. Elimination. Partially degraded LPS is slowly excreted from the body mainly through the gut and discharged in faeces. 20-30% of LPS can be collected in faeces during 14 days after injection. Another route of LPS excretion through the lung was reported via the migration of macrophages carrying LPS to the lung and passing into the alveolar and bronchiolar space. A small amount (4-7% during 14 days) of LPS-label is excreted in urine, which represents mainly small molecular weight metabolic products (**Freudenberg** et **Galanos**, 1988).

Tumour Necrosis Factor α (TNF-α) and Endotoxemia

The observation that serum from animals treated with endotoxin contains proteins that cause the hemorrhagic necrosis of tumors led to the discovery of tumor necrosis factor (TNF) (**Carswell** et al., 1975), a cytokine produced by stimulated macrophages which has been shown to be toxic to a variety of malignant cells (**Old** et al., 1986; **Pennica** et al., 1984).

Biochemistry of TNF-α

The TNF family includes two structurally and functionally related proteins: TNF-α or cachectin and TNF-ß or lymphotoxin. TNF-α is produced mainly by monocytes and/or macrophages, whereas TNF-ß is a product of lymphoid cells. TNF-α and TNF-ß (especially the former) are now grouped among the major "inflammatory cytokines" or "monokines". They are produced at the sites of inflammation by infiltrating mononuclear cells. The amino acid sequencing and cloning of the cDNA for the genes encoding TNF-α have confirmed that the TNF-α molecule is identical to cachectin, a protein factor, which was implicated in the genesis of cachexia (**Beutler** et al., 1985a; 1985b). Mature human TNF-α consists of 157 (156 in murine) amino acids. The genes encoding TNF-α are approximately 3 kb long, localized on the short arm of human chromosome 6 and murine

chromosome 17. TNF-α interacts with high-affinity membrane receptors in many normal tissues, including liver, muscle, lung, bowel, and kidney. But the post-receptor events leading to intracellular responses remain obscure. (**Tracey** et al., 1989; **Vilcek** et **Lee**, 1991).

Biological Properties of TNF-α

Among the hallmarks of TNF-α is the extremely pleiotropic nature of its actions. This has been ascribed to the following: 1) TNF-α receptors are present on virtually all cells examined, 2) TNF-α action leads to the activation of multiple signal transduction pathways, kinases, and transcription factors, and 3) TNF-α action leads to the activation of an unusually large array of cellular genes (**Vilcek** et **Lee**, 1991). In general, TNF-α is a primary mediator both in the pathogenesis of infection, injury and inflammation, and in the beneficial processes of host defence and tissue homeostasis. The net biological effects may be ultimately beneficial or deleterious to the host, depending on the quantity produced, the duration of release and the presence of other mediators in the environment of the responding cells. Thus, acute systemic overproduction of TNF-α causes septic shock and tissue injury, persisting TNF-α production provokes cachexia, whereas when lesser amounts of TNF-α were released in affected tissues the beneficial effects may predominate to

enhance host defence against pathogens and to coordinate normal wound healing and tissue remodelling. These sequelae are synergistically influenced by other cytokines, such as IL-1, IL-6 and interferon-γ (**Tracey** et al., 1989).

Appearance and Disappearance of TNF-α during Endotoxemia

TNF-α is known to be synthesized by various activated phagocytic and non-phagocytic cells, including macrophages/ monocytes, lymphocytes, natural killer cells, astrocytes and microglial cells of the brain, and Kupffer cells of the liver. A wide variety of infectious or inflammatory stimuli are capable of triggering TNF-α biosynthesis, e.g. bacterial endotoxin/LPS, enterotoxin, complement, virus, fungal or parasitic antigens, IL-1, and TNF-α itself. During endotoxemia, LPS appears to be the most potent stimulus capable of inducing a rapid transcription of nascent TNF-α mRNA normally present in resting macrophages (**Beutler** et al., 1986). The translation of TNF-α genes, which may be normally under the control of short-lived suppressor molecules, is also stimulated in response to LPS, and large amounts of mature TNF-α can be released into the circulation within minutes. Persistent exposure of macrophages to LPS in vitro, however, does not lead to continuous production of TNF-α, and biosynthesis is shut off within several hours (**Tracey** et al., 1988; 1989; **Vilcek** et **Lee**, 1991).

The serum half-life of TNF-α is relatively short (6-20

min). Infusion of a lethal dose of LPS in rabbits, mice or baboons results in the appearance of serum TNF-α levels in the nanomolar range, maximal levels being detected between 1.5-2.0 hr following endotoxin bolus. The circulating TNF-α was cleared within 4-5 hr and serum levels returned to a nondetectable baseline value. The highest tissue levels of radiolabeled TNF-α, exogenously administered to experimental animals, was found in liver, lungs, kidneys and skin. TNF-α is rapidly degraded after tissue binding (**Beutler** et al., 1985b; **Tracey** et al., 1988).

Endotoxin and Liver

General Liver Structure

The rat liver is divided by the ligaments into four major lobes: the median lobe, the left lateral lobe, the right lateral lobe and the caudate lobe. The median lobe and the left lateral lobe are two main liver lobes which, together, account for about 70% of the total liver mass (**Waynforth**, 1979). Absolute liver weight varies widely between individuals and species. The hepatosomatic index, the liver mass as a percentage of body weight, is an indication of the general involvement of the liver in pathological processes (**Cotchin** et **Roe**, 1967). The normal

variation of the hepatosomatic index during development in rat is shown in **Table 1.1.**

Structurally, the basic unit of the liver is the hepatic lobule. It is composed of a central vein and a portal triad consisting of the branches of hepatic artery, portal vein and bile duct. The liver sinusoids are widened capillaries which carry mixed venous and arterial blood (**Luciano** et al., 1983).

Cells in the Liver

Liver cells can be classified into hepatocytes and nonhepatocytes (such as blood cells, sinusoid lining cells, portal tract and bile duct cells, etc.).

Hepatocytes, the parenchymal liver cells, are the main functional units of the liver. There are about 1.2×10^8 (**Krebs** et al., 1974) to 1.38×10^8 (**Carabaza** et al., 1990) liver cells per g of rat liver. The diameter of hepatocytes varies between 13-30 μm with an average of 25 μm (**Leffert** et al., 1988). Stereologic measurements based on morphometric techniques indicate that the individual hepatocyte in the normal fed rat has a mean surface area of 1,680 μm^2 and a mean volume of 4,940 μm^3 (**Weibel** et al., 1969).

Table. 1.1 Rat* Liver Mass Relative to Body Weight
(Modified from **Cotchin** et **Roe**, 1967)

Mean Body Weight (g)	Hepatosomatic Index (Mean ± SD)
20	3.72 ± 0.21
50	6.69 ± 0.78
75	6.08 ± 1.16
100	5.96 ± 0.63
150	5.53 ± 0.49
200	4.99 ± 0.38
250	4.42 ± 0.47
300	3.86 ± 0.55
350	4.10 ± 0.39
400	4.04 ± 0.39

* Male Sprague-Dawley rats of random-bred strain.

About 99.9% of the blood cells in the liver are erythrocytes. They are in the blood which mainly occupy the sinusoidal lumen in the liver parenchyma.

There are four types of hepatic sinusoid lining cells: (1) Kupffer cells (phagocytic), which reside within the sinusoid; (2) endothelial cells (pinocytic); (3) Ito cells or lipocytes (fat and vitamin A storing), which reside within the perisinusoidal space (Space of Disse), i.e. the space between the endothelial cell and hepatocyte; and (4) the pit cells (unknown function) (**Craig**, 1990). Sinusoidal cells account for about 30% of all cells in the liver and Kupffer cells for about 10%. Sinusoidal cells are much smaller than hepatocytes; only 2-10% of hepatic protein is in sinusoidal cells (**Bouwens** et al., 1986).

Hepatic Cellular Spaces

The total hepatic fluid space consists of cellular and extracellular compartments. The hepatic cellular compartment is composed of hepatocytes and nonhepatocytes including blood cells and sinusoid lining cells. Hepatic extracellular (or intercellular) compartment consists of the lumina of sinusoids, interstitial space (mainly the space of Disse) and bile canaliculi, i.e. mainly the volume of blood and interstitial fluid in the liver. Blood volume equals the volume of blood cells plus the volume of plasma. The volume of blood cells accounts for about 45% of the blood

volume and can be measured by hematocrit. The plasma volume can be calculated by substracting the volume of blood cells from the total blood volume.

In this thesis, extrahepatocellular volume refers to the volume of the hepatic extracellular space plus blood cells. Hepatocellular volume refers to the total intracellular volume of hepatocytes and nonhepatocytes except blood cells, which excludes not only the volume of all components of the hepatic extracellular space but also the volume of blood cells.

According to a stereological study after vascular perfusion fixation (**Blouin** et al., 1977), the volume of hepatocytes accounts for 78-80% of total liver fluid space; and nonhepatocytes account for 6.3%, consisting of endothelial cells (2.8%), Kupffer cells (2.1%) and fat-storing cells (0.4%). The hepatic extracellular compartment accounts for 16-20% of total liver fluid space (**Blouin** et al., 1977; **Aria** et al., 1988), of which about two-thirds represent the sinusoidal lumen (10.6%), one-third the space of Disse (4.9%) and the bile canaliculi (0.4%) (**Blouin** et al., 1977). Hepatocytes are larger than any other cells in the liver so they account for over 95% of the total hepatic cellular compartment but only 60-65% of the cell population.

Liver Growth and Regeneration

Liver is a highly differentiated organ. In the adult animal the liver is normally in a state of growth arrest. Hepatocytes are essentially in G_0 stage and few differentiated hepatocytes enter into the cell cycle. This corresponds to the low rate of hepatocyte aging and death. However, the liver can be stimulated to grow by a variety of means, such as extra work load (pregnancy or lactation) (**Bucher** et **Malt**, 1971), surgical resection, certain drugs and toxins or a group of putative hepatotrophic factors, including insulin, glucagon, epidermal growth factor (EGF), vasopressin, triodothyronine (T_3) and portal blood nutrients (**Bucher** et al., 1978).

Liver growth occurs in two ways. Generally, hepatocyte hyperplasia refers to an increase in cell number, or to an upward shift in ploidy as occurs in embryonic development; whereas hepatocyte hypertrophy is defined in terms of an increase in cell size or protein content without an increase in genetic substance. But recent studies on cardiac hypertrophy in human showed that hypertrophic heart muscle cells are capable of increased DNA synthesis even if they are unable to undergo mitosis (**Scarpell** et **Iannaccone**, 1990). The term "hepatotrophic" has been loosely used to designate the factors involved in both hepatic hyperplasia and hypertrophy. The hepatotrophic factors are thought to

act directly, indirectly or synergistically with each other to regulate physiologic and pathologic growth of the liver by mechanisms that are still obscured (**Bucher** et **Malt**, 1971; **Bucher** et al. 1978; **Cornell**, 1981).

In the rat, partial (67% of the whole liver) hepatectomy results in rapid liver cell proliferation (**Higgins** et **Anderson**, 1931). The residual lobes (33% of the whole liver) can double in size by 48 hr and the original liver mass is restored by 7 days. Biochemical changes in hepatocytes start almost immediately after the resection, but an increase in DNA synthesis, the index of cell proliferation, becomes evident only after a 14- to 16-hr delay, and rises rapidly to a peak at about 22 hr. Mitosis follows and peaks 6-8 hr later. The growth rate diminishes soon after, gradually ceasing in a few days as the size and cell population of the liver remnant approximates those of the original (**Bucher** et **McGowan**, 1985; **Craig**, 1990; **Leffert** et al., 1988). This phenomenon has been termed "regeneration" (**Higgins** et **Anderson**, 1931) but is now more accurately described as "compensatory hyperplasia" (**Bucher** et **McGowan**, 1985).

The Role of Endotoxin in Liver Injury and Regeneration

Endotoxin has been shown to be a normal constituent of portal venous blood in man (**Jacob** et al., 1977). It comes from the endogenous pool of endotoxin in the

gastrointestinal tract. This gut-derived endotoxin can be released from both the viable and dead gram-negative aerobic and anaerobic bacteria. It is suggested that sinusoidal lining cells, especially the Kupffer cells, which constitute 80-90% of fixed cells of the macrophage system of the liver, normally protect the systemic circulation from endotoxin (**Aria** et al., 1988). Systemic endotoxemia occurs only when liver function is impaired or exogenous endotoxin (e.g. gram-negative bacteremia) is present. It has been hypothesized that the gut-derived endotoxin initially "spills over" to the systemic blood when the liver barrier (mainly sinusoidal lining cell function) is impaired by liver disease, alcohol, toxicants, etc. The systemic endotoxemia may further damage the hepatocytes and hepatic detoxification in a vicious-cycle manner to increase the liver sensitivity to endotoxin and cause the extrahepatic syndrome (**Nolan** et **Camara**, 1982).

Cornell (1981) proposed that gut-derived endotoxin represents a physiological negative feedback system that regulates liver regeneration after acute liver injury. He reported that systemic endotoxemia introduced either by 67% hepatectomy, which markedly depressed normal phagocytosis and degradation of gut-derived endotoxin by Kupffer cells, or by pretreatment with exogenous endotoxin at 24 hr before 67% hepatectomy accelerated the liver regeneration as

quantified by [^{3}H]thymidine incorporation into hepatic DNA (**Cornell**, 1985a). Conversely, the restriction of gut-derived endotoxin by antibiotics impaired DNA synthesis in regenerating liver (**Cornell**, 1985b). **Cornell** (1981) also found, in the same study, that the putative hepatotrophic factors respond similarly to endotoxemia whether caused by administration of exogenous endotoxin or by endogenous endotoxin absorption from the gut after partial hepatectomy. He hypothesized that the systemic endotoxemia, due to "overspilled" gut-derived endotoxin, elicits the secretion of hepatotrophic factors for liver regeneration so as to recover the original liver capacity to detoxify endotoxin (**Cornell**, 1981).

However, while most studies on the effect of endotoxemia on liver regeneration were performed on liver-resected animals, prior intravenous administration of exogenous endotoxin did not affect [^{3}H]thymidine incorporation into hepatic DNA in sham-operated control rats fasted for 24 hr (**Cornell**, 1985a). There seems to be no evidence that systemic endotoxemia can affect hepatic DNA synthesis in the intact endotoxic animal, without hepatectomy.

Liver Histopathologic Changes after Endotoxin Administraion

The hepatic histologic changes produced by a single sublethal but very high dose of E. coli LPS (0.5-0.7 mg/per

mouse, i.p.) in the mouse have been reported to be rather nonspecific (**Levy** et **Ruebner**, 1968). Light microscopy and histochemistry showed extreme vesiculation of hepatocytes with vacuolation and swelling of the endoplasmic reticulum and mitochondria and increased lipid accumulation. The Kupffer cells had increased number of lysosomes and vacuoles. There was widening of the space of Disse and dilation of the bile ducts. The changes were seen as soon as in 30 min and became less prominent at 24 hr after treatment.

Studies Related to Increasee Liver Mass

Although hepatomegaly is a common clinical sign in various pathological processes, there appears to be little information concerning exactly which cellular components are responsible for the increased liver mass. The exception is alcoholic hepatomegaly where it has been clearly demonstrated that increase in liver weight is accounted for by an increase in fat (20-30%) and in protein (20%) and the accumulation of intracellular water (50-60%), with no significant change in the extracellular water compartment (**Baraona** et **Leo**, 1975).

Jepson et al. (1986) described a temporary slower growth, muscle wasting and hepatic enlargement in response to a sublethal dose (3 mg/kg, s.c.) of E. coli LPS (0127:B8) in rats. The hepatic protein mass increased by about 15.0%,

from 0.565 ± 0.032 g at 24 hr and 0.561 ± 0.035 g at 30 hr in fasted controls to 0.650 ± 0.040 g and 0.647 ± 0.034 g in fasted endotoxemic rats, respectively.

Pedersen et al. (1986) reported a 25.6% increase in liver weight (7.44 ± 0.13 g) and a 33.2% increase of hepatosomatic index (4.41 ± 0.08) in septic rats 24 hrs after ligation and puncture of the cecum compared with the controls (5.92 ± 0.11 g, 3.31 ± 0.07 respectively). These rats were all fasted 24 hrs before the operation. The total hepatic protein content increased by 18.6% from 1.18 ± 0.02 g in controls to 1.40 ± 0.03 g in septic rats at the same time.

Wusteman et al. (1990) investigated rats with aseptic trauma induced by subcutaneous injections of mineral turpentine. They found that while pair feeding caused a 20% reduction in liver size, the average liver weight (6.38 g) of turpentine-injected rats fed a 15% casein diet was 36.6% higher at 48 hr than that of pair-fed controls (4.67 g), but was similar to that of ad libitum controls (6.28 g). At 48 hr, the hepatic total protein content of turpentine-injected rats (1.014 g) was 26.6% more than that of the pair-fed control group (0.801 g) but not significantly different from the ad libitum fed controls (0.926 g).

Vary et **Kimball** (1992) studied rats with sepsis or

sterile inflammation created by induction of a stable intra-abdominal abscess following the implantation of a sterilized fecal-agar pellet containing E. coli LPS plus either Bacteriodes fragilis or an equal volume of sterile saline. After the intra-abdominal abscess was allowed to develop for 5 days, they found that the liver weights of both the sterile abscess group (11.28 ± 0.35 g) and the septic abscess group (11.35 ± 0.43 g) increased by about 24% compared to the non-operated controls (9.11 ± 0.32 g). The liver wet/dry weight ratio increased in both sterile and septic abscess groups (**Vary** et al., 1988a, 1988b). While the protein content per g wet or dry liver remained unaltered, the total amount of hepatic protein per liver increased by 20% in the sterile abscess group (2.05 ± 0.13 g/liver) and by 33% in the septic abscess group (2.27 ± 0.23 g/liver) compared to the nonoperated controls (1.71 ± 0.06 g/liver).

Feingold et **Grunfeld** (1987) found that TNF-α stimlates hepatic lipogenesis in the rat in vivo. This was accompanied by an increase in liver mass of 25% from 7.57 ± 0.13 g (control) to 9.18 ± 0.20 g (TNF-α). The content of liver triglycerides increase from about 7.4 mg/per liver to 16.0 mg/per liver while cholesterol ester content decreased from about 6.4 mg/per liver to 3.5 mg/per liver.

These studies show that the increase in liver mass is

a common host response to stress stimuli. The increase of hepatic protein and lipids cannot account for all of the increase in liver mass.

Cell Volume and Hepatic Metabolism

Cellular life involves the continuous operation of physiologic mechanisms to maintain cell volume. During the past two decades, many volume regulatory mechanisms have been discovered, and found in almost every cell studied (**Hoffmann** et **Simonsen**, 1989). In the past five years, however, the alterations in cell volume were found to markedly influence a variety of metabolic pathways which are not primarily related to cell volume regulation. Hepatic metabolic functions, such as protein and carbohydrate metabolism, are extremely sensitive to alterations in the cell volume. This may imply a new principle of metabolic control in the liver (**Häussinger** et **Lang**, 1991).

Changes in Cell Volume Homeostasis

Theoretically, cell volume is changed by an altered effective osmotic gradient across the cell membrane, which depends on the intracellular and extracellular concentrations of each solute. Since water permeability is very high, in all cases changes in cell volume are brought

about by movement of osmolytes, which are rapidly followed by water, to equilibrate the osmotic pressure across the cell membrane. At constant basal conditions, a change in the effective osmotic gradient is the only known cause of altered intracellular or extracellular osmolarity which can challenge the cell volume homeostasis of the liver (**Häussinger** et **Lang**, 1991). Alterations in cell volume may occur under the following situations.

Changes in Hepatic Extracellular Osmolarity

Under physiological situations, hepatic portal venous blood may become slightly hypo- or hypertonic and the liver volume has been shown to increase during intestinal absoption of water (**Häussinger** et **Lang**, 1991). However, the time course of these alterations is usually slow so that they do not impose a serious burden on liver cell volume regulation mechanisms.

Changes in Hepatic Extracellular Ion Composition

An increase in extracellular K^+ concentration reduces the chemical driving force for K^+ efflux and leads to accumulation of intracellular K^+ and depolarization, which in turn impairs Cl^- or HCO_3^- extrusion (**Kirk** et al., 1987; **Lang** et al., 1988b). An increase of extracellular HCO_3^- concentration, as in metabolic alkalosis, is expected to reduce the efflux of HCO_3^- and hyper- polarization , which in turn impairs the efflux of K^+. As a result, K^+, Cl^- and

HCO_3^- are accumulated within the cell with a consequent increase in cell volume (**Beck** et al., 1988).

Changes in Hepatic Cellular Metabolism

Hepatic protein and carbohydrate metabolism may result in formation and disappearance of osmotically active small molecules, such as amino acids and glucose-phosphate. Since little is known about the permeability of individual cellular metabolites, it is impossible at present to quantify the effect of a given metabolic reaction on cell volume (**Häussinger** et **Lang**, 1991). On the other hand, altered energy metabolism by hypoxia or toxicity may inhibit membrane Na^+/K^+-ATPase and impair the extrusion of Na^+ in exchange for K^+ across the cell membrane. This leads to accumulation of Na^+ and loss of K^+ and to depolarization, and eventually to accumulation of Cl^- within the cell. The accumulation of Na^+ and Cl^- will ultimately result in an increase of cell volume (**Lang** et al., 1984; **Macknight** et **Leaf**, 1977).

Changes in Hepatic Amino Acid Transport

The cumulative uptake of osmotically active substances, such as amino acids, is one of the most important challenges for cell volume homeostasis in the liver (**Häussinger** et **Lang**, 1991). Cumulative amino acid transport into hepatocytes initially leads to volume increase and

subsequently activates volume-regulatory ion transporters (**Baquet** et al., 1990; **Häussinger** et al., 1990a; **Hallbrucker** et al., 1991a, 1991b; **Kristensen**, 1980; **Kristensen** et **Folke**, 1986).

In perfused liver, the Na^+-dependent transporters (system A and ASC) have been shown to build up intra/ extracellular amino acid concentration gradients of up to 20. Na^+ entering the hepatocyte together with an amino acid is extruded in exchange for K^+ by Na^+/K^+-ATPase. The accumulation of amino acids and K^+ in the cells leads to the increase in hepatocyte volume, which in turn triggers volume regulatory K^+ efflux (**Häussinger** et al., 1990a; **Kristensen**, 1980; **Kristensen** et **Folke**, 1986). Enlargement of the hepatocyte and subsequent volume-regulatory K^+ efflux was shown to occur upon addition of glutamine, alanine, proline, serine, glycine, phenylalanine, hydroxyproline, aminoisobutyrate, or a complete amino acid mixture in physiological concentrations (**Baquet** et al., 1990; **Häussinger** et al., 1990a; **Hallbrucker** et al., 1991a). The response to glutamine is half-maximal at the concentration normally found in portal venous blood (0.6-0.8 mM), and is maximal at 2 mM. This suggests that physiological fluctuations of the portal amino acid concentration may be accompanied by parallel alterations of liver cell volume (**Hallbrucker** et al., 1991a). The degree of amino acid-

induced volume change in hepatocytes seems largely to be related to the steady state intra/extracellular amino acid concentration gradient, and is modified by hormones and the nutritional state (**Hallbrucker** et al., 1991a, 1991b).

Insulin and Glucagon

Hormones were recently recognized as potent modulators of liver cell volume. In contrast to cumulative substrate transport, they initially affect the activity of volume-regulatory transport systems which subsequently result in cell volume changes (**Fehlmann** et **Freychat**, 1981; **Fehlmann** et al., 1981; **Moule** et **McGivan**, 1990). It was shown in both perfused livers and isolated hepatocytes that insulin increases and glucagon decreases cellular volume and that these changes are dependent on the activation of the respective K^+ transport systems (**Hallbrucker** et al., 1991b, 1991c). Insulin activates both loop diuretic-sensitive Na^+-K^+-$2Cl^-$-cotransport and amiloride-sensitive Na^+/H^+ exchange, whereas glucagon stimulates cellular potassium release through barium- and quinidine-sensitive K^+ channels (**Hallbrucker** et al., 1991a, 1991b). Insulin-induced cell swelling can be counteracted by further addition of glucagon. Similarly, cyclic AMP shrinks liver cells in the intact organ (**Hallbrucker** et al., 1991c; **Vom Dahl** et al., 1991). Furthermore, hormone concentrations normally present in portal venous blood in vivo were sufficient to give half-

maximal insulin-induced cell swelling and half-maximal glucagon-induced cell shrinkage in the perfused rat liver, suggesting that physiological fluctuations of the portal insulin and glucagon concentrations may modify liver cell volume *in vivo* (**Vom Dahl** *et al.*, 1991).

Hormones can also affect cell volume by altering amino acid transport across the plasma membrane. These effects not only include alterations of the electrochemical Na^+ gradient as a driving force for Na^+-dependent amino acid transporters, but also induction of amino acid transport systems. Insulin-induced intracellular K^+ accumulation by activation of Na^+/K^+-ATPase will lead to hyperpolarization of the membrane potential. Sodium-coupled amino acid transport can be stimulated by the hyperpolarization and the cycloheximide-sensitive induction of system A by insulin (**Fehlmann** *et al.*, 1981; **Prentki** *et al.*, 1981). Both tend to swell hepatocytes. Glucagon similarly increases Na^+/K^+-ATPase activity and stimulates amino acid uptake. However, it also induces a net K^+ release and stimulates amino acid breakdown to dissipate the amino acid concentration gradient across the plasma membrane (**Häussinger** *et al.*, 1983, 1985; **Jois**, 1990). Thus glucagon in fact shrinks the cells (**Moule** *et* **McGivan**, 1990; **Hallbrucker** *et al.*, 1991b, 1991c).

Mechanisms of Cell Volume Regulation

Most studies on cell volume regulation have been performed following anisoosmotic cell volume alterations (**Häussinger et Lang**, 1991; **Hoffmann et Simonsen**, 1989). Cells exposed to hypotonic media initially swell like osmometers but then almost regain their original volume within minutes. This behavior is called regulatory cell volume decrease (RVD). Conversely, cells exposed to hypertonic media initially shrink but also almost regain their original volume within minutes. This behavior is called regulatory cell volume increase (RVI). Both RVD and RVI have been demonstrated in rat hepatocytes (**Graf et al.**, 1988; **Haddad et al.**, 1989; **Häussinger et al.**, 1990b).

It should be noted that the initial cell volume is not restored completely following RVD or RVI. The cells remain in an either slightly swollen or shrunken state after RVD or RVI for the duration of anisoosmotic challenge. It has been postulated that the extent of this remaining cell volume deviation influences cell function (**Häussinger et Lang**, 1991).

Regulatory Cell Volume Decrease (RVD)

RVD is achieved by reduction of intracellular osmotic activity. In various cell types of vertebrates, several

transport mechanisms have been proposed to be activated during RVD. The principal types are shown in **Figure 1.2**: (1) conductive K^+ flux functionally coupled to conductive Cl^- flux; (2) electroneutral K^+-Cl^- cotranport; (3) electroneutral K^+-H^+ exchange functionally coupled to Cl^--HCO_3^- exchange, giving net KCl loss without change in pH (**Hoffmann** et **Simonsen**, 1989).

In rat liver, RVD is mainly (70%) due to extrusion of osmotically active substances by parallel activation of K^+ and Cl^- channels at the plasma membrane. Exposure of the perfused liver to hypoosmotic extracellular perfusate leads to rapid cell swelling and subsequent activation of Ba^{2+}-, quinidine- and SIS-sensitive K^+, Cl^- and HCO_3^- efflux, which partially restores the initial cell volume within about 8 min (**Graf** et al., 1988; **Haddad** et al., 1989; **Häussinger** et al., 1990b). Hepatocyte swelling is also reported to open stretch-activated non-selective cation channels, which allow passage of Ca^{2+} into the cell. The increase of intracellular Ca^{2+} then activates Ca^{2+}-sensitive K^+ channels (**Bear**, 1990). But it has been described that the activation of K^+ channels in hepatocytes does not require an increase in intracellular Ca^{2+} activity. If sufficient K^+ channels are operative at normal intracellular Ca^{2+}, RVD is not dependent on the activation of Ca^{2+}-sensitive K^+ channels (**Henderson** et al., 1989).

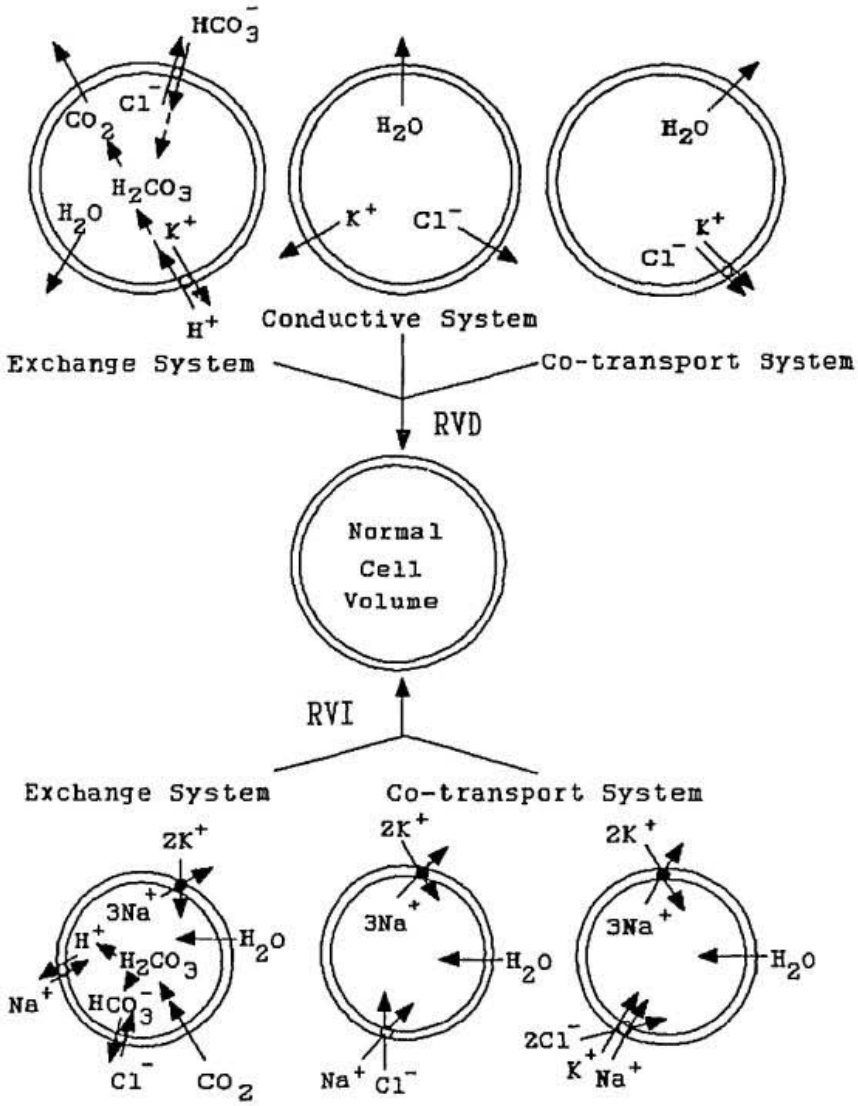

Figure 1.2 Regulatory cell volume decrease (RVD) and regulatory cell volume increase (RVI) (Modified from **Hoffmann** et **Simonsen**, 1989)

Regulatory Cell Volume Increase (RVI)

RVI is at least in part accomplished by uptake of ions across the cell membrane. The principal types of ion fluxes activated in various cell types during RVI are shown in **Figure 1.2**: (1) Na^+-K^+-$2Cl^-$ cotransport; (2) Na^+-Cl^- cotransport; and (3) electroneutral Na^+-H^+ exchange functionally coupled to Cl^--HCO_3^- exchange, giving NaCl uptake without change in pH. In all cases cells take up NaCl with subsequent replacement of Na^+ by K^+ via Na^+/K^+-ATPase, which is the only primary active transport system involved (**Hoffmann** et **Simonsen**, 1989).

In the perfused liver, a sudden increase in extracellular perfusate osmolarity stimulates amiloride- and ouabain-sensitive K^+ uptake, which eventually leads to RVI. Loop diuretics do not appreciably modify the cell volume regulatory K^+ uptake. RVI in liver is apparently accomplished by activation of Na^+/K^+ exchange with subsequent extrusion of Na^+ in exchange with K^+. Na-K-2Cl cotransport appears not to appreciably participate in hepatic RVI (**Häussinger** et al., 1990b).

Modulation of Hepatic Metabolism by Cell Volume

Residual Deviation of Cell Volume

Neither RVD nor RVI completely restore the initial cell volume, and the cells are left in either a slightly swollen or shrunken state. It has been proposed that it is the extent of these remaining deviations of cell volume that influences the metabolic functions in hepatocytes (**Häussinger** et **Lang**, 1991; **Hoffmann** et **Simonsen**, 1989).

Cell Volume and Metabolic Changes in Hepatocytes

The volume increase in hepatocytes (swelling) induced by either hypoosmotic exposure, amino acids or insulin triggers an anabolic pattern of hepatocellular function, including the inhibition of glycogenolysis, glycolysis and proteolysis, and the stimulation of glycogen synthesis, protein synthesis and amino acid uptake. Conversely, the volume decrease in hepatocytes (shrinkage) induced by either hyperosmotic exposure, amino acid deprivation or glucagon acts as a catabolic signal which stimulates proteolysis, glycogenolysis and glycolysis, and inhibits protein and glycogen synthesis (**Figure 1.3** and **Table 1.2**) (**Häussinger** et **Lang**, 1991).

These experiments have been taken to suggest that cell volume alterations may act as a second or third messenger mediating hormone and amino acid effects. Accordingly,

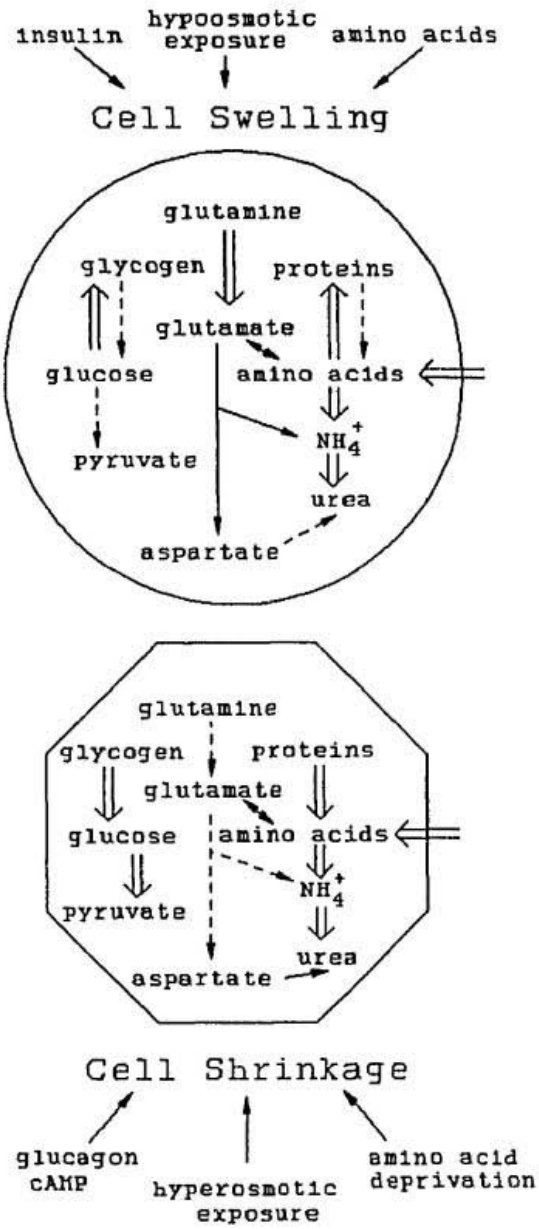

Figure 1.3 **Cell volume and metabolic changes in Hepatocytes** (Modified from **Häussinger** <u>et</u> **Lang**, 1991)

Table 1.2 Cell volume and metabolic changes in hepatocytes
(Modified from **Häussinger** et **Lang**, 1991)

Hepatocyte swelling

Stimulates:
Protein synthesis (Häussinger et al., 1990d)
Glycogen synthesis (Baquet et al., 1990; Lavoinne et al., 1987)
Glutaminase (Häussinger et al., 1990a)
Amino acid uptake (Häussinger et al., 1990a, 1990c; Häussinger et Lang, 1990)
Ureogenesis from amino acid (Häussinger et al., 1990a; 1990c; Häussinger et Lang, 1990)

Inhibits:
Proteolysis (Häussinger et al., 1990b, 1990e, 1991; Häussinger et Lang, 1991a; Hallbrucker et al., 1991b)
Glycogenolysis (Graf et al., 1988; Lang et al., 1989)
Glutamine synthesis (Häussinger et al., 1990a)
Ureogenesis from NH_4^+ (Häussinger et al., 1990c)

Hepatocyte shrinkage

Stimulates:
Proteolysis (Häussinger, 1990; Hallbrucker et al., 1991a; Vom Dahl et al., 1991)
Glycogenolysis (Graf et al., 1988; Häussinger, 1990)
ß-Hydroxybutyrate release at the expenses of acetoacetate (Häussinger et Lang, 1991)

Inhibits:
Ketone body formation from ketoisocaproate (Häussinger et Lang, 1991)

---

concentrative amino acid transport systems and hormone-modulated ion transporters in the plasma membrane appear to be a part of transmembrane signalling systems (**Häussinger** et **Lang**, 1991).

Objectives of This Study

As reviewed and discussed above, no previous study has been carried out on alterations in liver mass and hepatocyte volume as a host response to endotoxemia.

The present research was designed, using the endotoxic rat treated with E. coli LPS, to investigate: (1) Does E. coli LPS consistently increase rat liver mass in vivo? (2) Since the answer to this question was in the affirmative we then undertook a series of studies to determine whether the increase could be due to dry mass components, intracellular space, extracellular space, etc. (3) We also investigated whether the effect of LPS on the hepatic mass might be mediated by the cytokine TNF-α.

CHAPTER 3 of this thesis describes the observations during the preliminary experiments in which we established our animal model.

CHAPTER 4 covers all ensuing investigations on the phenomenon of the increase in the liver mass, as compared to the corresponding saline-controls, after LPS administration.

CHAPTER 2

MATERIALS AND METHODS

CHAPTER 2 MATERIALS AND METHODS

Materials

Animals

Adult male Sprague-Dawley rats (Charles River, Montreal, Que.) weighing 250-450 g were used for all experiments. They were caged two or three in a room, at 22 ± 2 °C, with free access to tap water and Purina rat chow (Ralston Purina of Canada, Ltd., Don Mills, Ontario). The feeding and housing conditions during experiments are described in "Experimental Protocol".

Pharmaceuticals

1. E. coli Lipopolysaccharides (LPS, endotoxin) (serotype O127:B8, phenol extraction) was obtained from Sigma Chemical Inc. (St. Louis, MO).

2. Recombinant human tumour necrosis factor α (rhTNF-α, biological activity: 5×10^6 U/mg as determined by cytolysis of murine L929 cells in the presence of actinomycn-D; LPS content: <100 ng/mg TNF-α) was purchased from Upstate Biotechnology, Inc. (Lake Placid, NY).

3. Goat anti-mouse-TNF-α serum (anti-mTNFα, 22.8 mg/ml)

and goat non-immune IgG (IgG, 20.5 mg/ml) were gifts of Dr. Gregory Bagby (Department of Physiology, Louisiana State University Medical Center).

4. 0.9% NaCl Injection (pyrogen-free saline, 310 mOsmol) was the product of Astra Pharma Inc. (Mississauga, Ont.).

5. SOMNOTOL^{R} (sodium pentobarbital injection) was made by Canada Packers Inc. (Cambridge, Ont). Each ml contained: sodium pentobarbital 65 mg and 2% benzyl alcohol in an aqueous propylene glycol base.

4. Heparin Sodium Injection (heparin, 1000 USP units/ml) was produced by Glaxo Canada, Ltd. (Toronto, Ont).

Radioisotopes

[^{14}C-carboxyl-]inulin (M.W. 5,000-5,500) was purchased from Dupont New England Nuclear Corp. (Mississauga, Ont).

Enzymes, Coenzymes and Other Chemicals

All enzymes and coenzymes used in this study were obtained from Sigma Chemical Co. (St. Louis, MO) or Boehringer Mannheim GmbH (Dorval, Que). All other chemicals used in this study were of analytical grade.

Methods

Experimental Protocol

In the preliminary studies, we found that fed rats were not an appropriate control for endotoxin-treated rats, since the endotoxic rats fed ad libitum manifested a profound decrease in spontaneous food intake and displayed distended stomach with marked food stagnation (**CHAPTER 3**). In order to keep the same post-absorptive status we therefore fasted both the endotoxin-treated and saline-control group. A group of normal fed rats was also included in each experiment.

(1) Animals were conditioned for at least 7 days under reversed 12 hr/12 hr-light/dark cycle, in which the dark period was from 8:00-20:00. On the experiment day, the rats in the normal fed group were allowed rat chow ad libitum until surgery; the rats in all other groups were deprived of food 1-2 hr (6:00-7:00) before the onset of the dark period and remained fasted during the entire experiment. All rats had free access to tap water and were caged separately.

(2) Four hours after the deprivation of food (10:00-11:00), initial body weights were recorded. Rats in endotoxic group, anti-TNF+LPS group and IgG+LPS group were all treated with E. coli LPS in pyrogen-free saline (1 mg/ml, 3 mg/kg, i.p. or at various doses as required in

the dose-response experiment). The rats in the TNF group were injected with rhTNF-α (in 1.0 ml pyrogen-free saline, 25 ug/250 g rat, tail vein). The rats in the saline group, as the corresponding controls for the endotoxic group and the TNF group, were injected i.p. or i.v. with the same volume of pyrogen-free saline. Two hours prior to the LPS treatment (8:00), the rats in the anti-TNF+LPS group and the IgG+LPS group were treated with anti-mouse TNF-α antiserum (20 mg/300 g rat, i.p.) or non-immune IgG (20 mg/300 g rat, i.p.).

(3) The liver was removed by complete hepatectomy 24 hr after the injection of LPS/saline or at various times in the time-course experiment. The hepatectomy for the uninjected normal fed rats was carried out at the same clock-time as for the rats in the endotoxic, TNF, or anti-TNF groups and their corresponding controls. All rats were weighed for final body weight at anaesthesia.

(4) The liver removed by hepatectomy was used to measure total liver weight and the water content was determined by drying a portion of the liver at 55-60 °C to a constant weight. The liver wet/dry weight ratio was then calculated. A portion of the liver was freeze-clamped in liquid nitrogen, then ground to a fine powder and extracted by different procedures to measure the hepatic content of glycogen, protein, lipids, DNA, potassium and sodium. In

some experiments, portal venous blood was obtained immediately before the hepatectomy to measure the activity of glutamate-pyruvate transaminase in serum.

(5) In a series of separate experiments, the liver tissue was obtained by direct open-biopsy and either prepared for morphometric study of hepatocytes or rapidly freeze-clamped for the assay of hepatic adenine nucleotides.

Hepatectomy

Complete hepatectomy was used to remove the whole liver without loss of blood or tissues. The surgical technique was based on the procedures described by **Waynforth** (1979) with some modifications. The rat was anaesthetized with Somnotol^{R} (sodium pentobarbital, 60 mg/kg, i.p.) and placed on a heating pad. After a mid-line laparotomy, the gut was deflected to the rat's left to expose and locate the liver lobes and splanchnic vessels. Suspensory ligaments were then cut down as near as possible to the blood vessels using a blunt-ended curved scissors. The portal vein, hepatic artery and inferior vena cava were exposed by blunt dissection. Silk surgical threads (4/0) were loosely placed around these vessels. They were simultaneously ligated and the liver was removed by severance of blood vessels at the sites of these ligatures. Finally, any non-hepatic tissues attached were removed. The time between the mid-line incision and severance of all blood vessels was less than 10

min.

Determination of Hepatic Extracellular Spaces In Vivo

The extrahepatocellular spaces in the liver are (1) the vascular space which contains blood and plasma and (2) interstitial space which is largely the space of Disse (see "Hepatic Cellular Space" in **Chapter 1**). The hemoglobin content of the liver can be used to determine the hepatic content of blood cells and the vascular space (cells plus plasma) can be calculated on the assumption that the sinusoidal hematocrit is the same as that in peripheral blood. The extracellular space (plasma plus interstitial fluid) can be determined by use of a marker that distributes in this space and is not taken up into cells. [^{14}C-carboxyl] inulin (^{14}C-inulin, M.W. 5,000-5,500), a fructose polysaccharide, was chosen as the extracellular space marker. The assumption that the ^{14}C-inulin is not taken up by hepatic cells was checked in an experiment in which, after ^{14}C-inulin infusion as detailed below, the liver was flushed with 200 ml of saline and the inulin washed out was determined. The ^{14}C-inulin removed in the wash-out was found to be 93.0 ± 1.7% (n=3).

Rats were anaesthetized and treated as for the hepatectomy. After anaesthesia and laparotomy, a priming dose of 8 μCi ^{14}C-inulin in 0.8 ml 0.9% NaCl was injected through the left saphenous vein and followed immediately by

a continuous infusion of 5 μCi ^{14}C-inulin in 1.5 ml 0.9% NaCl at a rate of 0.037 ml/min at the bifurcation of the inferior vena cava. From preliminary experiments (not shown) we determined that plateau levels of ^{14}C-inulin were obtained between 20-40 min. After 25 min, 0.15 ml of heparin (1,000 USP units/ml) was injected via the left saphenous vein and at 30 min, 0.2 - 0.3 ml of blood was slowly withdrawn from the hepatic portal vein. A portion of this blood was used for hematocrit determination and 20 μl of blood was used for hemoglobin determination by the cyanomethemoglobin method (**Oser** et **Hawk**, 1965) using crystalline hemoglobin (Sigma) as standard. Plasma, obtained from the remaining blood, was used for ^{14}C determination in a scintillation counter using ScintiVerse E (Fisher) as scintillation fluid. Immediately after the blood sample was taken from the portal vein, the whole liver was removed by total hepatectomy and homogenized with 20 ml of deionized water. The homogenate was frozen overnight, and, after thawing, the homogenate was centrifuged at 120,000 x g for 60 min at 4°C. An aliquot of the supernatant was used for hemoglobin determination. Another aliquot was deproteinized with an equal volume of 0.5 M $HClO_4$ and ^{14}C was determined in the deproteinized extract. The liver extracellular space was calculated as follows:

$$\text{Liver Blood Content (ml/liver)} = \frac{\text{Liver Hb (mg/liver)}}{\text{Portal Vein Blood Hb (mg/ml)}}$$

$$\text{Liver Plasma Space (ml/liver)} = \text{Liver Blood Content (ml/liver)} \times (1 - \text{hematocrit})$$

$$\text{Liver Inulin Space (ml/per liver)} = \frac{\text{Liver Inulin Concentration (dpm/liver)}}{\text{Plasma Inulin Concentration (dpm/ml)}}$$

$$\text{Liver Interstitial Space (ml/liver)} = \text{Liver Inulin Space (ml/liver)} - \text{Liver Plasma Space (ml/liver)}$$

$$\text{Liver Extrahepatocellular Space (ml/liver)} = \text{Liver Blood Content (ml/liver)} + \text{Liver Interstitial Space (ml/liver)}$$

Morphometric Study of Hepatocytes

In addition to the physical and biochemical examinations to measure the hepatic cellular space, it was also necessary to use a morphometric technique to estimate hepatocyte volume.

1. Preparation of liver specimen. Since some of the reagents used in these experiments were both expensive and scarce (i.e. TNF-α and anti-TNFα) it was necessary to get as much information as possible from each experiment.

Therefore we used the same liver for estimation of mass, wet/dry weight ratio and for morphometry. Since we had to fix tissue very rapidly for histology we devised a procedure of partial hepatoctomy whereby we tied off the two main liver lobes (median and left lateral lobes) for measuring the wet and dry weight. Immediately, 0.5-1.0 g liver tissue, incised from right lateral lobe, was diced into 1 x 1 x 1 mm blocks and fixed in Karnovsky's fixative (pH 7.4) at room temperature (**Karnovsky**, 1965). The fixed tissue blocks were further processed for both morphometric study under light microscopy and subcellular examination under electron microscopy (not reported in this thesis) by the procedures described by **Hyam** (1981). Briefly, four to five fixed blocks were chosen at random and each was first dehydrated and defatted by a series of treatments with sodium cacodylate, osmium tetroxide, uranyl acetate, ethanol and acetone. The treated block was then embedded, dried, polymerized and sectioned serially at 0.5-1.0 μm. Four to five technically perfect sections chosen from each block were finally stained for one min at 60 °C with 1% toluidine blue and mounted on the slide. Toluidine blue was the stain of choice as it gave the clearest outline of each hepatocyte which was necessary for the morphometric analysis.

2. Morphometric analysis. The morphometric analysis of hepatocytes was performed by a "blind" investigator (who

was unaware of the treatment of the animals) using an image analysis system (Bioquant™ System IV, R & M Biometrics, Inc.). At x10 magnification level, an area large enough to include two hepatic lobules (each with a central vein at the center) was chosen as the representative structure of the liver. Measurement of perimeters was restricted to those hepatocytes located in the portal area, i.e. hepatocytes in the areas distant from the center vein but proximal to the edges between the two adjacent lobules chosen. At x40 magnification level, four adjacent microscope fields within the portal area were chosen provided they met the requirement of sufficient resolution for unambiguous recognition of the cell boundary. The micrograph of individual microscope field was projected on the monitor with the reversed enhancement which minimized the background interference so as to optimize contrast of hepatocyte outline. The outline, i.e. the perimeter, of all individual mononuclear hepatocytes (150-250 in total for each liver) with clear and intact nuclei (i.e. excluding damaged cells at the edge of the section) in these four fields were then traced on the screen by a visible cursor. The image was digitalized and integrated by the Bioquant™ system to give the perimeter, transsectional area, longest diameter and shape factor of each individual hepatocyte. The shape factor is the ratio of the shortest diameter over the

longest diameter of an individual cell body on the transsectional profile (where, 0 = a straight line; 1 = a perfect circle). It helps to identify variations in different cell populations. All binucleate and mononucleate hepatocytes within the four microscope fields chosen were counted to give the percentage of binucleate hepatocytes for each liver. The calculation of hepatocyte volume from its transsectional area will be described later in detail (see "Does liver become bigger because of larger hepatocytes" in **CHAPTER 4**). A photograph taken from the video micrograph projected on the monitor of the Bioquant™ system is presented as **Figure 4.3** in **CHAPTER 4.**

Analyses of Hepatic Dry Mass Components

Glycogen was extracted from frozen liver powder and hydrolysed to glucose (**Hassid** et **Abraham**, 1957) which was determined by the glucose oxidase method (PGO kit, Sigma). Hepatic protein content was determined, after homogenization of frozen liver powder in a medium (containing 225 mM mannitol, 75 mM sucrose, 5 mM HEPES, EGTA 1 mM, pH 7.4) by the biuret method (**Gornall** et al., 1949), following solubilization with 5% (w/v) deoxycholate (**Jacobs** et **Jacob**, 1956). Bovine serum albumin was used as standard. Total lipids were measured by the gravimetric method (**Folch** et al., 1957; **Bligh** et **Dyer**, 1959) with modifications. The frozen liver powder was homogenized in a Polytron blender

and extracted three times in 2:1 (v/v) chloroform/methanol mixture. The top organic phases from each extraction were combined and allowed to evaporate from a preweighed aluminium weighing pan, which was then reweighed. For hepatic potassium and sodium content, the frozen liver powder was first defatted by overnight extraction with petroleum-ether and then dried overnight at 90 °C. The fat-free dry tissue was re-extrated with 2 N HNO_3. The nitric acid extract was collected and diluted with deionized water for potassium and sodium assay which were carried out on an atomic absorption spectrophotometer (Varian Techtron AA-5, wavelength: 766.9 nm for K^+, 589.4 nm for Na^+), using KCl and NaCl as standard (**Bergstrom**, 1962; **Bergstrom** et al., 1987; **Landin** et al., 1988). Hepatic DNA was extracted by trichloracetic acid (TCA) as described by **Schneider** (1945) and **Enesco** et **Leblond** (1962) except that the successive washings of TCA-extracted pellet by distilled water and absolute ethanol were omitted. The DNA concentration in the liver tissue was determined by Burton's method (**Burton**, 1956). Single-strand calf thymus DNA (Sigma) was used as standard. Hepatic adenine nucleotides were determined in freeze-clamped liver described by **Hems** et **Brosnan** (1970).

Determination of Free Amino Acids in Liver and Blood

The analysis of amino acids was performed by ion-exchange chromatography on a Beckman amino acid analyser

(Model 121M). The liver tissue and blood specimen were extracted essentially as described by **Brosnan** et al. (1983). For the liver tissue, a portion (0.5 g) of frozen powder was homogenized with 2.5 ml 0.5 M $HClO_4$ and kept standing on the ice for 30 min. The homogenate was centrifuged at 18,000 x g for 15 min at 4 °C. The supernatant was mixed with 100 µl 1.25 mM 2-aminoethyl-cysteine (AEC) as internal standard and was neutralized by 1 ml of 3 M K_2CO_3 and 20% (w/v) KOH to pH 7.0 with 10 µl of 1:1 diluted universal indicator. To the neutralized extract was added 0.4 ml of Lithium Citrate Sample Dilution Buffer (0.2 N Li^+ with 1% thiodiglycol and 0.1% phenol, pH 2.20 ± 0.01, Pierce Chemical, Rockford, IN) and pH was adjusted to 2.20 ± 0.01 with 10 N HCl and 3 M LiOH. For whole blood: 200 µl blood was mixed with 550 µl deproteinization mixture consisting of 50 µl 1.25 mM AEC, 200 µl SSA/LiOH (1 ml 10% sulfosalicylic acid in 9.10 ml 3 N LiOH) and 350 µl lithium citrate buffer, then thoroughly vortexed and kept standing on ice for 30 min. After centrifuged at 10,000 x g (Eppendorf) for 4 min, the supernatant (pH around 2.5) was collected for analysis.

Determination of Other Metabolic Substrates in Plasma or Blood

0.6 ml of whole blood or 0.3 ml of plasma, collected from the abdominal aorta and/or the inferior vena cava, was mixed with an equal volume of 0.5 M $HClO_4$ for

deproteinization and neutralized as described for the liver tissue. The neutralized extract was used for the following assays by enzymatic methods: D-(+)-glucose (**Bergmeyer** et al., 1974), L-(+)-lactate (**Noll**, 1974), pyruvate and acetoacetate (**Mellanby et Williamson**, 1974), D-3-hydroxy-butyrate (**Williamson**, 1974); L-alanine (**Bergmeyer**, 1974). Plasma long-chain fatty acids was determined by a colorimetric method using palmitic acid as standard (**Bergmann** et al., 1980)

Determination of Activity of Glutamate-Pyruvate Transaminase in Serum

The activity of glutamate-pyruvate transaminase (EC 1.1.1.27) in plasma was determined as described by **Bergmeyer** et **Bernt** (1974) using L-lactate dehydrogenase (Boehringer Mannheim from bovine heart) which was first dialysed through a commercial PD 10 column (Sephadex^{R} G25M) to remove $(NH_4)_2SO_4$.

Measurement of Portal and Abdominal Aortic Blood Flow

Portal vein and abdominal aortic blood flow were measured by a transonic perivascular flowmeter (Transonic^{R} Small Animal Flowmeter T206, Transonic Systems Inc., Ithaca, NY). Following routine anaesthesia and laparotomy, the hepatic portal vein and and lower abdominal aorta were exposed by blunt dissection. Vessels were dissected free of surrounding connective tissue, and a 2RB perivascular probe

with an L type bracket was placed around the abdominal aorta at its bifurcation into iliac arteries or the hepatic portal vein as close as possible to the liver. H-R^{R} Lubricating Jelly (Carter-Wallace Inc., New York, NY) was applied to the probe to improve acoustic coupling. The blood flow (ml/min) was monitored on the digital display and the fluctuations recorded with a chart recorder. When the trace became constant, the average of the blood flow during the last four minutes was recorded and taken as the measured blood flow.

Presentation and Analysis of Data

Results are expressed as means ± SD (number of rats). Significant difference between two individual means were determined by unpaired t-test as appropriate. Significant differences (**Zar**, 1984) among three or more individual means were determined by one-way analysis of variance (ANOVA) followed by Bonferroni t-test for multiple comparisons. A two-tailed P value less than 0.05 was taken as indicating statistical significance. Statistical analyses were conducted with the aid of PC software: GraphPAD InStat™ (Motulsky, 1989^{c}) and/or QUATTRO PRO™ (Borland, 1989^{c}).

CHAPTER 3

RESULTS AND DISCUSSION:

OBSERVATIONS IN PRELIMINARY EXPERIMENTS

CHAPTER 3 RESULTS AND DISCUSSION: OBSERVATIONS IN THE PRELIMINARY EXPERIMENTS

Introduction

Before we defined our endotoxic animal model, a series of preliminary experiments had been carried out after the administration of E. coli LPS to fed or fasted male Sprague-Dawley rats. We examined the clinical signs of endotoxemia, changes in food intake and body weight, arterial blood and plasma concentration of metabolic fuels, aortic and portal blood flow, changes in the mass of visceral organs and isolated skeletal muscles. Many features characteristic of acute infections were observed.

Results

Anorexia and Wasting

We first investigated fed rats injected with E. coli LPS at 3 mg/kg, i.p. They were allowed free access to water and food throughout. Their daily food intake, weight gain and growth curve were recorded from 10 days prior to the treatment to 15 days after treatment. The endotoxic rats

fed ad libitum showed a profound decrease in spontaneous food intake. The daily food intake was reduced almost to zero during the first 24 hr and returned to normal level 72-96 hr after the single endotoxin injection (**Figure 3.1.A**). A marked stagnation of food in distended stomachs was found in the endotoxic rats 24 hr after endotoxin administration. The fed endotoxic rats lost about 10% of their initial body weight during the first 24 hr as the result of a combination of decreased food intake, discharge of faeces and wasting of body mass (**Figure 3.1.B**). Although the growth rate tended to return to the normal level on the third day after endotoxin administration, the endotoxic rats did not demonstrate catch-up growth so that the final body weight remained about 10% less than that of controls even 15 days after the single endotoxin injection (**Figure 3.1.C**).

Since the endotoxic rats fed ad libitum ate much less, they could not be compared with the fed saline-treated rats having normal daily food intake. We decided to fast both endotoxin- and saline-treated rats so as to maintain the same post-absorptive status in both groups.

Figure 3.1.A-3.1.C Food Intake, Weight Gain and Growth Curve Before and After LPS/Saline Administration Animals were all fed ad libitum and injected with E. coli LPS (3 mg/kg, i.p.) or sterile saline (3 ml/kg, i.p.) at day 0. Values are means ± SD. The error bars in panel A are only shown for day 1, 2, and 3. * $p<0.05$ vs. corresponding Control or Endotoxic rats (two-tailed P values by unpaired t-test).

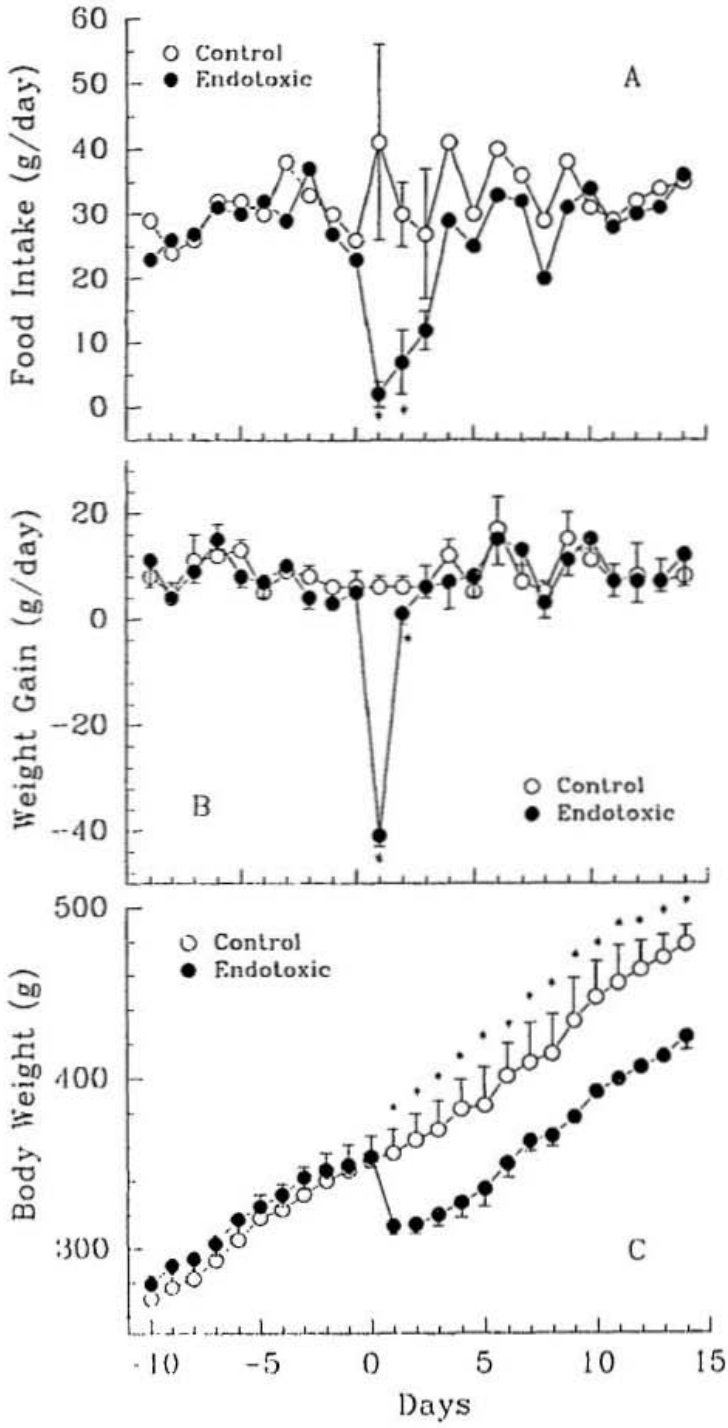
Food Intake (g/day)
60
50
40
30
20
10
0
Control
Endotoxic
A
Weight Gain (g/day)
20
0
-20
-40
B
Control
Endotoxic
Body Weight (g)
500
400
300
C
Control
Endotoxic
-10
-5
0
5
10
15
Days

Clinical Signs of Endotoxemia

During several other time-course experiments, the endotoxic rats were injected with the same dose of E. coli LPS (0.3 mg/kg, i.p.) but fasted from 2 hr prior to the treatment. The clinical signs of endotoxemia, arterial plasma or blood concentration of metabolic substrates (described later), the changes in the body weight and in the mass of visceral organs and isolated muscles (described later) were examined. **Table 3.1** shows seven clinical signs of endotoxemia manifested by the fasted endotoxic rats. They were also used as the criteria to judge the efficacy of intraperitoneal endotoxin administration in all experiments. Occasionally, if endotoxic rats showed less than four signs, at 24 hr after endotoxin injection, they were not used in the experiments.

The typical febrile body temperature curve was not observed in the fasted endotoxic rats during the time-course experiments, under either the regular light-cycle (lights on between 8:00-20:00) or reversed light cycle (lights on between 20:00-8:00). At 1, 3, 6, 7.5, 9, 12 and 24 hr after treatment, the mean colonic temperatures of the endotoxic rats, which varied from 36.5 ± 0.7 to 37.3 ± 0.8 °C, were not significantly different from the corresponding saline-controls.

Table 3.1 Clinical Manifestations after Endotoxin Administration The rats were fasted and treated with E. coli LPS (3 mg/kg, i.p.).

Post-Injection Signs	3h	6h	12h	24-48h
Inactivity	+	+	+	+
Piloerection	+	+	+	+
Peritonitis	-	+	+	+
Hepatosplenomegaly	-	-	+	+
Diarrhea	-	-	+	+
Lethargy	-	-	+	+
Chromodacryorrhea*	-	-	-	+

* (Pacitti, 1992)

Plasma Concentration of Major Metabolic Substrates

The temporal changes in metabolic substrates in arterial plasma from fasted endotoxic rats were determined to outline the general alteration in energy metabolism. Data in **Figure 3.2.A-3.2.F** and **Table 3.2.A-3.2.F** indicate an immediate hyperglycemia (during 1-2 hr) followed by hypoglycemia (at 9 hr) with increases in the plasma concentrations of pyruvate and lactate (during 6-12 hr); and an elevated plasma long-chain fatty acid level with sustained hypoketonemia (during 6-12 hr), as well as increases in blood concentration of both total and many individual free amino acids (described later).

Figure 3.2.A-3.2.C Plasma glucose, lactate and pyruvate Blood was collected from the lower abdominal aorta at the bifurcation into the iliac arteries of the fasted rats treated with endotoxin (3 mg/kg, i.p.) (●) or sterile saline (3 ml/kg, i.p.) (o). Values are expressed as mean ± SD with 3-5 rats at each time-point. * $p<0.05$; ** $p<0.01$; *** $p<0.001$ vs. corresponding (o) or (o) (two-tailed P values by unpaired t-test). (Also see **Table 3.2.A-3.2.C**).

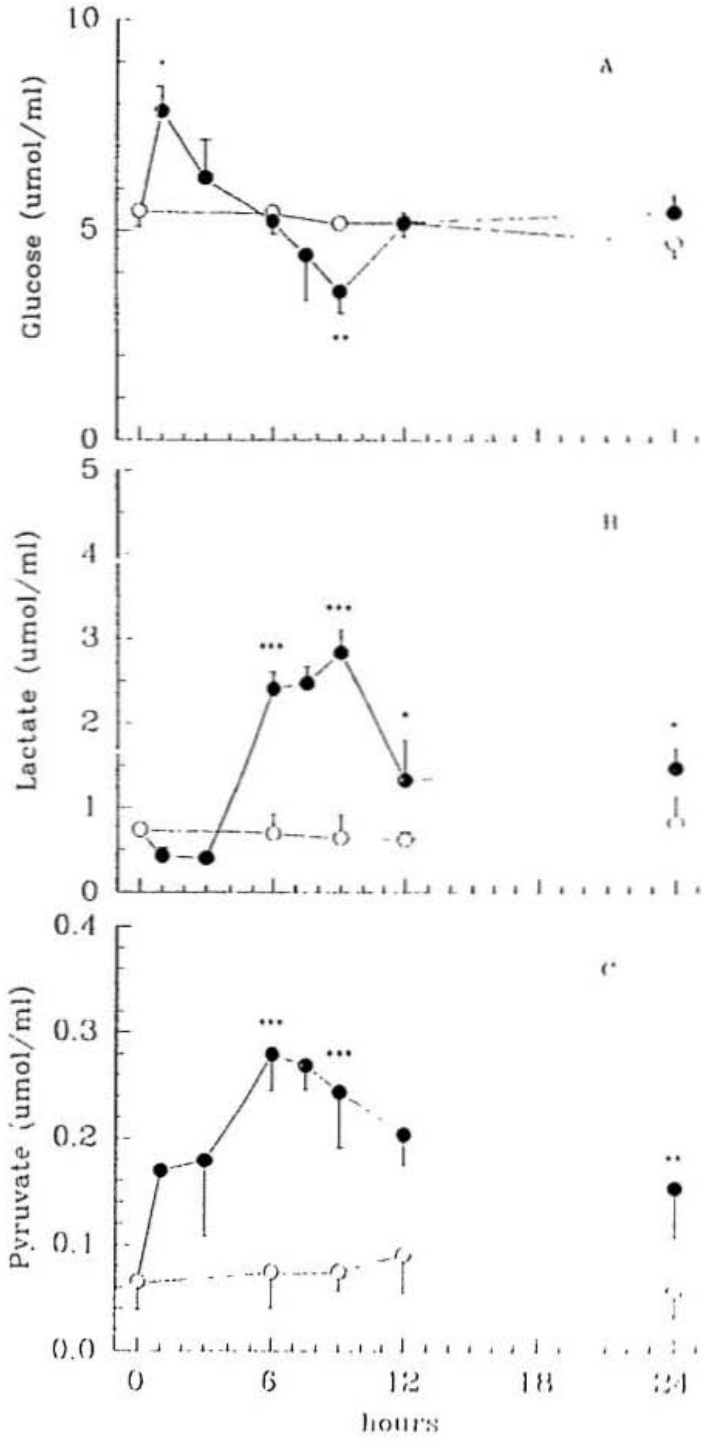
Glucose (umol/ml)
Lactate (umol/ml)
Pyruvate (umol/ml)
hours
A
B
C

Figure 3.2.D-3.2.F Plasma acetoacetate, ß-hydroxybutyrate and long-chain fatty acids Blood was collected from the lower abdominal aorta at the bifurcation into the iliac arteries of the fasted rats treated with endotoxin (3 mg/kg, i.p.) (●) or sterile saline (3 ml/kg, i.p.) (o). Values are expressed as mean ± SD with 3-5 rats at each time-point. * $p<0.05$; ** $p<0.01$; *** $p<0.001$ vs. corresponding (●) or (o) (two-tailed P values by unpaired t-test). (Also see **Table 3.2.D-3.2.F**).

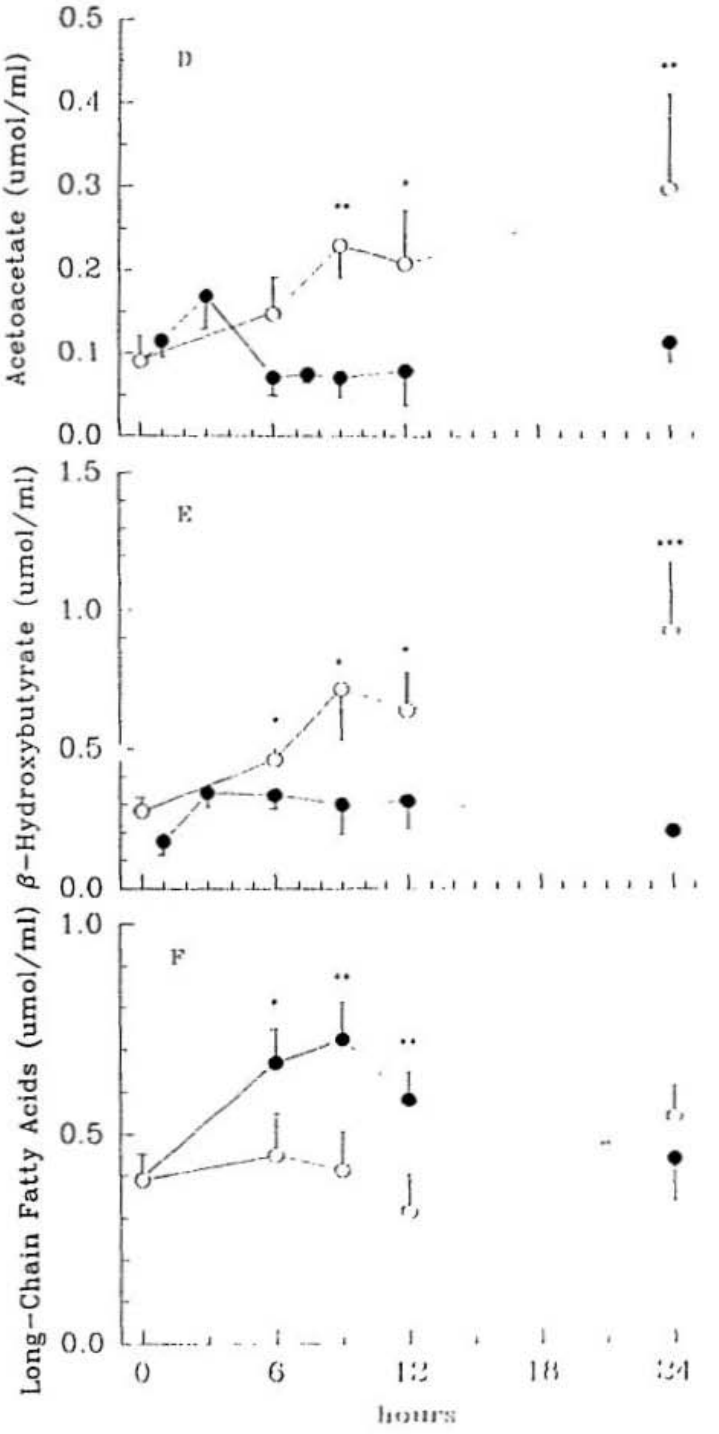
D
E
F
Acetoacetate (umol/ml)
β-Hydroxybutyrate (umol/ml)
Long-Chain Fatty Acids (umol/ml)
0.0
0.1
0.2
0.3
0.4
0.5
0.5
1.0
1.5
0.5
1.0
0
6
12
18
24
hours

Table 3.2.A-3.2.B Arterial Plasma Concentration of Glucose and Lactate Blood was collected from the lower abdominal aorta at the bifurcation into iliac arteries of the fasted rats treated with E.coli LPS (3 mg/kg, i.p.) or sterile saline (3 ml/kg, i.p.). Values are mean ± SD with the number of rats in parentheses. Significant difference was determined as the two-tailed P value less than 0.05 by unpaired t-test (superscription a vs. 0-hr untreated controls; b vs. 6-hr saline-controls; c vs. the time-matched saline-controls). (Also see **Figure 3.2.A-3.2.B**)

Table 3.2.A Plasma Glucose

	Plasma Glucose (μmol/ml)	
	Saline-Control	Endotoxic
0 hr	5.47 ± 0.39 (5)	-
1 hr	-	7.83 ± 0.58 (3)[a]
3 hr	-	6.25 ± 0.91 (3)
6 hr	5.45 ± 0.07 (3)	5.23 ± 0.31 (3)
7½ hr	-	4.42 ± 1.08 (3)
9 hr	5.18 ± 0.08 (3)	3.56 ± 0.54 (3)[c]
12 hr	5.18 ± 0.31 (4)	5.21 ± 0.24 (4)
24 hr	4.75 ± 0.36 (7)	5.47 ± 0.41 (7)

Table 3.2.B Plasma Lactate

	Plasma Lactate (μmol/ml)	
	Saline-Control	Endotoxic
0 hr	0.74 ± 0.08 (5)	-
1 hr	-	0.43 ± 0.10 (3)[a]
3 hr	-	0.41 ± 0.04 (3)[a]
6 hr	0.70 ± 0.23 (3)	2.41 ± 0.19 (3)[c]
7½ hr	-	2.47 ± 0.17 (3)[b]
9 hr	0.65 ± 0.28 (3)	2.83 ± 0.27 (3)[c]
12 hr	0.62 ± 0.09 (4)	1.33 ± 0.48 (4)[c]
24 hr	0.83 ± 0.31 (7)	1.47 ± 0.23 (7)[c]

Table 3.2.C-3.2.D Arterial Plasma Concentration of Pyruvate and Acetoacetate Blood was collected from the lower abdominal aorta at the bifurcation into the iliac arteries of the fasted rats treated with E.coli LPS (3 mg/kg, i.p.) or sterile saline (3 ml/kg, i.p.). Values are mean ± SD with the number of rats in parentheses. Significant difference was determined as the two-tailed P value less than 0.05 by unpaired t-test (superscription a vs. 0-hr untreated controls; b vs. 6-hr saline-controls; c vs. the time-matched saline-controls). (Also see **Figure 3.2.C-3.2.D**)

Table 3.2.C Plasma Pyruvate

	Plasma Pyruvate (μmol/ml)	
	Saline-Control	Endotoxic
0 hr	0.07 ± 0.03 (5)	-
1 hr	-	0.17 ± 0.00 (3)[a]
3 hr	-	0.18 ± 0.07 (3)[a]
6 hr	0.08 ± 0.03 (3)	0.28 ± 0.04 (3)[c]
7½ hr	-	0.27 ± 0.02 (3)[b]
9 hr	0.08 ± 0.02 (3)	0.24 ± 0.05 (3)[c]
12 hr	0.09 ± 0.04 (4)	0.20 ± 0.03 (4)[c]
24 hr	0.06 ± 0.02 (7)	0.15 ± 0.05 (7)[c]

Table 3.2.D Plasma Acetoacetate

	Plasma Acetoacetate (μmol/ml)	
	Saline-Control	Endotoxic
0 hr	0.09 ± 0.03 (5)	-
1 hr	-	0.12 ± 0.02 (3)
3 hr	-	0.17 ± 0.04 (3)[a]
6 hr	0.15 ± 0.04 (3)	0.07 ± 0.02 (3)
7½ hr	-	0.08 ± 0.01 (3)[b]
9 hr	0.23 ± 0.04 (3)	0.07 ± 0.02 (3)[c]
12 hr	0.21 ± 0.06 (4)	0.08 ± 0.04 (4)[c]
24 hr	0.30 ± 0.11 (7)	0.12 ± 0.02 (7)[c]

Table 3.2.E-3.2.F Arterial Plasma Concentration of 3-Hydroxybutyrate and Long-Chain Fatty Acids Blood was collected from the lower abdominal aorta at the bifurcation into the iliac arteries of the fasted rats treated with E. coli LPS (3 mg/kg, i.p.) or sterile saline (3 ml/kg, i.p.). Values are mean ± SD with the number of rats in parentheses. Significant difference was determined as the two-tailed P value less than 0.05 by unpaired t-test (superscription a vs. 0-hr untreated controls; b vs. 6-hr saline-controls; c vs. the time-matched saline-controls). (Also see **Figure 3.2.E-3.2.F**)

Table 3.2.E Plasma 3-Hydroxybutyrate

	Plasma 3-Hydroxybutyrate (μmol/ml)	
	Saline-Control	Endotoxic
0 hr	0.28 ± 0.05 (5)	-
1 hr	-	0.17 ± 0.05 (3)[a]
3 hr	-	0.31 ± 0.05 (3)
6 hr	0.46 ± 0.04 (3)	0.33 ± 0.05 (3)[c]
7½ hr	-	-
9 hr	0.71 ± 0.18 (3)	0.30 ± 0.11 (3)[c]
12 hr	0.64 ± 0.14 (4)	0.31 ± 0.10 (4)[c]
24 hr	0.92 ± 0.25 (7)	0.20 ± 0.01 (7)[c]

Table 3.2.F Plasma Long-Chain Fatty Acids

	Plasma Long-Chain Fatty Acids (μmol/ml)	
	Saline-Control	Endotoxic
0 hr	0.39 ± 0.06 (5)	-
1 hr	-	-
3 hr	-	-
6 hr	0.45 ± 0.10 (3)	0.67 ± 0.08 (3)[c]
7½ hr	-	-
9 hr	0.41 ± 0.09 (3)	0.72 ± 0.09 (3)[c]
12 hr	0.31 ± 0.09 (4)	0.58 ± 0.07 (4)[c]
24 hr	0.54 ± 0.07 (7)	0.44 ± 0.10 (7)

Blood Spectrum of Free Amino Acids

The temporal changes in free amino acid spectrum of the arterial blood from the fasted rats during 24 hr after endotoxin or saline treatment are shown in **Table 3.3.A** and **3.3.B**. Generally, endotoxin administration to the fasted rats elicited a biphasic change in the total amino acid level of the arterial blood. The change in various individual amino acids largely paralleled that in the total amino acid level.

Initially, there was a rapid depression (1 hr after endotoxin injection) in the levels of total amino acid and many glucogenic amino acids, such as Ala, Ser, Met, His, Pro, Asn, compared to the 0-hr uninjected controls. The concentration of branched-chain amino acids, however, did non decrease. Three hr after endotoxin injection, the depressed amino acid levels largely returned to or became higher than that in the untreated 0-hr controls (**Table 3.3.A**).

The initial depression and recovery were followed by an increase in the total amino acid level. It became most prominent at 9 hr when the total amino acid level in the endotoxic rats reached over 10 mM, the peak of the 24-hr time-course. The increase in individual amino acids, such as Ala, His, Thr, Gly, Cit, Leu, Val, Phe and Trp, ranged from 119% to 367%, compared to that in the time-matched

Table 3.3.A Arterial Blood Concentration of Free Amino Acids (0-7½ hr) Blood was collected from the lower abdominal aorta at the bifurcation into the iliac arteries of the fasted rats treated with E.coli LPS (3 mg/kg, i.p.) or sterile saline (3 ml/kg, i.p.). Values are mean ± SD with the number of rats in parentheses. Significant difference was determined as the two-tailed P value less than 0.05 by unpaired t-test (superscript a and b vs. 0-hr untreated controls; c vs. 1-hr endotoxic rats; d vs. the time-matched saline-controls).

Amino Acid (nmol/ml)	0 hr Control (n=3)	1 hr Endotoxic (n=3)	3 hr Endotoxic (n=4)	6 hr Control (n=3)	6 hr Endotoxic (n=3)	7½ hr Endotoxic (n=3)
Alanine	347 ± 41	278 ± 8[a]	383 ± 34[c]	419 ± 69	1021± 737	632 ± 277
Glycine	321 ± 32	281 ± 33	366 ± 37[c]	366 ± 52	547 ± 240	445 ± 142
Threonine	210 ± 37	195 ± 30	236 ± 27	226 ± 54	349 ± 167	321 ± 220
Serine	243 ± 23	190 ± 11[a]	211 ± 21	257 ± 17	344 ± 145	294 ± 157
Cysteine	54 ± 5	51 ± 4	47 ± 3[b]	58 ± 8	59 ± 13	55 ± 11
Asparagine	52 ± 25	19 ± 4[a]	38 ± 5[c]	57 ± 11	83 ± 35	72 ± 31
Glutamic Acid	221 ±148	124 ± 10	174 ± 27[c]	273 ± 42	253 ± 84	196 ± 43
Glutamine	474 ± 28	446 ± 19	558 ± 29[bc]	624 ± 64	709 ± 163	559 ± 130
Histidine	59 ± 6	43 ± 3[a]	72 ± 11	64 ± 9	133 ± 72	109 ± 51
Proline	123 ± 28	56 ± 9[a]	104 ± 14	118 ± 10	227 ± 161	156 ± 74
Valine	128 ± 32	142 ± 15	211 ± 26[bc]	206 ± 27	331 ± 153	278 ± 63
Leucine	106 ± 21	114 ± 4	151 ± 23[bc]	147 ± 19	247 ± 116	209 ± 37
Isoleucine	68 ± 17	64 ± 3	87 ± 14	99 ± 11	124 ± 46	109 ± 12
Lysine	594 ± 53	554 ± 5	509 ±126	635 ± 60	1039± 399	791 ± 338
Methionine	64 ± 10	48 ± 2[a]	57 ± 8	90 ± 5	134 ± 58	120 ± 51
Tyrosine	61 ± 11	55 ± 5	69 ± 9	80 ± 20	227 ± 182	163 ± 106
Phenylalanine	59 ± 8	49 ± 2[a]	78 ± 9[bc]	76 ± 8	123 ± 50	98 ± 22
Tryptophane	61 ± 11	31 ± 2	42 ± 6[bc]	37 ± 5	59 ± 13[d]	55 ± 11
Citrulline	78 ± 5	78 ± 9	91 ± 12	89 ± 15	151 ± 33[d]	122 ± 10
Arginine	256 ± 34	227 ± 2	210 ± 24[b]	257 ± 26	278 ± 50	198 ± 33
Ornithine	94 ± 12	76 ± 5	89 ± 7	97 ± 9	153 ± 77	124 ± 57
Taurine	436 ± 62	356 ± 32[a]	328 ± 17[b]	487 ± 18	551 ± 204	476 ± 90
Hydroxyproline	81 ± 28	23 ± 6[a]	34 ± 6[b]	54 ± 11	70 ± 32	68 ± 34
Total	4507±504	3730± 61[a]	4443±299[c]	5191±488	7597±3104	5962±1920

The value of aspartic acid, which includes glutathione, is omitted from the table.

Table 3.3.B Arterial Blood Concentration of Free Amino Acids (9-24 hr) Blood was collected from the lower abdominal aorta at the bifurcation into the iliac arteries of the fasted rats treated with E.coli LPS (3 mg/kg, i.p.) or sterile saline (3 ml/kg, i.p.). Values are mean ± SD with the number of rats in parentheses. Significant difference was determined as the two-tailed P value less than 0.05 by unpaired t-test (superscript d vs. the time-matched saline-controls).

Amino Acid (nmol/ml)	9 hr Control (n=3)	9 hr Endotoxic (n=3)	12 hr Control (n=4)	12 hr Endotoxic (n=4)	24 hr Control (n=7)	24 hr Endotoxic (n=7)
Alanine	348 ± 77	1627 ± 884[d]	388 ± 29	597 ± 212	250 ± 25	543 ± 16[d]
Glycine	353 ± 31	772 ± 282[d]	344 ± 24	361 ± 38	297 ± 11	274 ± 37
Threonine	171 ± 35	504 ± 146[d]	215 ± 22	241 ± 51	156 ± 12	172 ± 33
Serine	234 ± 16	431 ± 156	235 ± 27	209 ± 28	197 ± 15	195 ± 20
Cysteine	45 ± 4	56 ± 6	45 ± 4	55 ± 14	34 ± 5	32 ± 1
Asparagine	52 ± 3	120 ± 58	61 ± 15	64 ± 10	35 ± 10	59 ± 10[d]
Glutamic Acid	299 ± 17	312 ± 72	303 ± 44	229 ± 37	234 ± 15	193 ± 4[d]
Glutamine	526 ± 5	827 ± 303	556 ± 53	637 ± 39	562 ± 54	564 ± 17
Histidine	51 ± 6	202 ± 92[d]	56 ± 2	84 ± 33	59 ± 6	68 ± 3
Proline	102 ± 15	337 ± 175	125 ± 7	151 ± 53	80 ± 13	132 ± 13[d]
Valine	166 ± 4	424 ± 63[d]	189 ± 30	245 ± 30	166 ± 20	197 ± 30
Leucine	112 ± 6	330 ± 52[d]	126 ± 20	186 ± 12[d]	134 ± 23	141 ± 28
Isoleucine	82 ± 2	154 ± 23[d]	90 ± 16	108 ± 15	88 ± 12	81 ± 18
Lysine	512 ± 67	1409 ± 720	592 ±140	547 ± 150	467 ± 29	430 ± 43
Methionine	82 ± 7	229 ± 167	86 ± 6	120 ± 38	45 ± 2	67 ± 9[d]
Tyrosine	77 ± 13	344 ± 197	77 ± 14	94 ± 27	67 ± 11	74 ± 0
Phenylalanine	63 ± 3	174 ± 45[d]	66 ± 2	112 ± 27[d]	65 ± 19	91 ± 2
Tryptophan	30 ± 5	70 ± 13[d]	38 ± 11	45 ± 3	38 ± 5	40 ± 3
Citrulline	76 ± 15	186 ± 16[d]	70 ± 6	126 ± 6	56 ± 5	52 ± 10
Arginine	179 ± 30	194 ± 39	209 ± 46	196 ± 41	175 ± 12	220 ± 11[d]
Ornithine	78 ± 9	258 ± 145	87 ± 16	92 ± 16	80 ± 13	86 ± 5
Taurine	427 ± 34	751 ± 88[d]	451 ± 4	489 ± 160	360 ± 26	182 ± 8[d]
Hydroxyproline	53 ± 3	99 ± 31[d]	68 ± 12	36 ± 12[d]	34 ± 14	19 ± 0
Total	4413±255	10178±3675[d]	4858±407	5295± 765	4067±225	4228±266

The value of aspartic acid, which includes glutathione, is omitted from the table.

controls which remained the same as the 0-hr controls. The increased amino acid levels fell after 9 hr and finally returned to the pre-injection level at 24 hr (**Table 3.3.B**).

This biphasic pattern of the changes in blood amino acid spectrum mirrored the changes in plasma glucose concentration, which peaked at 1 hr (hyperglycemia) and decreased most profoundly at 9 hr (hypoglycemia) (**Figure 3.2.A** and **Table 3.2.A**).

On the other hand, the significant increase of Phe/Tyr ratio in the endotoxic rats was also remarkable. The Phe/Tyr ratio at 0 hr was close to 1. Both blood Phe and Tyr levels in the endotoxic rats tended to increase after 3 or 6 hr but this trend was more marked in Tyr level, so the Phe/Tyr ratios were all less than 1 at 6, 7.5 and 9 hr. At 12 hr and 24 hr, blood Phe level in the endotoxic rats significantly increased while Tyr level did not change, the mean Phe/Tyr ratios at 12 hr (1.19) and 24 hr (1.23) were significantly higher than either the 0-hr group (0.97) or the time-matched controls (0.86 at 12 hr; 0.97 at 24 hr). At the same time, the total amino acid levels in the endotoxic and controls rats were similar (**Table 3.3.A** and **3.3.B**).

Changes in Portal and Aortic Blood Flow Rate

The alterations in energy metabolism during endotoxemia often occurred with hemodynamic changes (**Lang** et al., 1985).

Table 3.4 shows the rate of blood flow in the portal vein and lower abdominal aorta of the fasted endotoxic rats. Twenty-four hr after endotoxin treatment, the portal blood flow was depressed by 39% compared to the time-matched controls. The flow in the lower abdominal artery was also only about half that in the controls, possibly reflecting a decreased cardiac output. No significant difference was found between the fasted saline-controls and normal fed groups.

Changes in the Mass of Visceral Organs and Skeletal Muscles

Enlargement of liver and spleen was visually noticeable during the laparotomy 24 hr after endotoxin treatment. Therefore we removed and weighed the heart, kidneys, intestines, left soleus muscle and left extensor digitorum longus (EDL) muscle, as well as the liver and spleen, so as to determine the effect of endotoxin administration on the mass of visceral organs in our animal model. This was done at both 24 hr and 48 hr after endotoxin injection. The total mass of various organs was expressed as the relative weight (percentage of the body weight at sacrifice) (**Table 3.5**).

(1) Heart, intestines, left soleus and left EDL muscles. At 24 hr, the heart mass of endotoxin-injected rats was neither significantly different from their time-matched saline-controls nor from the 0-hr uninjected

Table 3.4 Portal and Aortic Blood Flow Rate Fasted rats treated with E. coli LPS (3 mg/kg, i.p.) or sterile saline (3 ml/kg, i.p.) were examined 24 hr after treatment. The untreated rats fed ad libitum were examined at the same clock hour as the other two groups. Values are mean ± SD with the number of rats in parentheses. [a] $p<0.001$ vs. saline-controls; [b] $p<0.001$ vs. Normal fed group (by ANOVA plus Bonfferroni t-test).

Flow Rate (ml/min)	Normal Fed (n=5)	Saline-Control (n=8)	Endotoxic (n=8)
Portal Vein	27.7 ± 2.8	24.2 ± 3.1	11.5 ± 3.4[ab]
Abdominal Aorta, Lower	13.4 ± 2.1	11.2 ± 1.8	6.8 ± 1.2[ab]

Table 3.5 Loss of Body Weight and Changes in Relative Weight of Visceral Organs and Skeletal Muscles Data were obtained during two separate experiments from the fasted rats treated with E. coli LPS (3 mg/kg, i.p.) or sterile saline (3 ml/kg, i.p.). The organs and muscles were removed by open biopsy after anaesthesia with sodium pentobarbital (60 mg/kg, i.p.). Values (% of body weight) are mean ± SD with the number of rats in parentheses. Significant difference was determined as the two-tailed P value less than 0.05 by unpaired t-test (superscript a vs. 0 hr; b vs. the time-matched controls).

	Saline-Control	Endotoxic
Final B.W. (g)		
24 hr	305 ± 17 (4)	295 ± 14 (6)
48 hr	296 ± 13 (3)	309 ± 10 (3)
Loss of B.W. (%)		
24 hr	6.96 ± 0.21 (4)	8.44 ± 1.31 (6)[b]
48 hr	12.41 ± 0.81 (3)	13.76 ± 0.31 (3)[b]
Heart (%)		
0 hr	0.40 ± 0.02 (4)	-
24 hr	0.39 ± 0.02 (4)	0.41 ± 0.03 (6)
Intestines* (%)		
0 hr	3.45 ± 0.34 (4)	-
24 hr	2.99 ± 0.17 (4)[a]	2.67 ± 0.15 (6)[ab]
Muscles** (%)		
0 hr	0.081 ± 0.005(4)	-
24 hr	0.076 ± 0.005(4)	0.074 ± 0.002(4)[a]
Liver (%)		
0 hr	3.13 ± 0.32 (3)	-
24 hr	2.82 ± 0.07 (4)	3.69 ± 0.19 (6)[ab]
48 hr	2.56 ± 0.11 (3)	3.82 ± 0.53 (3)[b]
Spleen (%,		
0 hr	0.25 ± 0.06 (3)	-
24 hr	0.22 ± 0.02 (4)	0.26 ± 0.04 (6)
48 hr	0.20 ± 0.03 (3)	0.37 ± 0.05 (3)[ab]
Kidneys (%)		
0 hr	0.71 ± 0.04 (3)	-
24 hr	0.71 ± 0.04 (4)	0.85 ± 0.08 (6)[ab]
48 hr	0.72 ± 0.03 (3)	0.84 ± 0.04 (3)[ab]

* From pylorus to caecum with digesta.

** Isolated soleus and extensor digitorum longus muscle.

controls. A decrease in the mass of intestines of bothendotoxic (by 23%) and saline-control rats (by 13%) from 0-hr controls was to be expected since the luminal contents of intestines decreased due to the digestion of food and the discharge of faeces after the rats were fasted for 24 hr. However, the significant difference between the endotoxic group and their time-matched controls, which equals about 1.1 g more loss in the mean mass of the intestines in endotoxic rats during 24 hr, suggested that the wasting of the intestinal wall itself was exaggerated after endotoxin administration. The mass of two isolated muscles tended to reduce in both endotoxic rats and saline-controls at 24 hr, but only the decrease (by 18%) in endotoxic group was significant compared to the 0-hr controls (**Table 3.5**).

(2) Parenchymal organs. In contrast to the decrease in the mass of intestines and isolated muscles, the mass of kidneys in the endotoxic rats significantly increased at 24 hr (by 20%) and at 48 hr (by 18%) compared to both the 0-hr controls and their time-matched controls, while the values in saline-controls maintained essentially unaltered during 48 hr. The splenic mass was also constant in the controls, but in the endotoxic group, it dramatically increased after 48 hr compared to both the time-matched controls (by 85%) and the 0-hr controls (by 48%). The hepatosomatic index, the relative weight of the liver, in the endotoxic rats

increased by 18% at 24 hr and by 22% at 48 hr, whereas it decreased by 10% and 18% in the saline-controls at the same time, as compared to 0-hr uninjected controls. The hepatosomatic index was 31% and 49% higher in the endotoxic rats than that in their time-matched controls, which equals about 2.5 and 4 g more wet weight at 24 hr and 48 hr, respectively (**Table 3.5**).

Temporal Increase of the Hepatic Mass after Endotoxin Administration

Figure 3.3.A-3.3.C shows that the total liver mass, hepatosomatic index and body weight increased time-dependently after endotoxin administration during the same time-course experiment in which the blood or plasma concentration of fuel substrates was also determined (**Figure 3.2.A-3.2.F** and **Table 3.2.A-3.2.F**). During the 48-hr time-course, the endotoxin-treated rats lost slightly more body weight (13.84 ± 0.47%) than the saline-control rats (12.76 ± 0.81%) (**Figure 3.3.C**). Six hr after endotoxin administration, the mean hepatosomatic index in the endotoxic rats (3.19 ± 0.15) was not significantly different from the 0-hr uninjected controls (3.19 ± 0.60) and the time-matched saline-controls (3.05 ± 0.23). At 24 hr, however, the hepatosomatic index of the endotoxic rats increased by 9.4% but it decreased by 18.2% in the saline-controls, as compared with the 0-hr controls. During the

Figure 3.3.A-3.3.C Temporal Changes in Body Weight, Liver Weight and Hepatosomatic Index During a 48-hr Time-Course
The livers were removed by open biopsy from the fasted rats treated with E. coli LPS (3 mg/kg, i.p.) or sterile saline (3 ml/kg, i.p.). The mean initial body weights were 321 ± 36 g and 332 ± 28 g for the endotoxin-treated (●) and the saline-control (o) rats (n=19), respectively. Values are means ± SD with 3-5 rats in each group at various times, except 7 rats for each group at 24 hr. * $p<0.05$, ** $p<0.01$, *** $p<0.001$ vs. the time-matched controls (two-tailed P values by unpaired t-test).

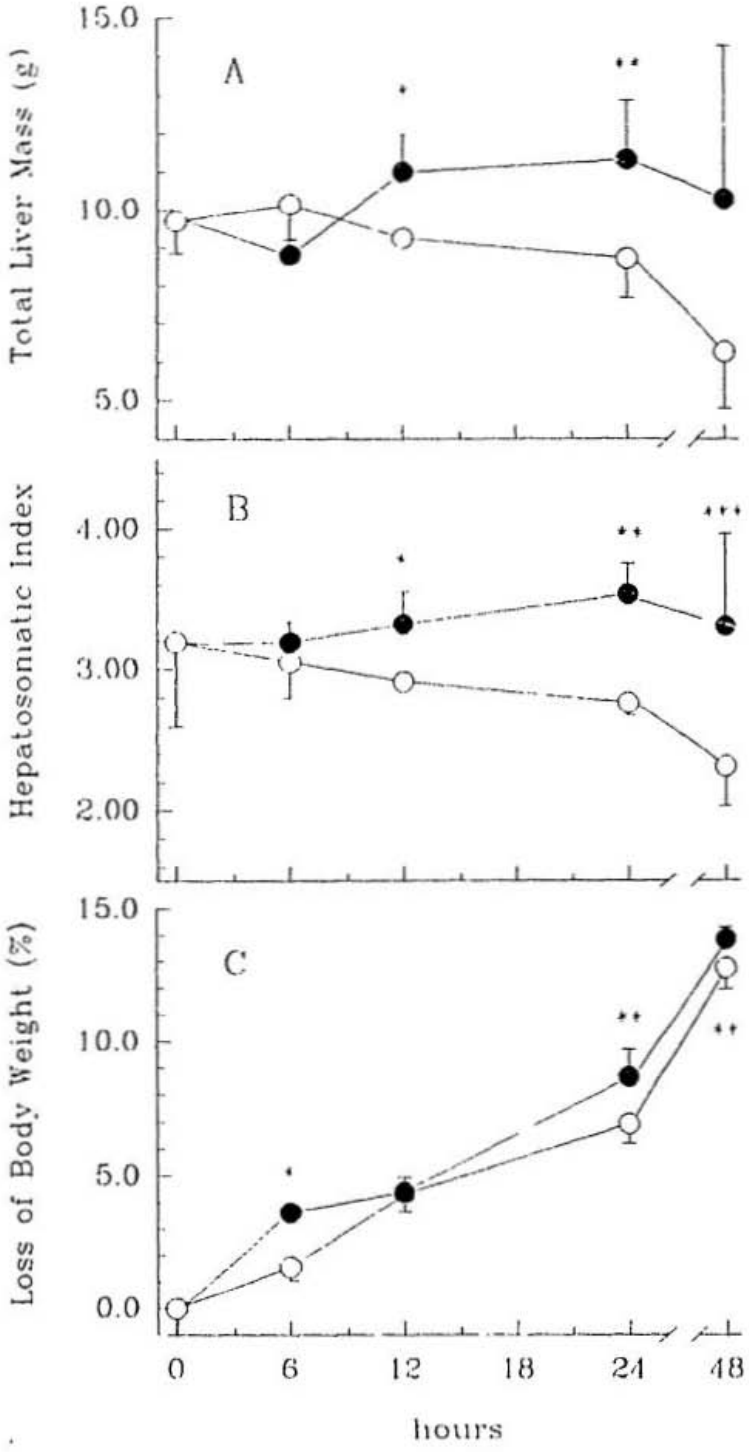
A
B
C
Total Liver Mass (g)
Hepatosomatic Index
Loss of Body Weight (%)
15.0
10.0
5.0
4.00
3.00
2.00
0.0
0
6
12
18
24
48
hours

second 24 hr, the endotoxic group maintained the similar hepatosomatic index; whereas the saline-control group had a further decrease by 11.5%, giving a total decrease of 28% during 48 hr. The hepatosomatic index in the endotoxic group, at 12 hr (3.33 ± 0.22), 24 hr (3.50 ± 0.22) and 48 hr (3.41 ± 0.68), was 17%, 34% and 48% higher than their time-matched saline-controls (2.91 ± 0.04; 2.61 ± 0.25; 2.31 ± 0.28) (**Figure 3.3.B**). This amounts to about 1.9, 2.6 and 4.0 g more in average wet liver weight, respectively, compared to the saline-treated controls (**Figure 3.3.A**).

Discussion

The dose (3 mg/kg, i.p.) of *E. coli* LPS (0127:B8) used in this study is sublethal. It is equivalent to 1/10 of the subcutaneous LD_{90} dose (**Jepson** *et al.*, 1987) and between the intravenous LD_{95} (10 mg/kg) and LD_{10} (1 mg/kg) dose (**Lang** *et al.*, 1985) reported for the same serotype of LPS. It resulted in 5% lethality (LD_5) in the rats within the first 24 hr. All of the rats that died had initial body weight less than 300 g. They all died in the first 12 hr. The characteristic signs of LPS toxicity, such as piloerection, anorexia, lethargy, diarrhea and chromodacryorrhea (**Pacitti** *et al.*, 1992), were evident in the injected animals.

The reason for the absence of the typical febrile response in our animal model is unclear. It may be attributable to the different route and dose of endotoxin administration. The intravenous administration of endotoxin was reported to induce a dose-dependent febrile response (**Sacca** et al., 1974; **Splawinski** et al., 1977). Severe lethal doses (10 and 1.0 mg/kg, i.v.) of endotoxin resulted in a sustained hypothermia (-1.5 to -2.0 °C) which occurred immediately, while relatively milder, nonlethal doses (0.1 - 0.001 mg/kg, i.v.) elicited a two-hour delayed hyperthermia (1.0-1.5 °C) (**Lang** et al., 1985). The relatively slower absorption of LPS via intraperitoneal injection might compromise both extremes of the response.

The decrease in spontaneous food intake (anorexia) is well known in stress states, particularly in infections. Anorexia results in fasting, which, together with other host neurohormonal response to the stress, will mobilize endogenous carbohydrate, lipid and protein reserves to provide energy and precursors for the increased hepatic synthesis of proteins. This has been suggested to have beneficial significance. A possible explanation for anorexia is the inhibition of gastric empyting due to the constriction of the pyloric sphincter by TNF-α (**Evans** et al., 1989; **Patton** et al., 1987) with resulting gastric distention. Since endotoxic rats fed ad libitum eat much

less (**Figure 3.1.A**), the normal fed rat is not an appropriate control. Therefore, the definitive model determined for this study involved fasted endotoxic rats and fasted saline-injected controls. A group of normal fed rats was also included in each experiment.

Although data on turnover or the net flux of metabolic fuels were not available in this study, the temporal changes in arterial plasma fuel substrates, such as plasma glucose, lactate, pyruvate, long-chain fatty acids and blood amino acids, essentially agree with the well documented metabolic response to sepsis and endotoxemia (**Beisel**, 1975; **Warren** et al., 1987; **Watters** et **Wilmore**, 1989), in particular glucose dyshomeostasis and enhanced peripheral proteolysis. In our animal model, those alterations were evident after LPS administration, became prominent during 6-12 hr and subsided but were partly evident until 24 hr (**Figure 3.2.A-3.2.F** and **Table 3.2.A-3.2.F**).

Glucose dyshomeostasis and depressed hepatic blood flow (**Table 3.2.A** and **Table 3.4**) developed as "ebb phase" signs indicating that the LPS challenge to our animals is quite severe. Hypoglycemia following the early hyperglycemia have been known to occur upon intravenous injection of a high dose of LPS to animals (**Lang** et al., 1985). The initial hyperglycemia, primarily from glycogenolysis, is a direct consequence of the elevated rate of glucose appearance

exceeding an increased rate of glucose disappearance (**Wolfe** et al., **Lang**, et al., 1985). The subsequent hypoglycemia is attributed to an inability of hepatic gluconeogenesis to maintain blood glucose levels in the face of glycogen reserves which are depleted while peripheral glucose uptake and utilization rates are maintained or even enhanced (**Wolfe** et al., 1977). In our animal model, the hypoglycemia was most profound at 9 hr post-injection, while plasma pyruvate and lactate as well as the levels of blood total amino acid, Ala and other glucogenic amino acids all remained high (**Figure 3.2.A-3.2.C**, **Table 3.2.A-3.2.C** and **Table 3.3.B**). Studies into the cause of impaired gluconeogenesis have determined that endotoxin blocks the glucocorticoid induction of gluconeogenic enzymes, such as glucose-6-phosphatase, fructose-1,6-diphosphatase, phosphoenolpyruvate carboxykinase and tryptophan oxygenase (**Shackleford** et al., 1986).

Endotoxin-induced alterations of carbohydrate metabolism have also been attributed to hemodynamic impairments. Only endotoxin administration at a dose that disturbs the hemodynamic status has been reported to affect glucose kinetics (**Lang** et al., 1985). The hypoglycemia that occurred in our animal model 9 hr after the endotoxin injection (**Figure 3.2.A** and **Table 3.2.A**) could partially have resulted from a decreased hepatic blood flow due to

impaired cardiac output and/or lower mean arterial blood pressure. Decreased liver perfusion after endotoxin treatment could reduce the metabolic clearance of major gluconeogenic precusors such as pyruvate, lactate, alanine in the liver, since the hepatic blood flow, as well as the substrate extraction, determines the efficiency of gluconeogenic substrate clearance by the liver (**McGuinness** et **Spitzer**, 1984). However, **Pacitti** et al. (1992) reported an increase of 59% in total hepatic blood flow, as a result of a 2.5-fold increase in hepatic arterial flow and unchanged portal flow, 12 hr after rats were treated with E. coli LPS of the same serotype at a higher dose (7.5 mg/kg, i.p.) than that we administered. Our data on the aortic and portal blood flow, which indicated an decrease in both, were obtained at 24 hr after endotoxin injection (**Table 3.4**). Although the hepatic arterial blood flow is not available, the net change in the hepatic blood flow is expected to decrease the liver perfusion in our animals, since portal blood flow normally accounts for about 75% of total hepatic blood flow. However, depressed plasma glucose level returned to normal and the elevated plasma lactate, pyruvate and blood Ala became much lower, although still significantly higher than the corresponding controls, during the second 12-hr after endotoxin injection (**Figure 3.2.B-3.2.C**, **Table 3.2.B-3.2.C** and **Table 3.3.B**). These seem to

argue against severe impairment of hepatic clearance due to a poor liver perfusion between 12 hr and 24 hr after endotoxin injection.

Data in **Figure 3.2.B-3.2.E** and **Table 3.2.B-3.2.E** on plasma levels of lactate, pyruvate, acetoacetate and ß-hydroxybutyrate also give information on the adequacy of oxygenation of tissues. When tissues become hypoxic the ratio of NADH/NAD increases both in the cytoplasm of cells and in mitochondria (**Brosnan**, 1970). The increase in cytoplasmic NADH/NAD is indicated by an increase in the ratio of lactate/pyruvate since lactate dehydrogenase is a highly active enzyme that catalyzes a near-equilibrium reaction in most tissues. An increase in mitochondrial NADH/NAD is indicated by an increase in the ratio of ß-hydroxybutyrate/acetoacetate, at least in liver where ß-hydroxybutyrate dehydrogenase catalyses a near-equilibrium reaction in mitochondria. The plasma levels of lactate, pyruvate, ß-hydroxybutyrate and acetoacetate generally reflect tissue levels. It is significant, therefore, that there were no major changes in the plasma ratio of lactate/pyruvate and of ß-hydroxybutyrate/acetoacetate during the 24-hr after LPS administration. In particular, the increase in plasma lactate, that occurred between 6 and 24 hr, was not accompanied by an increase in the lactate/pyruvate ratio. It seems highly unlikely that our

LPS protocol was accompanied by tissue hypoxia.

Hyperaminoacidemia after endotoxin injection (**Table 3.3.B**) reflects an algebraic sum of the changes, mainly in the amino acid release from peripheral tissue (such as skeletal muscle, intestines), and in the rate of utilization by liver (as major substrate) for gluconeogenesis and protein synthesis. An increase in blood Phe/Tyr ratio (at 12 and 24 hr) of the endotoxic group due to elevated Phe and unaltered or decreased Tyr level (**Table 3.3.A** and **3.3.B**) is an index of an enhanced release of amino acids from skeletal muscles (**Wannemacher**, 1971; 1975a). The accelerated net breakdown of skeletal muscle is supposed to provide amino acids as the substrates for hepatic gluconeogenesis and protein synthesis, which is a major part of the host metabolic response to infection (**Millward**, 1986). But this also depends on the capability of the hepatic uptake of amino acids. During the first 3 hr after endotoxin injection, there was an initial depression (at 1 hr) in blood amino acid level (**Table 3.3.A**), as well as hyperglycemia (at 1 hr). Since the decrease in blood amino acid level occurred at 1 hr after the treatment, it could not be explained by the diminished dietary intake of protein due to fasting. The studies on human subjects revealed that the decrease in amino acids during the early stage of infections was due to greater increase in the uptake of

amino acids by the liver, relative to the release from skeletal muscle (**Feigin et Dangerfield**, 1967; **Feigin et al.**, 1968; **Wannemancher et al.**, 1972). Between 3 hr and 9 hr after endotoxin injection, the blood total amino acid level, as well as plasma lactate and pyruvate levels, was increasing or remained high while the plasma glucose level was continuously decreasing. This reciprocal change suggests a mismatch between an impaired hepatic gluconeogenesis due to the possible decrease in hepatic uptake and the enhanced mobilization of gluconeogenic precursors from the periphery. Between 9 hr and 24 hr after treatment, the total blood amino acids in the endotoxic rats decreased and eventually became similar to the levels of the 24-hr or 0-hr controls. The blood Phe/Tyr ratio, however, was still significantly higher (at 12 and 24 hr) than that in the time matched controls, indicating that the increased muscle breakdown continued. The plasma glucose level restored and remained normal while plasma lactate and pyruvate were decreasing. We could speculate that the capabilities of the liver to handle the amino acids and other gluconeogenic substrates might gradually recovered during the second 12-hr after the endotoxin injection (**Figure 3.2.A-3.2.C**, **Table 3.2.A-3.2.C** and **Table 3.3.B**).

Hypoketonemia (**Figure 3.2.D-3.2.E** and **Table 3.2.D-3.2.E**) is characteristically observed in sepsis and

endotoxemia. The concentration of blood ketones is inversly related to the severity of the insult (**Neufeld** et al., 1980; **Vary** et al., 1986). Although it is known that liver failed to enhance ketogenensis during carbohydrate deprivation in sepsis and endotoxemia, the precise mechanisms of hypoketonemia remain uncertain (**Takeyama** et al., 1990). Most evidence indicates that hyperinsulinemia, rather than lack of substrate or accelerated peripheral utilization of fatty acids, results in the inhibited ketosis in infection (**Wannemacher** et al., 1979; **Neufeld** et al., 1980).

Finally, the most interesting discovery during the preliminary experiments was the increase in the mass of the parenchymal organs after endotoxin administration. In contrast to the decrease in the intestines and isolated muscles, the mass of the liver, spleen and kidney, increased markedly in the fasted endotoxic rats at 24 hr and/or 48 hr compared to the 0-hr untreated rats or the time-matched saline-controls, whereas the loss of body weight in the endotoxic group was only slightly more than that in the corresponding controls during 48 hr. The time-course experiment revealed that the mean liver mass in the fasted endotoxic rats remained almost unaltered while the mean liver mass of fasted saline-controls decreased continuously during 48 hr. This made the difference in both the absolute and relative liver weight between the two

groups, which amounts to about 2-3 g wet mass, significant at 12 and 24 hr after endotoxin treatment.

CHAPTER 4

RESULTS AND DISCUSSION:

TNFα-MEDIATED EFFECT OF *E.COLI* LPS INCREASES LIVER MASS AND HEPATOCYTE VOLUME *IN VIVO*

Chapter 4 Results and Discussion: TNFα-Mediated Effect of E.coli LPS Increases Liver Mass and Hepatocyte Volume In Vivo

Introduction

The most striking result in our preliminary experiments was the marked increase in liver mass after E. coli LPS administration. We therefore decided to examine this phenomenon in detail.

To confirm the increase in the liver mass after endotoxin injection, rat livers were removed by more standardized surgical procedures - complete hepatectomy instead of open biopsy. The endotoxin-treated and the saline-treated controls were fasted as described in the previous chapters, and a group of normal rats fed ad libitum was also included. In all experiments the animals were distributed to the three groups such that the initial body weights of each group were as similar as possible. They were all kept under the reversed light cycle in which the light-period was between 20:00-8:00. The food was removed at 6:00-7:00 and endotoxin or saline was injected at 10:00. Hepatectomy was performed 24 hr after the treatment. That is also the time when the maximal difference of the liver

weight, compared to the time-matched saline-controls, occurred with less variation, during the previous time-course experiment (**Figure 3.3.A-3.3.B**). The livers in the fed animals were removed at the same clock-time as for the other two groups of treated animals.

Figure 4.1 shows the combined results from five separate experiments using complete hepatectomy to remove the liver. At 24 hr after treatment, the total liver mass (11.36 ± 1.05 g) and hepatosomatic index (3.60 ± 0.21) of the endotoxic rats (n=21) were 25% higher than that of saline-controls (9.09 ± 0.88 g and 2.80 ± 0.27, n=19), but not significantly different from the normal fed rats (11.46 ± 1.29 g and 3.52 ± 0.36, n=9), whereas that of saline-controls decreased by 21% compared to the normal fed group. The increase (25%) in the hepatosomatic index calculated for the endotoxic livers removed by the complete hepatectomy was slightly less than that (34%) shown in the previous experiments using open biopsy technique (**Table 3.3.A-3.3.B**).

Figure 4.1 Absolute and relative weight of the rat liver removed by hepatectomy The rats in FED group were untreated and fed ad libitum. Endotoxic group (ETX) and saline-control group (CTR) was treated with E. coli LPS (3 mg/kg i.p.) and sterile saline (3 ml/kg, i.p.), respectively. Results are the combined data from five separate experiments in which the rat livers were removed by complete hepatectomy, 24 hr after the treatment. The final body weight at sacrifice for ETX, CTR and FED group was 314 ± 15, 321 ± 22 and 325 ± 13 g, respectively. Values are means ± SD with the number of rats in parentheses. * $p<0.001$ vs. CTR group; @ $p<0.001$ vs. FED group (by ANOVA plus Bonferroni t-test).

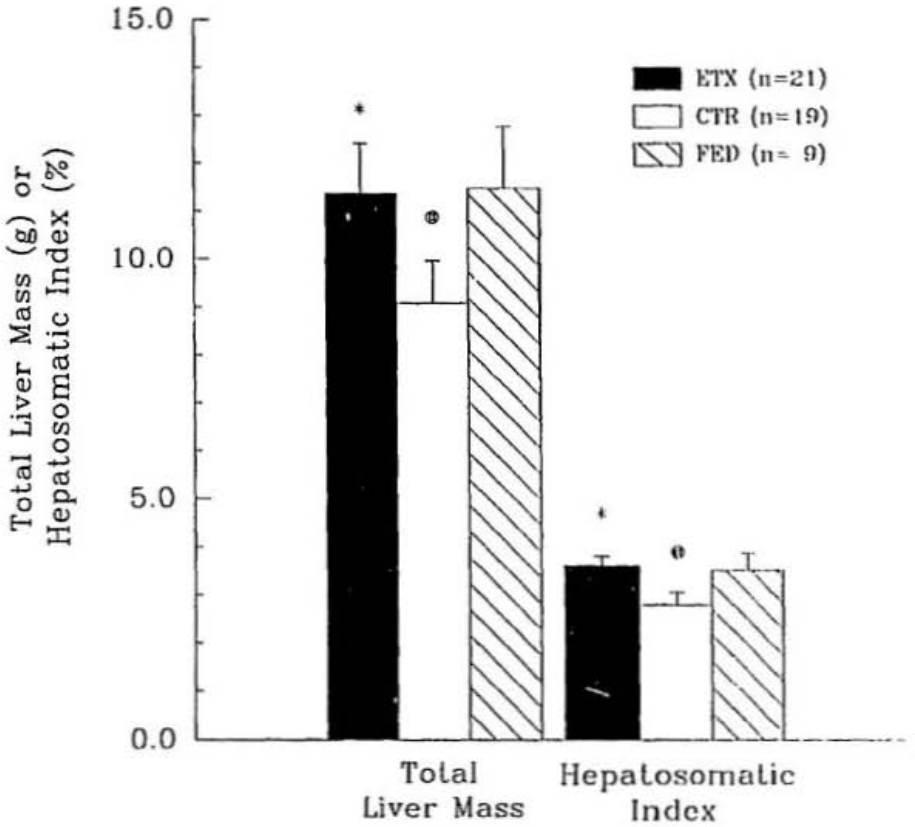
15.0
10.0
5.0
0.0
Total Liver Mass (g) or Hepatosomatic Index (%)
ETX (n=21)
CTR (n=19)
FED (n= 9)
*
⊕
*
⊕
Total Liver Mass
Hepatosomatic Index

Results and Discussion

E. coli LPS Increases Liver Mass Dose-Dependently

Figure 4.2.A-4.2.B show the dose-dependence of the endotoxin-induced change in the hepatic mass, measured in fasted rats, 24 hr after treatment. The effect was generally dose-dependent between 0.03 and 3.0 mg/kg i.p. A dose of 0.3 mg/kg i.p. was the minimal dose required to introduce an unambiguous change in the liver mass. The dose (3.0 mg/kg, i.p.) we used for all other experiments in this study caused a large increase in the liver mass and was well tolerated by the animals with a mortality of less than 5% in all experiments. The body weight loss by the animals was also dose-dependent (**Figure 4.2.C**).

More Water, Rather Than More Dry Mass, Underlies the LPS-Induced Effect on Hepatic Mass

Since water comprises about 70% of the total liver weight, we assumed that changes in water content of the liver, rather than dry mass components, would account for the dramatic changes in liver mass. Indeed, **Figure 4.2.D** shows a dose-dependent increase in hepatic wet/dry weight ratio. **Table 4.1** shows changes in water content and various dry mass components. It is clear that the increased liver mass in the endotoxic rats, compared with the saline-controls, was largely due to increased water content.

Figure 4.2.A-4.2.D Dose-response curve of the changes in the liver mass, hepatosomatic index, loss of body weight and heptatic wet/dry weight ratio after endotoxin administration

These studies were performed on the fasted rats at 24 hr after endotoxin administration at doses of 0.03-3.0 mg/kg, i.p. All values are means ± SD with 3 rats for each dose except 5 rats for 0.3 mg/kg and 1.0 mg/kg groups. * $p<0.05$, ** $p<0.01$, *** $p<0.001$ (two-tailed P values by unpaired t-test) for the endotoxic group (●) treated with various doses vs. the corresponding values of the same saline-control group (n=4). The dashed line (---) represents the control values of liver mass (6.49 ± 0.79 g) in panel A; hepatosomatic index (3.07 ± 0.38) in panel B; loss of body weight (7.34 ± 1.31%) in panel C and liver wet/dry weight ratio (2.25 ± 0.03) in panel D, respectively.

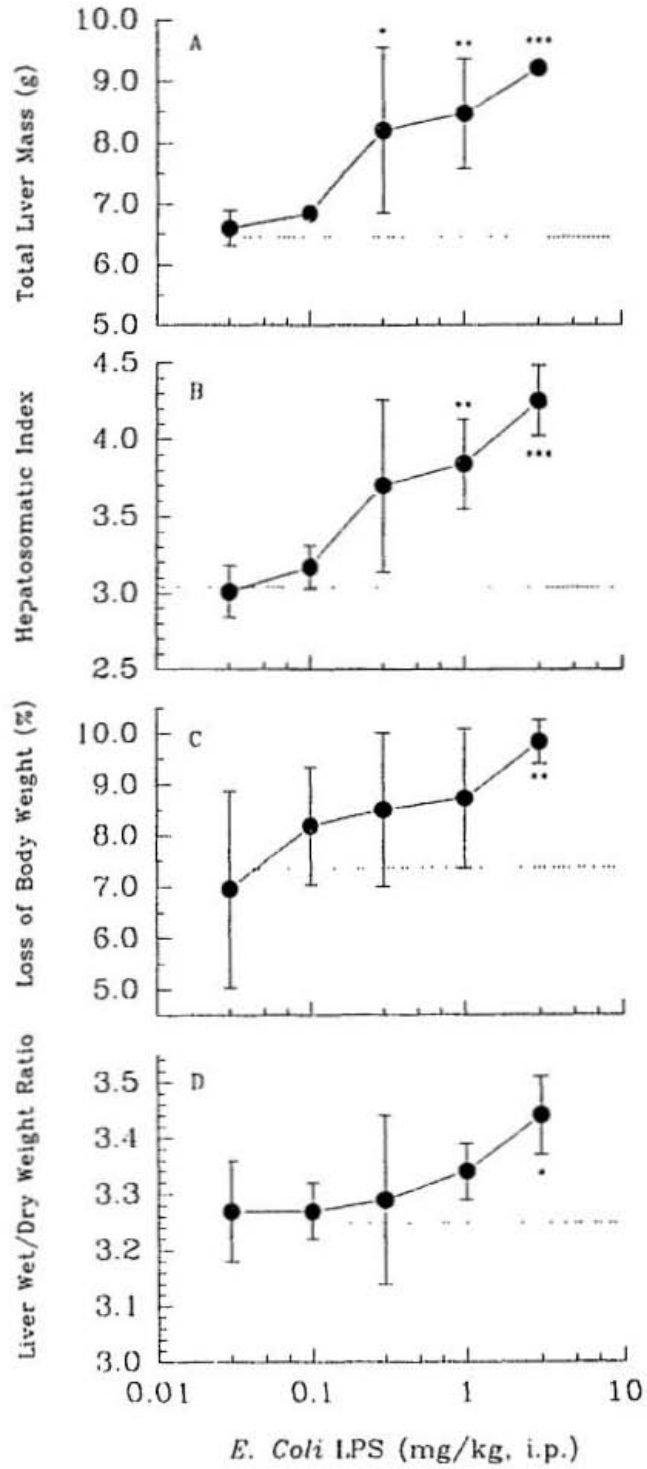
Total Liver Mass (g)
10.0
9.0
8.0
7.0
6.0
5.0
A
*
**
***
Hepatosomatic Index
4.5
4.0
3.5
3.0
2.5
B
**
***
Loss of Body Weight (%)
10.0
9.0
8.0
7.0
6.0
5.0
C
**
Liver Wet/Dry Weight Ratio
3.5
3.4
3.3
3.2
3.1
3.0
D
*
0.01
0.1
1
10
E. Coli LPS (mg/kg, i.p.)

Table 4.1 Total liver mass, water content and dry mass components of the liver Normal Fed group was untreated and fed ad libitum. Endotoxic and Saline-Control were fasted and treated with E. coli LPS (3 mg/kg, i.p.) and sterile saline (3 ml/kg, i.p.), respectively. Values are means ± SD with the number of rats in parentheses. * $p<0.01$, ** $p<0.001$ vs. saline-Control group; ‡ $p<0.001$ vs. normal fed group; † $p<0.01$ vs. Endotoxic group (by ANOVA plus Bonferroni t-test). [a] The glycogen data could not be obtained from the same livers as the other data since it required freeze-clamping. The glycogen content per gram, obtained in a separate experiment, was multiplied by the mean of the total liver mass for each group.

	Normal Fed (n=5)	Saline-Control (n=8)	Endotoxic (n=8)
Final Body Weight (g)	326 ± 17	325 ± 10	322 ± 12
Total Liver Mass (/per liver)			
Wet Weight (g)	12.07 ± 0.66	9.60 ± 0.72‡	11.78 ± 0.71**
Hepatosomatic Index	3.71 ± 0.71	2.96 ± 0.26	3.66 ± 0.18**
Water (g)	8.53 ± 0.48	6.74 ± 0.54‡	8.54 ± 0.61**
(%)	70.34 ± 0.52	70.14 ± 0.76	72.58 ± 0.89**
Dry Mass (g)	3.54 ± 0.19	2.86 ± 0.20‡	3.24 ± 0.13**
Wet/Dry Ratio	3.41 ± 0.04†	3.36 ± 0.09	3.63 ± 0.13**
Dry Mass Components			
Glycogen (g)[a]	0.633	0.009	0.046
Lipids (g)	0.863 ± 0.091	0.676 ± 0.023‡	0.783 ± 0.096*
Proteins (g)	1.620 ± 0.109	1.368 ± 0.106‡	1.540 ± 0.095*

Twenty-four hr after endotoxin administration, the water content in the whole rat liver was about 27% more than that in the corresponding saline-controls, which is essentially the same (about 26%) as the increase in the total liver mass at 24 hr (**Figure 4.1**). The percentage of water content in the liver of endotoxic rats was also significantly higher than in either the normal fed rats or the saline-controls (**Table 4.1**). The major components of the dry mass are also given in **Table 4.1**. The dry mass, which comprises about 30% of the total liver weight, was 0.38 g more in endotoxic livers 24 hr after treatment, but this is obviously not enough to account for 2.18 g increase in the total liver weight, compared with saline-control rats. It can be seen that protein, glycogen and lipids are all slightly increased in the endotoxin-treated rats compared to the saline-controls. A number of other studies have also reported small increases (0.1-0.2 g per liver) in hepatic protein content after endotoxin administration (**Jepson** et al., 1986) or in sepsis (**Pedersen** et al., 1986; **Vary** et **Kimball**, 1992).

These data, therefore, demonstrated that the major effect of E. coli LPS, in terms of increasing the liver mass, compared with saline-controls, is to increase the water content of the liver.

The Increased Hepatic Water Content Cannot be Accounted for by an Increase in Extrahepatocellular Water (Blood and/or Interstitial Fluid)

The increase in the liver water content may result from an increase in the volume of hepatocytes, nonhepatocytes, blood or interstitial fluid, or any combination of these. Since cells make up more than 80% of the total hepatic fluid space and hepatocytes make up more than 90% of the liver cellular space (**Blouin** et al., 1977, also see "Hepatic Cellular Spaces" in **Chapter 1**), we hypothesized that hepatocellular space, the hepatic cellular space which excludes blood cells, rather than extrahepatocellular space (the total volume of plasma, blood cells and interstitial fluid), would be primarily responsible for the change in the liver mass. **Table 4.2** contains data on the volume of the major components of hepatic cellular spaces. The inulin space was determined following inulin infusion and the plasma space from the hepatic hemoglobin content, assuming that the hematocrit of sinusoidal blood in the liver is the same as that of vascular blood collected from the hepatic portal vein. Since hepatic blood content and plasma volume did not change after endotoxin injection , thus the blood volume did not change (**Table 4.2**).

Table 4.2 Hepatic cellular and extracellular volume The Normal fed group was untreated and fed ad libitum. Endotoxic and Saline-Control rats were fasted and treated with E. coli LPS (3 mg/kg, i.p.) or sterile saline (3 ml/kg, i.p.). The calculation of the hepatic fluid spaces was detailed in **Methods** of **CHAPTER 2.**
[a] Extrahepatocellular volume was calculated by adding the mean volume of the hepatic interstitial space to the mean volume of the hepatic blood content for each group.
[b] Hepatocellular volume was calculated by substracting the mean volume of the extrahepato-cellular space from the mean volume of the hepatic water content for each group. Values are means ± SD with the number of rats in parentheses. * $p<0.05$, *** $p<0.001$ vs. Saline-Control group; † $p<0.05$, ‡ $P<0.001$ vs. Normal Fed group (all by ANOVA plus Bonferroni t-test).

	Normal Fed (n=4)	Saline-Control (n=5)	Endotoxic (n=7)
Final Body Weight (g)	339 ± 19	325 ± 20	326 ± 17
Total Liver Mass (g)	13.76 ± 0.77	10.08 ± 0.67‡	12.84 ± 0.51***
Hepatosomatic Index	4.06 ± 0.26	3.10 ± 0.34‡	3.94 ± 0.40***
Hepatic Fluid Spaces (ml/per liver)			
Water Content	9.72 ± 0.68	7.11 ± 0.49†	9.36 ± 0.81***
Inulin Space	2.48 ± 0.41	1.57 ± 0.43†	2.13 ± 0.42
Plasma Space	0.99 ± 0.13	0.81 ± 0.17	0.87 ± 0.13
Interstitial Space	1.49 ± 0.29	0.77 ± 0.28	1.26 ± 0.49
Blood Content	2.04 ± 0.24	1.79 ± 0.29	1.72 ± 0.22
[a]Extrahepatocellular Vol.	3.53 ± 0.44	2.56 ± 0.31†	2.97 ± 0.43
[b]Hepatocellular Volume	6.19 ± 0.42	4.55 ± 0.40†	6.39 ± 0.89*

Table 4.2 shows that the total hepatic extracellular space (inulin space), which is the liver fluid space excluding all liver cells (hepatocytes and nonhepatocytes including blood cells), in the endotoxic group was not significantly different from that in the normal fed rats. In contrast, there was a 37% decrease in this parameter in saline-controls. The total hepatic extrahepatocellular volume, which is the hepatic interstitial space plus blood content (the volume of plasma and blood cells), in the endotoxic rats (2.97 ± 0.43 ml/liver) tended to become larger compared to that in the saline-controls (2.56 ± 0.31 ml/liver), however that was not statistically significant. Even if we add this 0.41 ml increase in extrahepatocellular space (i.e. 0.41 g more water) to the 0.38 g of net increase in dry mass (**Table 4.1**), we can only account for one third (0.79 g) of the increase in the total liver mass (2.18 g). These data support the idea that an increase in extrahepatocellular space is not the primary source responsible for the increase in the total liver mass of the endotoxic rats.

Table 4.2 also shows the calculated increase in the hepatic cellular volume by substracting the extrahepatocellular volume from the total volume of hepatic water content. After endotoxin injection, the liver extrahepatocellular volume did not significantly change

while hepatocellular volume increased by 40% compared to the saline-treated controls. Compared to the untreated rats fed ad libitum, the hepatocellular (by 26%) and extrahepatocellular (by 27%) volume decreased in parallel in the fasted saline-controls. There were no significant differences between the fasted endotoxic rats and the normal fed rats.

Since the hepatic content of osmotically active solutes must parallel the change in cellular volume, we predicted that an increase in hepatic intracellular space must be reflected in the hepatic K^+ content, the predominant intracellular cation. **Table 4.3** shows that total hepatic content of K^+ in the endotoxic livers was 25% higher than the saline-controls and not significantly different from that in normal fed rats. This percentage increase was conparable in magnitude to the increases in the total liver mass (about 23%) and hepatic water content (about 27%) (**Table 4.1**). Since about 97% of hepatic K^+ ions are present in intracellular space, this is a strong evidence suggesting for increase in hepatic cellular space. There was also an appreciable (25%) increase in the hepatic sodium content. By multiplying the volume of inulin space (mainly plasma plus interstitial space) (**Table 4.2**) by the plasma sodium concentration (taken as 145 mM), we can calculate the mean total extracellular sodium as 360 μmoles in the fed livers,

Table 4.3 Hepatic Content of Potassium and Sodium

These data were obtained for the livers in which dry mass and water content were determined (**Table 4.1**). Normal fed group was untreated and fed ad libitum. Endotoxic and Saline-Control rats were fasted and treated with E. coli LPS (3 mg/kg, i.p.) or sterile saline (3 ml/kg, i.p.). Values are means ± SD with the number of rats in the parentheses. * $p<0.05$; *** $p<0.001$ vs. Saline-Control; † $p<0.01$; ‡ $p<0.001$ vs. Normal Fed group (by ANOVA plus Bonferroni t-test).

	Normal Fed (n=5)	Saline-Control (n=8)	Endotoxic (n=8)
Final Body Weight (g)	326 ± 17	325 ± 10	322 ± 12
Liver Mass (g)	12.07 ± 0.66	9.60 ± 0.72‡	11.78 ± 0.71***
Hepatosomatic Index	3.71 ± 0.71	2.96 ± 0.26	3.66 ± 0.18***
Potassium (μmol/liver)	1018 ± 58	852 ± 50†	1062 ± 86***
Sodium (μmol/liver)	466 ± 23	405 ± 42	514 ± 95*

229 μmoles in the livers from the saline-injected controls and 309 μmoles in the livers from the endotoxin-injected rats. Subtracting these values from the total hepatic sodium content one can estimate the intracellular sodium at 106, 176 and 195 μmoles per liver for the fed, saline-control and endotoxin-treated rats, respectively. These numbers include sodium within blood cells but this is relatively minor. Thus fasting increased the intracellular sodium concentration but it was not appreciably further modified by endotoxin treatment.

Does Liver Become Bigger Because of More Hepatocytes ?

As shown in **Table 4.1** and **Table 4.2**, about one third of the total (2.18 g) increase in the liver mass of endotoxic rats, as compared to the saline-controls, can be accounted for by the sum of the net increase of dry mass components (0.38 g) and extrahepatocellular water (0.41 g). The other two thirds of the change, therefore, must result from the increase of the liver cellular space, i.e. hepatocytes and/or nonhepatocytes including blood cells in the liver. The total volume of nonhepatocytes (6.4%) in the liver is very small compared to that of hepatocytes (78%) (**Blouin et al.**, 1977). Since the hepatic blood content and plasma volume did not significantly change after endotoxin injection (**Table 4.3**), an increase in blood cell volume can be excluded. Therefore, the increase in the total volume of

hepatocytes must be the major source of the increase in the liver mass after endotoxin administration. This could be either due to an increased number of hepatocytes (hyperplasia) and/or an increased volume of hepatocytes (hypertrophy or swelling).

The number of cells (more strictly, the number of cell nuclei) present in an organ or tissue can be estimated from its total DNA content, because of the constancy of the quantity of DNA per nucleus in most organs and tissues of mature animals (**Enesco** et **Leblond**, 1962). Data in **Table 4.4** were obtained from the liver of male rats at 100-110 days of age, at 24 hr after treatment. The total hepatic DNA content of the saline-controls was not significantly different from the normal fed animals, although the latter had significantly lower hepatic DNA concentration when expressed per gram wet liver. The hepatic DNA content of the endotoxic rats, however, increased by 14% compared to the saline-controls or normal fed rats. This suggests an increase in the number of liver cells after endotoxin administration. An increase in hepatic DNA content after endotoxin administration to intact rat has not been reported. TNF-α has been reported to stimulate hepatic DNA synthesis in intact rat (**Feingold** et al., 1988). The increase in DNA synthesis is first seen at 20 hr and peaked at 24 hr after TNF-α treatment. However, the enhanced

Table 4.4 Hepatic DNA Content Data were obtained in the same experiment reported in **Table 4.1.** The Normal fed group was untreated and fed ad libitum. Endotoxic and Saline-Control rats were fasted and treated with E. coli LPS (3 mg/kg, i.p.) or sterile saline (3 ml/kg, i.p.). Values are means ± SD with the number of rats in parentheses. *** $p<0.001$ vs. Saline-Control; ‡ $p<0.01$ vs. Normal Fed; † $p<0.05$ vs. Endotoxic group (by ANOVA plus Bonferroni t-test).

	Normal Fed (n=5)	Saline-Control (n=8)	Endotoxic (n=8)
Final Body Weight (g)	326 ± 17	325 ± 10	322 ± 12
Liver Mass (g)	12.07 ± 0.66	9.60 ± 0.72‡	11.78 ± 0.71***
Hepatosomatic Index	3.71 ± 0.71	2.96 ± 0.26	3.66 ± 0.18***
Hepatic DNA			
(mg/g liver)	2.15 ± 0.16†	2.64 ± 0.21‡	2.44 ± 0.09
(mg/per liver)	25.85 ± 1.12†	25.21 ± 1.54	28.71 ± 1.55***

hepatic DNA synthesis is localized in non-parenchymal cells, which are clearly identified as Kupffer cells and some portal tract cells, whereas the low level of DNA synthesis normally found in hepatocytes remained unaffected (**Feingold** et al., 1991). Therefore, the increase in hepatic DNA content after endotoxin injection suggests an increase in the liver cell numbers but does not necessarily represent the proliferation in hepatocytes, the predominant hepatic parenchymal cells.

Does Liver Become Bigger Because of Larger Hepatocytes ?

The total hepatocellular volume was 31% larger after endotoxin administration, compared to the saline-treated controls (**Table 4.2**). Thus if the increase (by 14%) in hepatic DNA content (**Table 4.4**) represents an increased number of hepatocytes, one would still expect a 15-20% increase in average hepatocyte volume. If, as is likely from the work of **Feingold** et al. (1991), the increased hepatic DNA synthesis is restricted to non-parenchymal cells, the hepatocyte volume would be expected to increase even more. Therefore, we required additional independent means of determining hepatocyte volume.

Morphometric analysis was, therefore, conducted to estimate hepatocyte volume quantitatively. It involved (1) measurement of the perimeter and transsectional area of individual hepatocyte cell bodies in micrographic profiles

of liver tissue, which are projected on the monitor, by an image analysis system (Bioquant™); (2) calculation of hepatocyte volume from the transsectional area given by the Bioquant™ system. **Figure 4.3** is a photograph, taken from the micrograph projected on the Bioquant™ system monitor, showing the transsectional profile of hepatocytes from an endotoxic liver. The solid circle represents the outline of a hepatocyte, i.e. its perimeter. The perimeter of an individual hepatocyte was the value directly measured by the "blind" examiner and digitalized and integrated by the Bioquant™ system to give the hepatocyte transsectional area. Assuming one hepatocyte is an approximate sphere, the volume (V) of an individual hepatocyte can be calculated from its radius (r) by equation $V = 4\pi r^3/3$. Transsectional area (A) of a hepatocyte cell body is integrated from its perimeter by the Bioquant™, and $A = \pi r^2$, the average r can be calculated. By substitution of πr^2 in the equation $V = 4\pi r^3/3$ with the A given by the Bioquant™, the equation can be rearranged as $V = 4rA/3$. The hepatocyte volume (V) in the morphometric data shown in this study was calculated by the equation $V = 4rA/3$.

The shape or volume of hepatocytes might also vary with the different histological locations or functional groups (i.e. periportal or perivenous hepatocytes), their own polymorphism during cell cycle and artefactual changes in

Figure 4.3 Transsectional profile of hepatocytes from an endotoxic liver

The photograph was taken from the video micrograph projected on the monitor of the Bioquant™ image analysis system. It shows the transsectional profile of hepatocytes from the portal area of an endotoxic liver under light microscope (x40). The liver specimen was removed by open biopsy from the rat at 24 hr after E. coli LPS treatment (3 mg/kg, i.p.). The specimen was immediately fixed in Karnovsky's fixative (pH 7.4) and processed as described in **Method** in **CHAPTER 2.** The slide was stained by toluidine blue. The micrograph was projected with reversed enhancement to minimize background interference and optimize contrast of the hepatocyte outline. The solid circle is the visible cursor traced by the examiner on the screen. It represents the perimeter of the hepatocyte being measured, which will be digitalized and integrated by the Bioquant™ system at the same time to give the transsectional area and hepatocyte shape factor. The transsectional area given by the Bioquant™ system will be used to calculate the volume of the hepatocyte by the procedures detailed in the text.

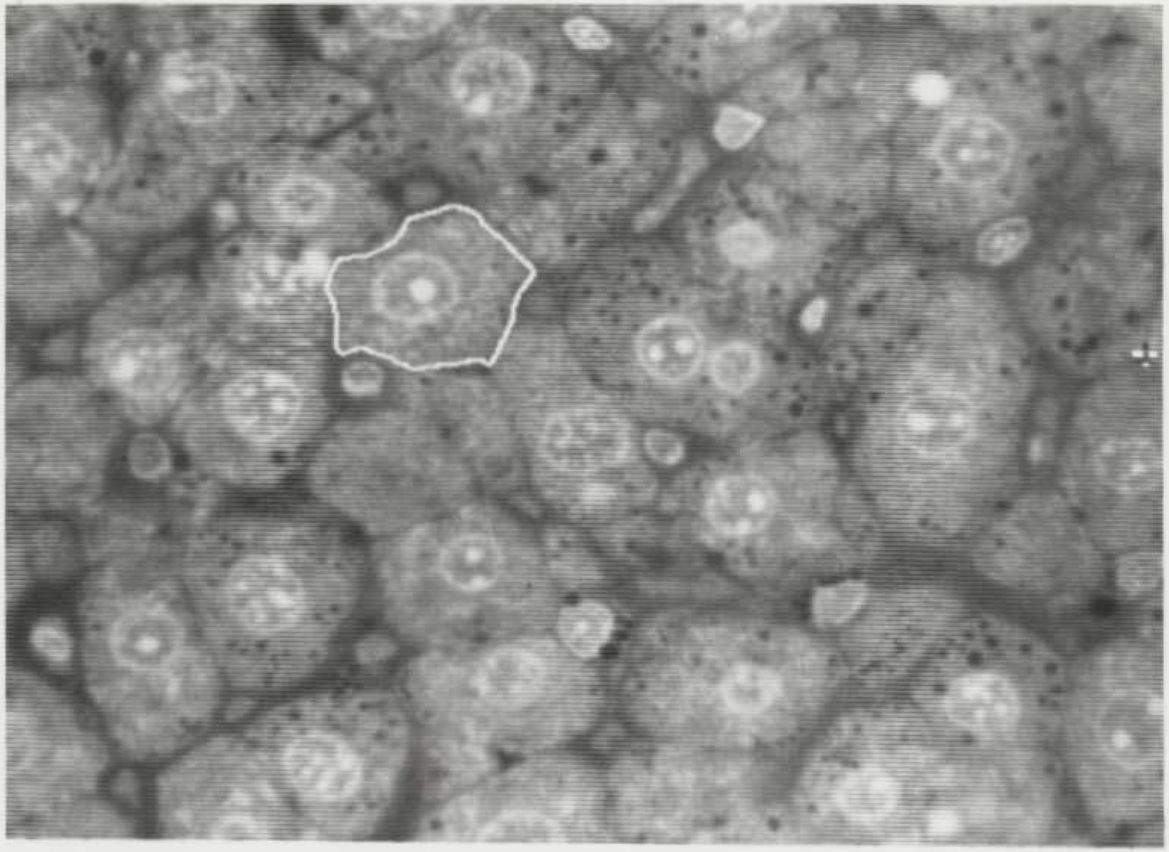

cell shape during thepreparation of tissue slides. In order to identify these possible non-specific changes in hepatocyte volume, the following criteria were followed during the morphometric studies: (1) The measurement of perimeter and transsectional area were restricted to those hepatocytes located in portal area, i.e. the area distant from the center veins but proximal to the edges between two adjacent hepatic lobules (this can be easily identified under x10 magnification). (2) The measurement of perimeter and transsectional area were restricted to those mononucleate hepatocytes showing a clear and intact nucleus. (3) The percentage of binucleate hepatocytes among all measured hepatocytes were calculated for each liver. (4) The distribution of transectional areas of all measured hepatocytes was examined for each liver. (5) The hepatocyte shape factor, ratio of the longest diameter over the shortest diameter, of an individual hepatocyte body on the transsectional profile was calculated for all hepatocytes measured.

Table 4.5 contains the morphometric data for the livers from the normal fed, saline- and endotoxin-treated rats. Since the other physical and biochemical investigations, described in previous sections, all suggested an increase, compared to the saline-controls, in the hepatocellular space, I used one-tailed t-test. **Table 4.5** shows that the

Table 4.5 Morphometry of Hepatocytes Normal fed group was untreated and fed ad libitum. Endotoxic and Saline-Control rats were fasted and treated with E. coli LPS (3 mg/kg, i.p.) or sterile saline (3 ml/kg, i.p.). Values are means ± SD with the number of rats in parentheses. * $p<0.05$ vs. Control (one-tailed P values, by unpaired t-test); $p>0.05$ for multiple comparisons between any two groups for each parameter (by ANOVA plus Bonferroni t-test). [a] Shape factor is the ratio of the shortest diameter over the longest diameter of the hepatocyte body on transsection profiles (0 = a straight line, 1 = a perfect circle).

Hepatocyte Morphometry	Normal Fed (n=4)	Saline-Control (n=4)	Endotoxic (n=4)
(P) Perimeter (μm)	63.84 ± 3.41	60.78 ± 1.50	63.10 ± 0.90
(A) Area (μm^2)	270.2 ± 31.3	246.2 ± 10.4	265.0 ± 10.2*
(V) Volume (μm^3)	3449 ± 585	2977 ± 189	3347 ± 202*
(r) Average Radius (μm)	9.17 ± 0.54	8.78 ± 0.19	9.09 ± 0.17
Longest Diameter (μm)	21.83 ± 1.24	20.96 ± 0.97	21.65 ± 0.20
Shape Factor[a]	0.82 ± 0.01	0.83 ± 0.01	0.82 ± 0.01
Binucleohepatocyte (%)	8.0 ± 2.6	11.1 ± 3.5	8.7 ± 3.4

mean transsectional area and the mean volume of hepatocyte was 8% and 12% larger in the endotoxic livers than in the livers from saline-controls, respectively. **Table 4.5** also shows that the percentages of binucleohepatocytes among all hepatocytes and the hepatocyte shape factors for the animals with the different treatments were not significantly different. These data suggest that the significant difference in the hepatocyte transsectional area between the endotoxin- and saline-treated animals is not attributable to the nonspecific variations due to hepatocyte polymorphism, artefactual change in processing specimens. Therefore, the increase in the hepatocyte transsectional area indicates an increase in the hepatocyte volume.

The morphometric data support the idea that larger hepatocytes (hepatocyte hypertrophy) rather than more hepatocytes (hepatocyte hyperplasia) are mainly responsible for the increase of hepatocellular fluid space, compared to the saline-controls, after endotoxin administration.

The Effect of *E. coli* LPS on the Liver Mass and Hepatocyte Volume Is Mediated by TNF-α

The pathogenesis of many well-known features of endotoxemia, such as fever, systemic toxicity and shock, acute phase protein synthesis and stress hormone secretion, are mediated by cytokines, TNF-α in particular (**Tracey** *et al.*, 1987; **Warren** *et al.*, 1988). This raises the question

as to whether the effect of E. coli LPS on the liver mass and hepatocyte volume is also mediated by cytokine TNF-α. Therefore, we first examined whether the effect of LPS on the liver mass and hepatocyte volume could be prevented by the passive immunization with antibodies against TNF-α. Data in **Table 4.6** show that the liver mass in the endotoxic rats pretreated with goat non-immune IgG, which was chosen as control for the TNF-α antibody, was 18-19% more than that in the endotoxic rats pretreated with the goat anti-mTNFα serum. Furthermore, the increased hepatic mass in this experiment was also accompanied by a significantly greater (by 20%) water content in the liver and a higher hepatic wet/dry weight ratio. This recalls the data from animals solely treated with E. coli LPS (**Table 4.1** and **Figure 4.2.D**). The subsequent morphometric study found that the mean transsectional area and the mean volume of hepatocyte cell bodies, in the endotoxic rats pretreated with non-immune IgG, was 11% and 17% larger, respectively, compared to the endotoxic rats protected by the specific anti-mTNFα serum (**Table 4.7**). The differences in the mean hepatocyte transsectional area and the calculated mean hepatocyte volume between the two groups were even more evident than that introduced by LPS- and saline-treatment. These data strongly suggest that the effect of E. coli LPS on the hepatic mass and hepatocyte volume are mediated by the

Table 4.6 The effect of specific TNF-α antibody on the liver mass of endotoxin-treated rats The animals were pretreated with goat anti-mouse-TNFα serum (20 mg/300 g rat, i.p.) (Anti-TNFα+LPS) or non-immune goat IgG (20 mg/300 g rat, i.p.) (Non-immune IgG+ LPS) 2 hr prior to the treatment of E. coli LPS (3 mg/kg, i.p.). The median and left lateral lobes, the two main lobes which account for 70% of the total liver mass, were removed by partial hepatectomy at 24 hr after LPS administration. Before the partial hepatectomy, a portion of the liver tissue was taken from the right lateral lobe for the morphometric analysis of hepatocytes (**Table 4.7**). [a] The values of liver mass and hepatosomatic index are of the median and left lateral lobes. [b] The values in parentheses are the calculated liver mass for the whole liver. All values are means ± SD with 4 rats in each group. † $p<0.05$; ‡ $p<0.01$ vs. IgG+LPS group (two-tailed P values by unpaired t-test).

	Anti-TNFα + LPS (n=4)	Non-Immune IgG + LPS (n=4)
Final Body Weight (g)	284 ± 8	281 ± 9
Liver Mass (g)	[a] 6.74 ± 0.48‡ [b](8.76 ± 0.62)	7.92 ± 0.50 (10.30 ± 0.64)
Hepatosomatic Index	[a] 2.37 ± 0.17† [b](3.08 ± 0.22)	2.83 ± 0.25 (3.68 ± 0.33)
Wet/Dry Weight Ratio	3.33 ± 0.14†	3.55 ± 0.06
Liver Water Content (%)	69.95 ± 1.34†	71.84 ± 0.49

Table 4.7 Morphometry of hepatocytes in the endotoxic rats pretreated with or without specific TNF-α antibody. The data were obtained from the same experiment as described in **Table 4.6**. The animals were pretreated with goat anti-mouse-TNFα serum (20 mg/300 g rat, i.p.) (Anti-TNFα+LPS) or non-immune goat IgG (20 mg/300 g rat, i.p.) (Non-immune IgG+ LPS) 2 hr prior to the treatment of E. coli LPS (3 mg/kg, i.p.). About 0.5 g of liver tissue was removed by open biopsy before the ligature of hepatic blood vessels for the partial hepatectomy (**Methods** in **CHAPTER 2**), at 24 hr after the LPS injetion. The liver specimen was immediately fixed in Karnovsky's fixative (pH 7.4) and prepared as described in **Methods** in **CHAPTER 2**. The morphometry of hepatocytes was analysed by the Bioquant™ system. The relative calculations were detailed in the previous section. Values are means ± SD with 4 rats in each group. * $P<0.05$ vs. IgG+LPS group (one-tailed P values by unpaired t-test).

Hepatocyte Morphometry	Anti-TNFα + LPS (n=4)	Non-Immune IgG + LPS (n=4)
(P) Perimeter (μm)	64.06 ± 2.90	67.10 ± 2.30
(A) Area (μm^2)	268.2 ± 16.7	297.2 ± 20.6*
(V) Volume (μm^3)	3378 ± 320	3966 ± 429*
(r) Average Radius (μm)	9.17 ± 0.28	9.63 ± 0.32
Longest Diameter (μm)	22.17 ± 1.19	23.02 ± 0.57
Shape Factor	0.81 ± 0.03	0.82 ± 0.00
Binucleohepatocyte (%)	5.3 ± 2.1	4.8 ± 3.1

cytokine TNF-α.

Increased production and serum level of TNF-α has been observed in patients with various liver diseases with detectable hepatomegaly (**Bird** et al., 1990). Long-term (**Fong** et al., 1989) or acute (**Feingold** et **Grunfeld**, 1987) administration of TNF-α to rats has also been reported to cause hepatic hypertrophy. Our own data in **Table 4.6** and **Table 4.7** demonstrated that the increase in the liver mass and hepatocyte volume after endotoxin injection could be prevented by the specific TNF-α antibody. This led us to question whether TNF-α administration could reproduce the effect of LPS on the liver mass and hepatocyte volume. **Table 4.8** shows that a bolus injection of rhTNF-α alone, which is essentially LPS-free, could also cause a 15-16% increase in the liver mass with significant increases in the hepatic water content and the wet/dry weight ratio, 24 hr after the treatment. **Feingold** et **Grunfeld** (1987) reported a 20% increase in liver mass 17 hr after a single rhTNF-α injection (25 μg/200 g rat, i.v.). The biological activity (5 x 10^7 U/mg) of the rhTNF-α they used is 10 times greater than ours (5 x 10^6 U/mg). The smaller increase of the liver mass in our experiments may be attributable to the slightly different experiment protocol, the lower dose (25 ug/250 g, i.v.) and activity of rhTNF-α that we used. Together with the data on anti-TNFα, this

Table 4.8 The Effect of rhTNF-α administration on the Liver Mass of Rat Animals were injected with rhTNF-α (25 μg/250 g rat, in 1.0 ml pyrogen-free saline, i.v.) or 1.0 ml pyrogen-free saline via tail vein. The livers were removed by hepatectomy 24 hr after the treatment. All values are means ± SD with 4 rats in each group. * $p<0.05$, ** $p<0.01$ vs. Saline group (the two-tailed P values by unpaired t-test).

	Recombinant Human TNF-α (n=4)	Pyrogen-free Saline (n=4)
Final Body Weight (g)	244 ± 10	244 ± 7
Liver Mass (g)	9.58 ± 0.80*	8.32 ± 0.75
Hepatosomatic Index	3.93 ± 0.25**	3.40 ± 0.23
Wet/Dry Weight Ratio	3.26 ± 0.06*	3.15 ± 0.05
Liver Water Content (g)	69.32 ± 0.58*	68.26 ± 0.58

experiment strengthens the conclusion that TNF-α plays a role in mediating the effect of E. coli LPS on liver mass. Obviously it is necessary to investigate, in the future, the changes in hepatocyte morphometry after rhTNF-α administration. One would expect that the hepatocyte transsectional area and hepatocyte volume should also increase after rhTNF-α administration.

Why Do Hepatocytes Become Larger After E. coli LPS administration ?

Although the mechanism of hepatocyte enlargement has not been directly determined in this study, the following observations are relevant.

Our preliminary experiments revealed that the blood flow of the portal vein and the lower abdominal aorta in the endotoxic rats was dramatically depressed (39% and 50%, respectively) 24 hr after endotoxin injection (**Table 3.4**). Poor perfusion and a reduction in oxygen supply to the liver could impair the hepatic oxidative phosphorylation and ATP production. This, in turn, could reduce Na^+-K^+-ATPase activity and result in the accumulation of Na^+ and Cl^- ions and a shift of extracellular water into cells (**Fitch et Rink**, 1983; **Garrison et al.**, 1982). One might therefore expect that the increase in hepatocyte volume after endotoxin injection could be hepatocyte swelling due to impairment in energy metabolism. However, the hepatic

concentration of adenine nucleotides in the endotoxic liver was not significantly different from the other two control groups (**Table 4.9**). Together with the results of the liver potassium content (**Table 4.3**), which increased by 25% after endotoxin injection, these data argue against a mechanism of cell swelling, as a result of impaired hepatic oxidative phosphorylation and ATP production. In addition, a recent study (**Pacitti** et al., 1992) reported an net increase (59%) in hepatic blood flow at 12 hr after the injection with LPS of the same serotype (as the result of a 2.5-fold increase in the hepatic arterial flow and unchanged portal flow). It is quite possible, therefore, that the net change in hepatic blood flow, at 24 hr, does not necessarily lead to decreased liver perfusion even though the portal blood flow was reduced. As discussed in **Chapter 3**, the values for blood lactate/pyruvate and ß-hydroxybutyrate/acetoacetate ratios throughout the 24 hr after endotoxin injection do not suggest tissue anoxia. Therefore there is no reason to suggest that the increased hepatocyte volume, after endotoxin injection, is an artefact of impaired energy metabolism.

Table 4.9 Hepatic concentration of adenine nucleotides

Normal fed group was untreated and fed ad libitum. Endotoxic and Saline-Control rats were fasted and treated with E. coli LPS (3 mg/kg, i.p.) or sterile saline (3 ml/kg, i.p.). A portion of liver was removed by open biopsy 24 hr after the treatment and rapidly freeze-clamped for the assay (see **Methods** in **CHAPTER 2**). Values are all means ± SD with the number of rats in parentheses. $p>0.05$ for comparisons between any two groups for ATP, ADP and AMP (by ANOVA plus Bonferroni t-Test).

(μmol/per g wet liver)	Normal Fed (n=4)	Saline-Control (n=3)	Endotoxic (n=5)
ATP	3.83 ± 0.31	3.56 ± 0.21	3.35 ± 0.45
ADP	1.18 ± 0.22	1.39 ± 0.08	1.18 ± 0.18
AMP	0.24 ± 0.06	0.28 ± 0.01	0.24 ± 0.07

Mobilization of amino acids from the periphery with a concomitant increase of hepatic amino acid uptake and protein synthesis are characteristics of infections including endotoxemia (**Rosenblatt** et al., 1983; **Fong** et al., 1990). Studies into the exchange of amino acids between skeletal muscles and the liver in sepsis have shown that both the release of amino acids from muscle and the uptake of amino acids by the liver were markedly increased (**Rosenblatt** et al., 1983). The cumulative transport of amino acids by Na^+-dependent transporters has been reported to build up intra /extracellular amino acid concentration gradients (see "Changes in amino acid transport" in **Chapter 1**). The accumulation of amino acids and K^+, which is pumped into hepatocytes by Na^+/K^+-ATPase in exchange for the Na^+ co-transported with amino acids, can lead to hepatocyte swelling (**Häussinger** et al., 1990a; **Häussinger** et **Lang**, 1991). Of course, the hepatic uptake of amino acids is not only enhanced by the increased availability of amino acids in the extracellular environment (**Collarini** et **Oxender**, 1987; **Häussinger** et al., 1990a), but also stimulated by the cytokine TNF-α and glucagon, the two important mediators during critical illnesses involving sepsis and endotoxemia. TNF-α has been shown to exhibit a permissive effect in enhancing the stimulation of amino acid transport by glucagon (**Warren** et al., 1987). A marked

increase in Na^+-dependent amino acid transport by TNF-α *in vivo* is, in part, mediated by the glucocorticoid hormones (**Pacitti** *et al.*, 1993). Alanine transport in hepatic membrane vesicles has been reported to be stimulated in the endotoxin-treated rat (**Pacitti** *et al.*, 1991). In our animal model 24 hr after treatment, the blood L-alanine level in the endotoxic rats was more than doubled that in the saline-controls, and the hepatic content of both total amino acids and L-alanine in the endotoxic rats were 64% and 270% higher, respectively, than the saline-controls (**Table 4.10**). Thus, it is possible that the enlargement of hepatocytes after endotoxin administration was due to the enhanced hepatic uptake of amino acids, especially of L-alanine, by the activation of Na^+-dependent systems in the liver.

Table 4.10 Hepatic and blood total amino acid and L-alanine concentrations Normal fed group was untreated and fed ad libitum. Endotoxic and Saline-Control rats were fasted and treated with E. coli LPS (3 mg/kg, i.p.) or sterile saline (3 ml/kg, i.p.). A portion of liver was removed by open biopsy 24 hr after the treatment and rapidly freeze-clamped. Blood was collected from the lower abdominal aorta at the bifurcation into the iliac arteries. The extraction and assay procedures were described in **Methods** in **CHAPTER 2**). Values are means ± SD with the number of rats in the parentheses. * $p<0.05$, ** $p<0.01$ vs. Saline-Controls; † $p<0.05$ vs. Normal Fed 0 hr; ‡ $p<0.001$ vs. Endotoxic (by ANOVA plus Bonferroni t-Test). [a] Since total liver mass was not available due to freeze-clamping, the total amino acids and L-alanine per liver were calculated by multiplying the hepatic amino acid concentration by the means of the total liver mass for each group in the combined data shown in **Figure 4.1.**

	Normal Fed	Saline-Control	Endotoxic
Total Aminoacids			
Blood (umol/ml)	4.51 ± 0.50(4)	4.07 ± 0.23(4)	4.23 ± 0.27(6)
Liver (umol/g)	15.17 ± 2.08(4)	14.69 ± 2.40(4)	19.03 ± 2.87(6)**
(umol/liver)[a]	174	134	216
L-Alanine			
Blood (umol/ml)	0.35 ± 0.04(5)‡	0.25 ± 0.03(3)†	0.54 ± 0.02(3)**
Liver (umol/g)	0.77 ± 0.10(5)‡	0.57 ± 0.37(3)	1.66 ± 0.65(3)*
(umol/liver)[a]	8.84	5.18	18.86

GENERAL DISCUSSION

Intraperitoneal administration of E. coli LPS (0127:B8) to fasted rats increased total liver mass and hepatic water content, temporally and dose-dependently, as compared with the fasted saline-controls (**Figure 3.3.A**, **3.3.B** and **Figure 4.1**). The effect of LPS on the liver mass could be reproduced by rhTNF-α and prevented by anti-mTNFα serum in vivo (**Table 4.8** and **Table 4.6**). Our results are consistent with other published studies on different animal models of infection (see "Studies related to the increase of liver mass" in **Chapter 1**). These data suggest that an increase in the liver mass appears to be a common TNF-α-mediated host response after such stress stimuli as endotoxemia, sepsis, trauma and chronic inflammation in either fasted or fed rats.

Twenty-four hr after treatment, the absolute and relative weight of the livers of fasted endotoxic rats remained similar to those of the normal fed rats although there was a significantly higher hepatic wet/dry weight ratio and a higher water content. The water content of the fasted saline-control rats was reduced by about 20% with a similar wet/dry weight ratio as in the normal fed rats (**Figure 4.1** and **Table 4.1**). The changes in wet/dry weight ratio and water content suggest that the alteration in the

total liver mass after E. coli LPS administration, while still within the bounds of the changes that occur during the shift between fasting and fed states, must involve a different process.

Although the increase in hepatic water content accounted for over 80% of the change in the liver mass (**Table 4.1**), less than 20% of this increase in the hepatic water content was attributable to the increase in the extracellular fluid space (mainly interstitial fluid) (**Table 4.2**). It suggests an increase in the hepatic cellular space after endotoxin administration, which was supported by a corresponding increase of hepatic K^+ content, the predominant intracellular cation (**Table 4.3**).

Systemic endotoxemia due to gut-derived or exogenous endotoxin was reported to enhance liver regeneration quantified by [^{3}H]thymidine incorporation into hepatic DNA in rats with 67% hepatectomy (**Cornell**, 1985a; 1985b). However, exogenous endotoxin did not stimulate [^{3}H]thymidine incorporation into hepatic DNA in intact rats (**Cornell**, 1985a). This suggested to **Leffert** et al. (1988) that the enhanced hepatic DNA synthesis in the regenerating liver is a "compensatory hyperplasia" after acute liver injury. In our endotoxic animals, however, the activities of serum glutamate-pyruvate transaminase (SGPT), an index of damage in hepatic parenchyma, was not significantly elevated at

different E. coli doses from 0.03 mg/kg, i.p. (22.6 ± 3.3 U/L) to 3.0 mg/kg, i.p. (30.0 ± 7.9 U/L), compared with the saline-controls (23.4 ± 4.8 U/L). No massive hepatocyte necrosis was found in the liver histopathological examination for the endotoxic rats. Thus, there is no evidence of profound damage in hepatic parenchyma causing "compensatory hyperplasia" so as to recover its capability of degrading endotoxin (**Cornell**, 1981).

The cytokine TNF-α has been reported to mediate the stimulation of hepatic DNA synthesis during liver regeneration both in rats after partial hepatectomy (**Akerman** et al., 1992) and in intact rats (**Feingold** et al., 1988). It was also proposed to be one of many putative hepatotrophic factors, such as insulin, glucagon, epidermal growth factor, vasopressin, and triiodothyronine (**Cornell**, 1985a; **Feingold** et al., 1988). In intact rats, the enhancement of hepatic DNA synthesis following TNF-α administration was shown to be a stimulation of de novo DNA replication rather than DNA repair in the liver (**Feingold** et al., 1988). A recent study (**Feingold** et al., 1991) demonstrated that TNF-stimulated hepatic DNA synthesis is localized in nonparenchymal cells including Kupffer cells and some portal tract cells which are most likely bile duct precursors, whereas the low level of DNA synthesis normally found in parenchymal hepatocytes remained unaffected. This

suggests that the increase in hepatic DNA content observed by us after endotoxin administration may not represent hyperplasia of parenchymal hepatocytes. The increased DNA synthesis in non-parenchymal cells might be a common hepatic inflammatory response involving mononuclear cell accumulation and bile duct proliferation to systemic illnesses such as sepsis and circulating toxins (**Tracey** et al., 1988; **Fong** et al., 1989; **Craig**, 1990). Since Kupffer cells and all non-hepatocytes account for 35-40% of the liver cell population but only for 5-10% (2.1% for Kupffer cells) of the total liver fluid space (**Blouin** et al., 1977), they represent a large proportion of hepatic DNA but a small proportion of intracellular space. Their proliferation may account for the increase in the total hepatic DNA content but the contribution to the increased total hepatic cellular volume, if any, should be very limited. Thus, larger hepatocytes rather than more hepatocytes or other cells are mainly responsible for the increase in the hepatic cellular volume. Our morphometric data support this hypothesis. However the mechanisms by which the volume changes come about together with their functional consequences remain to be determined.

Insulin has been shown in perfused liver, at physiological concentrations of portal venous blood, to affect the activity of volume-regulatory transport systems

on the hepatocyte membrane, which secondarily results in cell volume increase (**Häussinger** et **Lang**, 1991) (see "Insulin and glucagon" in **Chapter 1**). Insulin-induced increase in hepatocyte volume was known to act like an "anabolic signal" to inhibit glycogenolysis, glycolysis, proteolysis, and to stimulate glycogen synthesis, amino acid uptake and protein synthesis. Most of those features agree with the hepatic metabolic changes in infection including endotoxemia. On the other hand, hyperinsulinemia and insulin-resistance are characteristic metabolic alterations during trauma and/or sepsis (**Watters** et **Wilmore**, 1989). It is therefore tempting to speculate that the enlargement of hepatocytes after endotoxin administration is not merely a pathological "swelling" but an adaptive volume increase modulated by insulin as a response to the altered metabolism during endotoxemia.

SUMMARY AND CONCLUSIONS

1. A single intraperitoneal injection of E. coli LPS (O127:B8) at a sublethal dose (3 mg/kg, LD_5) induces, after 24 hr, an increase in hepatic mass of 25% in the fasted rat, compared with corresponding saline-controls. This phenomenon is generally time- and dose-dependent. It can be reproduced by a single intravenous administration of recombinant human TNF-α and prevented by the intraperitoneal injection of goat anti-mouse-TNFα serum.

2. In livers removed by complete hepatectomy 24 hr after endotoxin treatment, the difference in the absolute liver weight between the endotoxic group and their corresponding saline-controls is 2.0-2.5 g, i.e. 20-25% of the total liver mass of 300-350 g rats. The absolute liver weight and the hepatosomatic index of the fasted endotoxic rats remained similar to that of the normal rats fed ad libitum, but with a significantly higher water content and wet/dry weight ratio. The liver weight and hepatosomatic index of the fasted saline-controls were reduced by 20% compared to the normal fed rats. There was no change in water content on fasting. This suggests that although the change in liver mass after E. coli LPS treatment is similar in magnitude to the changes which occurs in the usual

physiologic shift from fasting to fed state, it must be a different process.

3. In the endotoxic liver, the hepatic water content increases by almost the same extent as the increase in the liver mass 24 hr after treatment, indicating that the effect of E. coli LPS is mainly on the hepatic water content, rather than on the dry mass components.

4. Only about one third (0.8 g) of the total increase (2.18 g) in the hepatic mass can be accounted for by the net increase (0.38 g) of the dry mass components plus the blood/plasma and/or interstitial fluid (0.41 ml) in the extrahepatocellular space, suggesting that an expansion of the hepatocellular space is mainly responsible for the increase in the liver mass of endotoxic rats. This is also supported by the increase of hepatic K^+ content by 25% in the endotoxic rats. The hepatocellular space calculated based on the extrahepatocellular space determined in vivo was 40% larger in the endotoxic rats.

5. A morphometric study demonstrates that the mean transsectional area and the mean volume is 8% and 12% larger, respectively, in the mononucleate hepatocytes from the endotoxic livers, and 11% and 17% larger in that from the livers of endotoxic rats treated with goat non-immune IgG, respectively, compared to their corresponding saline- or goat anti-mTNFα-serum-treated rats. This supports our

hypothesis that larger hepatocytes, rather than more hepatocytes, are responsible for the increase in the hepatocellular space.

6. The hepatic DNA content increases by 14% in the endotoxic liver, compared with the saline-controls and the normal fed rats, suggesting that an increase in the number of liver cells also occurs after the treatment of E. coli LPS. Whether the proliferation of hepatocytes (hepatocyte hyperplasia) or non-hepatocytes (portal lymphoid hyperplasia and/or lobule Kupffer cell hyperplasia as an inflammatory response) underlies the increase of hepatic DNA content needs to be further defined.

7. Twenty-four hr after the treatment with E. coli LPS, the concentrations of hepatic adenine nucleotides in the endotoxic rats are not significantly different from the saline-controls and the normal fed rats; and elevated total amino acid and L-alanine level in both blood and the liver, hyperlactacidemia, hyperpyruvacidemia, and hypoketonemia are evident in the endotoxic rats. In addition, there is no significant change in the activity of serum glutamate-pyruvate transaminase (SGPT) and the plasma ratio of lactate/pyruvate and ß-hydroxybutyrate/acetoacetate during the 24 hr after endotoxin treatment. These observations argue against a "compensatory hyperplasia" resulting from acute liver damage due to direct LPS toxicity or hepatocyte

"swelling" due to tissue anoxia and impaired energy status in the liver. Metabolic changes mediated by insulin, glucagon, TNF-α and/or other "hepatotrophic factors" may be responsible for the increase of liver mass after E. coli LPS administration.

BIBLIOGRAPHY

1. **Qian, D., M. Jois, and J.T. Brosnan.** (1992) Endotoxin administration to rats increases liver mass *in vivo*: Possible increase in hepatocyte volume. Proceedings of 35th annual meeting of the Canadian Federation of Biological Societies (CFBS, Victoria, B.C., Canada, June 18-20, 1992): 86 (Abstract No.260).

2. **Brosnan, J.T. *et* Qian, D.** (1992) Endotoxin administration increases rat liver mass *in vivo*. Proceedings of 21st annual meeting of the European Biochemical Societies (FEBS, Trinity college Dublin, Ireland, August 9-14, 1992): Abstract Th-90.

3. **Ewart, H.S., D. Qian, and J.T. Brosnan.** Activation of hepatic glutaminase in the endotoxin-treated rat. (Submitted to Journal of Surgical Research in August, 1993).

4. **Brosnan, J.T. *et* Qian, D.** Endotoxin-induced increase in liver mass and hepatocyte volume. Abstract chosen by the Biochemical Society Meeting No.649, Imperial College, London, December 21, 1993.

5. **Brosnan, J.T. *et* Qian, D.** (1994) Endotoxin-induced increase in liver mass and hepatocyte volume. Biochemical Society Transanctions (in press).

6. **Qian, D. *et* Brosnan, J.T.** TNFα-mediated effect of *E. coli* LPS increases hepatic mass and hepatocyte volume *in vivo*. (Submitted to the American Journal of Physiology).

REFERENCES

Akerman, P., P. Cole, S.Q. Yang, C. McClain, S. Nelson, G.J. Bagby, and A.M. Diehl. **(1992)** Antibodies to tumour necrosis factor-α inhibit liver regeneration after partial hepatectomy. Am J Physiol 263:G579-G585.

Ardawi, M.S.M., A.A. Ashy, Y.S. Jamal, and S.M. Khoja. **(1989)** Metabolic control of hepatic gluconeogenesis in response to sepsis. J Lab Clin Med 114:579-586.

Aria, I.M., W.B. Jacoby, H. Popper, D. Schachter, and D.A. Shafritz (eds.). **(1988)** The cells. In: The liver biology and pathobiology (2nd ed.). Raven Press, New York, pp9-10.

Baquet, A., L. Hue, A.J. Meijer, G.M. van Woerkom, and P.J.A.M. Plomp. **(1990)** Swelling of rat hepatocytes stimulates glycogen synthesis. J Biol Chem 265:955-959.

Baraona, E. et **Leo**, M.A. **(1975)** Alcoholic hepatomegaly: accumulation of protein in the liver. Science 190:794-795.

Bartlett, J.G., A.B. Onderdonk, T. Louie, D.L. Kasper, and S.L. Gorbach. **(1978)** Lessons from an animal model of intra-abdominal sepsis. Arch Surg 113:853-857.

Bear, C.E. **(1990)** A nonselective cation channel in rat liver cells is activated by membrane stretch. Am J Physiol 258:C421-C428.

Beck, F.X., A. Dorge, R. Rick, M. Schramm, and K. Thurau. **(1988)** The distribution of potassium, sodium and chloride across the apical membrane of renal tubular cells: effect of acute metabolic alkalosis. Pflüegers Arch physiol 411: 259-267.

Beisel, W.R. **(1975)** Metabolic response to infection. Ann Rev Med 26:9-20.

Bergmann, S.R., E. Carlson, E. Dannen, and B.E. Sobel. **(1980)** An improved assay with 4-(2-thiazolylazo)-resorcinol for non-esterified fatty acids in biological fluids. Clin Chim Acta 104:53-63.

Bergmeyer, H.U. (ed.) **(1974)** L-alanine. Determination with alanine dehydrogenase. In: Bergmeyer, H.U. (ed.) Methods of enzymatic analysis, Vol. IV. Academic Press, New York, pp. 1679-1682.

Bergmeyer, H.U. et **Bernt**, E. **(1974)** Glutamate-pyruvate transaminase. UV-assay, mannual methods. In: Bergmeyer, H.U. (ed.) Methods of enzymatic analysis, Vol. II. Academic Press, New York, pp. 752-758.

Bergmeyer, H.U., E. Bernt, F. Schmidt and H. Stork. **(1974)** D-glucose. Determination with HK and G6P-DH. In: Bergmeyer, H.U. (ed.). Methods of enzymatic analysis, Vol. III. Academic Press, New York, pp. 1196-1200.

Bergstrom, J.P. **(1962)** Muscle electrolytes in man. Scan J Clin Lab Invest 14(suppl.68):1-100.

Bergstrom, J.P., J. Larsson, H. Nordström, E.Vinnars, J. Askanazi, D.H. Elwyn, J.M. Kinney, and P.J. Fürst. **(1987)** Influence of injury and nutrition on muscle water and electrolytes: effects of severe injury, burns and sepsis. Acta Chir Scand 153:261-266.

Beutler, B., D. Greenwald, J.D. Hulmes, M. Chang, T.-C. E. Pan, J. Mathison, R. Ulevitch, and A. Cerami. **(1985a)** Identity of tumour necrosis factor and the macrophage-secreted factor cachectin. Nature 316:552-554.

Beutler, B., I.W. Milsark, A. Cerami. **(1985b)** Cachectin/tumour necrosis factor: production, distribution, and metabolic fate in vivo. J Immunol 135:3972-3977.

Beutler, B., N. Krochin, I.W. Milsark, C. Leudke, A. Cerami. **(1986)** Control of cachectin synthesis: mechanism of endotoxin resistance. Science 232:977-980.

Beutler, B. et **Cerami**, A. **(1988)** The history, properties, and biological effects of cachectin. Perspectives in Biochem 27:7576-7582.

Bird, G.L.A., N. Sheron, A.K.J. Goka, G.J. Alexander, R.S. Williams. **(1990)** Increased plasma tumor necrosis factor in severe alcoholic heatitis. Ann Intern Med 1990; 112:917-921

Bisell, D.M. et **Roll**, J.R. **(1990)** Connective tissue metabolism and hepatic fibrosis. In: Zakim, D. et Boyer, T.D. (eds.). Hepatology: a textbook of liver disease (2nd

ed.), Vol. I. Saunders, Philadelphia, pp424-444.

Bligh, E.G. et **Dyer**, W.J. **(1959)** A rapid method of total lipid extraction and purification. Can J Biochem Physiol 37:911-917.

Blouin, A., R.P. Bolender, and E.R. Weibel. **(1977)** Distribution of organelles and membranes between hepatocytes and nonhepatocytes in the rat liver parenchyma. A stereological study. J Cell Biol 72:441-455.

Boivin, A. et **Mesrobeanu**, L. **(1935)** Recherches sur les antigéenes somatiques et sur les endotoxines des bactéries. I. Considérations générales et exposé des techniques utilisées. Rev Immunol (Paris) 1:553-569.

Bouwens, L., M. Baekeland, R. de Zanger, and E. Wisse. **(1986)** Quantitation, tissue distribution and proliferation kinetics of Kupffer cells in normal rat liver. Hepatology 6:718-722.

Brade, H., L. Brade, U. Schade, U. Zahringer, O. Holst, H. Kuhn, A. Rozalski, E. Rohrscheidt, and E. Th. Rietschel. **(1988)** Structure, endotoxicity, immunogenicity and antigenicity of bacterial liopolysaccharides (endotoxins, O-antigens). In: Levin, J., H.R. Buler, J.W. ten Cate, S.J.H. van Deventer, and A. Sturk (eds.). Bacterial endotoxins. Pathophysiological effects, clinical significance, and pharmacological control. Alan R. Liss, New York, pp17-45.

Brosnan, J.T., H.A. Krebs, and D.H. Williamson. **(1970)** Effects of ischaemia on metabolite concentrations in rat liver. Biochem J 117:91-96.

Brosnan, J.T., K.-C. Man, D. Hall, S.A. Colbourne, and M.E. Brosnan. **(1983)** Interorgan metabolism of amino acids in streptozotocin-diabetic ketoacidotic rat. Am J Physiol 244:E151-E158.

Browne, M.K. et **Leslie**, G.G. **(1976)** Animal odels of peritonitis. Surg Gynecol Obstet 143:738-740.

Bucher, N.L.R. et **Malt**, R.A. **(1971)** Liver regeneration. In: Regeneration of liver and kidney. Little Brown, Boston, pp15-176.

Bucher, N.L.R., U. Patel and S. Cohen. **(1978)** Hormonal factors concerned with liver regeneration. In: Ciba

Foundation Symosium 55. Hepatotrophic factors. Elsevier/Excerpta Medica, Amstrdam, pp95-151.

Bucher, N.L.R. et **McGowan**, J.A. **(1985)** Regulatory mechanisms in hepatic regeneration. In: Wright, R., K.G.M.M. Alberti, and S.Karran (eds.). Liver and biliary disease. Saunders, London, pp251-265.

Bullock, B.L. **(1992)** Alterations in cellular processes. In: Bullock, B.L. et Rosendahl, P.P. (eds.). Pathophysiology. Lippincott, Philadelphia, pp32-40.

Burton, K. **(1956)** A study of the conditions and mechanism of the diphenylamine reaction for the colorimetric estimation of deoxyribonucleic acid. Biochem J 62:315-323.

Carabaza, A., M.D. Ricart, A. Mor, J. J. Guinovart, and C.J. Ciudad. **(1990)** Role of AMP on the activation of glycogen synthase and phosphorylase by adenosine, fructose and glutamine in rat hepatocytes. J Biol Chem 265:2724-2732.

Carswell, E.A., L.J. Old, R.L. Kassel, S. Green, N. Fiore and B. Williamson. **(1975)** An endotoxin-induced serum factor that causes necrosis of tumours. Proc Natl Acad Sci USA 72:3666-3670.

Cater, D.B., B.E. Holmes, and L.K. Mee. **(1957)** The effect of growth hormone upon cell division and nucleic acid synthesis in the regenerating liver of the rat. Biochem J 66:482-486.

Collarini, E.J. et **Oxender**, D.L. **(1987)** Mechanisms of transport of amino acids across membranes. Ann Rev Nutr 7:75-90.

Cornell, R.P. **(1981)** Endotoxin-induced hyperinsulinemia and hyperglucagonemia after experimental liver injury. Am J Physiol 241:E428-E435.

Cornell, R.P. **(1985a)** Gut-derived endotoxin elicits hepatotrophic factor secretion for liver regeneration. Am J Physiol 249:R551-R562.

Cornell, R.P. **(1985b)** Restriction of gut-derived endotoxin impairs DNA synthesis for liver regeneration. Am J Physiol 249:R563-R569.

Cotchin, E. et **Roe**, F.J.C. **(1967)** Pathology of the liver of rats and mice. In: Pathology of laboratory rats and mice.

Blackwell, Oxford, pp1-24.

Craig, J.R. **(1990)** Liver. In: Kissan, J.M. (ed.). Anderson's Pathology, Vol.III. Mosby, St. Louis, pp1199-1320.

Cuthbertson, D.P. **(1930)** The disturbance of metabolism produced by bony and non-bony injury, with notes on certain abnormal conditions of bone. Biochem J 24:1244-1263.

Douglas, R.G. et **Shaw**, J.H.F. **(1989)** Metabolic response to sepsis and trauma. Br J Surg 76:115-122.

Elwyn, D.H., H.C. Parikh, and W.C. Shoemaker. **(1968)** Amino acid movements between gut, liver and periphery in unanesthetized dogs. Am J Physiol 215:1260- 1275.

Enesco, M. **(1956)** Biochemical determination of the growth rate of several organs in male Sherman rats. Anat Rec 124:285-286.

Enesco M. et **Leblond**, C.P. **(1962)** Increase in cell number as a factor in the growth of the organs and tissues of the young male rat. J Embryol Exp Morph 10:530-562.

Evans, R.D., J.M. Argilés, and D.H. Williamson. **(1989)** Metabolic effects of tumour necrosis factor-α (cachectin) and interleukin-1. Clin Scin 77:357-364.

Fehlmann, M., Morin, P. Kitabgi, and P. Freychat. **(1981)** Insulin and glucagon receptors of isolated rat hepatocytes: cmoparison between hormone binding and amino acid transport stimulation. Endocrinology 109:253-261.

Fehlmann, M. et **Freychat**, P. **(1981)** Insuliin and glucagon stimulation of (Na^+-K^+)-ATPase transport activity in isolated rat hepatocytes. J Biol Chem 256:7449-7453.

Feigin, R.D. et **Dangerfield**, H.G. **(1967)** Whole-blood amino acid changes following respiratory acquired pasteurella tularensis infection in man. J Infect Dis 117:346-351.

Feigin, R.D., A.S. Klainer, W.R. Beisel, and R.B. Hornick. **(1968)** Whole-blood amino acids in experimentally induced typhoid fever in man. New Engl J Med 278:293-298.

Feingold, K.R. et **Grunfeld** C. **(1987)** Tumour necrosis factor-α stiulates hepatic lipogenesis in the rat in vivo. J Clin Invest 80:184-190.

Feingold, K.R., M. Soued, and C. Grunfeld. **(1988)** Tumour nectosis factor stimulates DNA synthesis in the liver of intact rats. Biochem Biophys Res Comm 153(2):576-582.

Feingold, K.R., M.E. Barker, A.L. Jones, and C. Grunfeld. **(1991)** Localization of tumor necrosis factor-stimulated DNA synthesis in the liver. Hepatology 13:773-779.

Felig, P., J.Wahren, and L. Räf. **(1973a)** Evidence of inter-organ amino-acid transport by cells in humans. Proc Natl Acad Sci USA 70:1775-1779.

Felig, P. **(1973b)** Glutamine and glutamate metabolism in normal and diabetic subjects. Diabetes 22:573-576.

Felig, P. **(1973c)** The glucose-alanine cycle. Metabolism 22:179-207.

Filkins, J.P. **(1978)** Phases of glucose dyshomeostasis in endotoxicosis. Circulatory Shock 5:347-355.

Fitch, K. et **Rink**, R. **(1983)** Hepatic oxygen supply during early and late sepsis int the rat. Circulation Shock 10:51.

Folch, J., M. Lees, and G.H. Sloane-Stanley. **(1957)** A simple method for the isolation and purification of total lipides from animal tissues. J Biol Chem 2265:497.

Fong, Y., L.L. Moldawer, M. Marano, H. Wei, A. Barber, K. Manogue, K.J. Tracey. **(1989)** Cachectin/TNF or IL-1a induces cachexia with reditribution of body proteins. Am J Physiol 256:R659-R665.

Fong, Y., M.A. Morano, L.L. Moldawer, H. Wei, S. Calvano, J.S. Kenney, A.C. Allison, A. Cerami, T.Shires, and S.F. Lowry. **(1990)** The acute splanchnic and peripheral tisue metabolic response to endotoxin in humans. J Clin Invest 85:1896-1904.

Freudenberg, M.A., N. Freudenberg, and C. Galanos. **(1982)** Time course of cellular distribution of endotoxin in liver lungs and kidneys of rats. Br J Exp Path 63:56-65.

Freudenberg, M.A., B. Kleine, C. Galanos. **(1984)** The fate of lipopolysaccharide in rats: evidence for chemical alteration in the molecule. Rev Infect Dis 6:483-487.

Freudenberg, M.A. et **Galanos**, C. **(1988)** The metabolic fate of endotoxins. In: Levin, J., H.R. Buller, J.W. ten Cate,

S.J.H. van Deventer, and A. Sturk. Bacterial endotoxins. Clinical significance, and pharmacological control. Alan R. Liss, New York, pp 63-76.

Fukuda, M. et **Sibatani**, A. **(1953)** Relation between the body weight and the average DNA content of liver nuclei in postnatal growth of the rat. Exp Cell Res 4:236- 238.

Garber, A.J., I.E. Karl, and D.M. Kipnis. **(1976)** Alanine and glutamine snthesis and release from skeletal muscle. I. Glycolysis and amino acid release. J Biol Chem 251:826-835.

Garrison, R., D.J. Ratcliff, and D.E. Fry. **(1982)** Hepatocellular function and nutrient blood flow in experimental peritoitis. Surgery 92:713-719.

Gornall, A.G., C.J. Bardawill, and M.M. David. **(1949)** Determinaiton of serum proteins by means of the biuret reaction. J Biol Chem 177:7751-7776.

Goldstein, S.A. **(1989)** The effects of injury and sepsis on fuel utilization. Ann Rev Nutr 9:445-473.

Graf, J. P., Haddad, D. Haussinger, and F. Lang. **(1988)** Cell volume regulation in liver. Renal Physiol Biochem 11:202-220.

Haddad, P., T. Thalhammer, and J. Graf. **(1989)** Effect of hypertonic stress on liver cell volume, bile flow and volume-regulatory K^+ fluxes. Am J Physiol 256:G563-G569.

Hallbrucker, C., S. Vom Dahl, F. Lang, and D. Häussinger. **(1991a)** Control of hepatic proteolysis by amino acid. The role of cell volume. Eur J Biochem 197:717-724.

Hallbrucker, C., S. Vom Dahl, F. Lang, W. Gerok, and D. Häussinger. **(1991b)** Inhibition of hepatic proteolysis by insulin. Role of hormone-induced alteration of the cellular K^+ balance. Eur J Biochem 199:467-474.

Hallbrucker, C., S. Vom Dahl, F. Lang, W. Gerok, and D. Häussinger. **(1991c)** Modification of liver cell volume by insulin and glucagon. Pflüegers Arch Physiol 418:510-521.

Hasselgren, P.O., R. Jagenburg, L. Karlström, P. Pedersen, and T. Seeman. **(1984)** Changes of protein metabolism in liver and skeletal muscle following trauma complicated by sepsis. J Trauma 24:224-228.

Hassid, W.Z. et **Abraham**, S. **(1957)** Chemical procedures for analysis of polysaccharides. I. Determination of glycogen and starch. Methods Enzymol 3:34-50.

Hau, T. et **Simmons**, R.L. **(1970)** Surgical pros and cons. Surg Gynecol Obstet 144:755-756.

Häussinger, D., W. Gerok, and H. Sies. **(1983)** Regulation of flux through glutaminase and glutamine synthase in isolated perfused rat liver. Biochim Biophys Acta 755:272-278.

Häussinger, D., S. Soboll, A.J. Meijer, W. Gerok, J.M. Tager, and H. Sies. **(1985)** Role of plasma membrane transport in hepatic glutamine metabolism. Eur J Biochem 152:597-603.

Häussinger, D. **(1990)** Nitrogen metabolism in liver: structural and functional organization and physiological relevance. Biochem J 267:281-290.

Häussinger, D. et **Lang, F. (1990)** Exposure of perfused liver to hypotonic conditions modifies cellular nitrogen metabolism. J Cell Biochem 43:355-361.

Häussinger, D., F. Lang, K. Bauers, and W. Gerok. **(1990a)** Interactions between glutamine metabolism and cell volume regulation in perfused rat liver. Eur J Biochem 188:689-695.

Häussinger, D., T. Stehle, and F. Lang. **(1990b)** Volume regulation in liver: further characterization by inhibitors and ionic substitutions. Hepatology 11:243-254.

Häussinger, D., F. Lang, K. Bauers, and W. Gerok. **(1990c)** Control of hepatic nitrogen metabolism and gutathione release by cell volume regulatory mechanisms. Eur J Biochem 193:891-898.

Häussinger, D., F. Lang, S. Vom Dahl, B. Stoll and W. Gerok. **(1990d)** Renal Physiol Biochem 13:167-168 (Abstract).

Häussinger, D., C. Hallbrucker, S.Vom Dahl, S. Lang, and W. Gerok. **(1990e)** Cell swelling inhibits proteolysis in perfused rat liver. Biochem J 272,:239-242.

Häussinger, D. et **Lang**, F. **(1991)** Cell volume in the regulation of hepatic function: A mechanism for metabolic control. Biochem Biophys Acta 1071:331-350.

Häussinger, D., C. Hallbrucker, S. Vom Dahl, S. Decker, U. Schweizer, F. Lang, and W. Gerok. **(1991)** Cell volume is a major determinant of proteolysis control in liver. FEBS Letter 283:70-72.

Hems, D.A. et **Brosnan**, J.T. **(1970)** Effects of ischaemia on content of metabolites in rat liver and kidney in vivo. Biochem J 120:105-111.

Henderson, R.M., J. Graf, and J.L. Boyer. **(1989)** Inward-rectifying potassium channels in rat hepatocytes. Am J Physiol 256:G1028-G1035.

Hensyl, W.R. **(1990)** In: Hensyl, W.R. (ed.) Stedman's medical dictionary (25th ed.). Williams and Wilkins, Baltimore.

Heys, M.R. et **McGivan**, J.D. **(1982)** Differential effects of starvation on alanine and glutamine transport in isolated rat hepatocytes. Biochem J 204:365-369.

Higgins, G.M. et **Anderson**, R.M. **(1931)** Experimental pathology of the liver: restoration of the liver of the white rat following partial surgical removal. Arch Rathol 12:186-202.

Hoffmann, E.K. et **Simonsen**, L. **(1989)** Membrane mechanisms in volume and pH regulation in vertebrate cells. Physiol Rev 69:315-382.

Holdstock, G., G.H.M. Balasegaram and R. Wright. **(1985)** The liver in infecton. In: Wright, R., K.G.M.M. Alberti, and S. Karran (eds.). Liver and biliary disease. Saunders, London, pp1077-1119.

Hyam, P.L. **(1981)** Same day electron microscopy. Canad J Med Tech 48:255-260.

Jacobs, E.E., et Jacob, M. **(1956)** Uncoupling of oxidative phosphorylation by cadmium ion. J Biol Chem 223:147-156.

Jacob, A.I., P.K. Goldberg, N. Bloom, G.A. Degenshein and P.J. Kozinn. **(1977)** Endotoxin and bacteria in portal blood. Gastroenterol 72:1268-1270.

Jepson, M.M. J.M. Pell, P.C. Bates, and D.J. Millward. **(1986)** The effects of endotoxemia on protein metabolism in skeletal muscle and liver of fed and fasted rats. Biochem J 235:329-336.

Jepson, M.M., M. Cox, P.C. Bates, N.J. Rothwell, M.J. Stock, E.B Cady, and D.J. Millward. **(1987)** Regional blood flow and skeletal muscle energy status in endotoxic rats. Am J Physiol 252:E581-E587.

Jois, M., B. Hall, and Brosnan, J.T. **(1990)** Stimulation of glycine catabolism in isolated perfused liver by calcium mobilizing hormones and in isolated rat liver mitochondria by submicromolar concentration of calcium. J Biol Chem 265:1246-1248.

Karnovsky, M.J. **(1965)** A formaldehyde-glutaraldehyde fixative of high osmolality for use in electron microscopy. J Cell Biol 27:137A-138A.

Kennedy, D.C. and Pearse, W.M. **(1958)** The relation between liver growth and somatic growth in the rat. J Endocrinol 17:149-157.

Kirk, K.L., D.R. DiBona, and J.A. Schafer. **(1987)** Cell volume regulation in rabbit proximal straight tubule perfused in vitro. Am J Physiol 252:F922-F932.

Krebs, H.A., N.W. Cornell, A.K. Walli, M. Ferraudi and U. Jost. **(1974)** Isolated liver cells as experimental material. In: Lundquist, F. et Tygstrup, N. (eds.). Regulation of hepatic metabolism. Academic Press, New York, pp715-750.

Kristensen, L.. **(1980)** Energization of alanine transport in isolated rat hepatocytes. J Biol Chem 255:5236-5243.

Kristensen, L.O. et **Folke**, M. **(1986)** Effect of perturbation of the Na^+-electrochemical gradient on influx an efflux of alanine in isolated rat hepatocytes. Biochim Biophys Acta 855:49-57.

Kushner, I. **(1986)** The phenomenon of acute phase response. Ann N.Y. Acad Sci 389:39-48.

Landin, K., F. lindärde, B. Saltin, and L. Wilhelmsen. **(1988)** Increased skeletal muscle potassium in obesity. Acta Med Scand 223:507-513.

Lang, F., G. Messner, W. Wang, M. Paulmichl, H. Oberleithner, and P. Deetjeno. **(1984)** The influence of intracellular sokium activity on the transport of glucose in proximal tubule of frog kidney. Pflüegers Arch Physiol 401:14-21.

Lang, C.H., G.J. Bagby, and J.J. Spitzer. **(1985)** Glucose kinetics and body temperature after lethal and nonlethal doses of endotoxin. Am J Physiol 248:R471-R478.

Lang, F., H. Voldl, and M. Paulmichl. **(1988)** How do cells regulate their volume? Pflüegers Arch Physiol 411:R4-R5 (No.3).

Lang, F., H. Volkl, and D. Haussinger. **(1989)** Water, K^+, H^+, lactate and glucose fluxes during cell volume regulatrion in perfused rat liver. Pflüegers Arch Physiol 413:209-216.

Lavoinne, A., A. Baquet, and L. Hue. **(1987)** Stimulation of glycogen synthesis and lipogenesis by glutamine in isolated rat hepatocytes. Biochem J 248:429-437.

Leblond, C.P., N.J. Nadler, and M. Enesco. **(1956)** Rates of desoxyribonucleic acid formation and cell production in regenerating rat liver. J Biol Chem 221:727-733.

Leffert, H.L., K.S. Koch, P.J. Lad, I.P. Shapiro, H.Skelly, and B.de Hemptinne. **(1988)** Hepatocyte Regeneration, Replication, and Differentiation. In: Aria, I.M., W.B. Jacoby, H. Popper, D. Schachter, and D.A. Shafritz (eds.). The liver: Biology and pathobiology (2nd ed.). Raven Press, New York, pp833-849.

Levin, J., H.R. Buler, J.W. ten Cate, S.J.H. van Deventer, and A. Sturk (eds.). **(1988)** Introlduction. In: The liver bioogy and pathobiology (2nd ed.). Raven Press, New York, pp833-849.

Levy, M. et **Ruebner**, B.H. **(1968)** Hepatic changes produced by a single dose of endotoxin in the mouse: light microscopy and histochemistry. Am J Pathol 52:477-502.

Long, C.L., L. Spencer, J.M. Kinney, and J.W. Geiger. **(1971)** Carbohydrate metabolism in man: effect of elective operation and major injury. J Appl Physiol 31:110-116.

Lovtrup, S. et **Swanson**, V.L. **(1958)** Changes in content of nucleic acid in organs of young rats during arrested growth. Acta Physiol Scand 43:51-70.

Luciano, D.S., A.J. Vander and J. H. Sherman (eds.). **(1983)** Chapter 25: Digestive system. In: Human anatomy and physiology (2nd ed.). McGraw-Hill, New York, pp592-684.

Macknight, A.D.C. et **Leaf**, A. **(1977)** Regulation of cell volume. Physiol Rev 57:510-573.

MacNicol, M.F. et **Clowes**, G.H.A. **(1972)** Comparison of proteolysis induced by starvation, sepsis and infusion of bradykinin or endotoxin. Surg Forum 25:45

Mallette, L.E., J.H. Exton, and CR. Park. **(1969)** Control of gluconeogenesis from amino acids in the perfused rat liver. J Biol Chem 244:5713-5723.

Mathison, J.C. et **Ulevitch**, R.J. **(1979)** The clearance, tissue distribution, and cellular localization of intravenously injected lipopolysaccharide in rabbits. J Immunol 123:2133-2143.

McGuinness, O.P. et **Spitzer**, J.J. **(1984)** Hepatic glycerol flux after E. Coli endotoxin administration. Am J Physiol 247:R687-692.

Mellanby J. et **Williamson** D.H. **(1974b)** Acetoacetate. In: Bergmeyer, H.U. (ed.). Methods of enzymatic analysis, Vol. IV. Academic Press, New York, pp. 1840-1843.

Michie, H.R., D.R. Spriggs, K.R. Manogue, M.L. Sherman, A. Revhaug, S.T. O'Dwyer, K. Arthur, C.A. Dinarello, A. Cerami, S.M. Wolff, D.W. Kufe, and D.W. Wilmore. **(1988)** Tumour necrosis factor and endotoxin induce similar metabolic responses in human beings. Surgery 104:280-286.

Millward, D.J. **(1986)** The physiological regulation of proteolysis in muscle. Biochem Soc Trans 13:1023-1026.

Moule, S.K. et **McGivan**, J.D. **(1990)** Regulation of the plasma membrane potential in hepatocytes - mechanism and physiological significance. Biochim Bophys Acta 1031:383-397.

Neufeld, H.A., J.G. Pace, M.V. Kaminske, D.T. George, P.B. Jahrling, R.W. Wannemacher, Jr., and W.R. Beisel. **(1980)** A probable endocrine basis for the depression of ketone bodies during infectious or inflammatory state in rats. Endocrinology 107:596-601, 1980.

Nolan, J.P. **(1975)** The role of endotoxin in liver injury. Gastroenterol 69:1346-1356.

Nolan, J.P. et **Camara**, D.S. **(1982)** Endtoxin, sinusoidal cells and liver injury. In: Popper, H. et Schaffuer, F.

(eds.). Progress in liver disease, Vol. VII. Grune & Stratton, N.Y., pp361-375.

Noll, F. **(1974)** L-(+)-lactate. Determination with LDH, GPT and NAD. In: Bergmeyer, H.U. (ed.). Methods of enzymatic analysis, Vol. III. Academic Press, New York, pp. 1475-1478.

Old, L.J. **(1986)** Tumor necrosis factor. Science (Washington DC) 37:173-178.

Old, L.J. **(1987)** Another chapter in the long history of endotoxin. Nature 330:602-603.

Oser, B.L. et **Hawk**, P.B. **(1965)** Determination of hemaglobin (Chapter 29). In: Hawk's physiological chemistry (14th ed.). McGraw-Hill, New York, pp. 1095-1097.

Pacitti, A.J., T.R. Augsten, and W.W. Souba. **(1991)** Adaptive regulation of alanine transport in hepatic membrane vesicles (HPMV's) from the endotoxin-trated rat. J Sur Res 51:46-53.

Pacitti, A.J., Augsten, T.R., and Souba, W.W. **(1992)** Mechanisms of increased hepatic glutamine uptake in the endotoxin-treated rat. J Surg Res 53:298.

Pacitti, A.J., Y. Inoue, and W.W. Souba. **(1993)** Tumor necrosis factor stimulates amino acid transport in plasma membrane vesicles from rat liver. J Clin Invest 91:474-483.

Patton, J.S., P.M. Peters, J. McCabe, D. Crase, S. Hansen, A.B. Chen, and D. Liggitt. **(1987)** Development of partial tolerance to gastrointestinal effects of high doses of recombinant tumor necrosis fator-α in rodents. J Clin Invest 80:1587-1596.

Pennica, D., G.E. Nedwin, J.S. Hayflick, P.H. Seeburg, R.Derynck, M.A. Palladino, W.J. Kohr, B.B. Aggarwal, and D.V. Goeddel. **(1984)** Human tumour necrosis factor: Precursor structure, expression and homology to lymphotoxin. Nature (Lond.) 312:724-729.

Perbellini, A., C.H. Shatney, D.J. DacCarter, and R.C. Lillehi. **(1978)** A new model for the study of septic shock. Surg Gynecol Obstet 147:69-74.

Perkash, J., P. Satpati, K.C. Agarwal, R.N. Chakravarti, P.N. Chhttani. **(1970)** Prolonged peritoneal lavage and fecal peritonitis. Surgery 68:842-845.

Pedersen, P., T. Seeman, and P. Hasselgren. **(1986)** Protein synthesis and degradation in liver tissue following induction of septic peritonitis in rats. Acta Chir Scand 152:29-34.

Pfaller, W., C. Willinger, B. Stoll, C. Hallbrucker, F. Lang, and D. Häussinger. **(1993)** Structural reaction pattern of hepatocytes following exposure to hypotonicity. J Cell Physiol 154:248-253.

Pfeiffer, R. **(1892)** Untersuchungen über das Cholera gift. Zeitschrift Hyg Infektionskran 11:393-412.

Powanda, M.C., R.E. Dinterman, R.W. Wannemacher, Jr., and G.D. Herbrandson. **(1974)** Distribution and metabolism of phenyulalanine and tyrosine during tularaemia in the rat. Biochem J 144:173-176.

Postel, J. et **Scholoerb**, P.R. **(1977)** Metabolic effects of experimental bacteremia. Ann Surg 185:475-480.

Prentki, M., M. Crettaz, and B. Jeanrenaud. **(1981)** Role of microtubules in insulin and glucagon stimulation of amino acid transport in isolated rat hepatocytes. J Biol Chem 256:4336-4340.

Rennie, M.J. **(1985)** Muscle protein turnover and the wasing due to injury and disease. Br Med Bull 41:257-264.

Rosenblatt, S.G., H.A. Clowes, B.C. George, E. Hirsch, and B. Lindberg. **(1983)** Exchange of amino acids by muscle and liver in sepsis. Comparative studies in vivo and in vitro. Arch Surg 118:167-175.

Sacca, L.G., G.Perez, F. Rengo, and M. Condoreli. **(1974)** Effects of different prostaglandins on glucose kinetics in the rat. Diabetes 23:532-535.

Scarpell, D.G. et **Iannaccone**, P.M. **(1990)** Cell injury and errors of metabolism. In: Kissane, J.M. (ed.) Anderson's pathology, Vol.I. Mosby, St. Louis, pp1-65.

Schneider, W.C. **(1945)** Phosphorous compounds in animal tissues. I. Extraction and estimation of deoxypentose nucleic acid and of pentose nucleic acid. J Biol Chem

161:293-303.

Shackleford, G.M., S.F. Hart, and L.J. Berry. **(1986)** Endotoxin treatment inhibits glucocorticoid induction of hepatic enzymes at a late induction step. Am J Physiol 250:E218-E225.

Splawinski, J.A., E. Zacny, and Z. Gorka. **(1977)** Fever in ats after intravenous E. coli endotoxin administration. Pfluegers Arch 368:125-128.

Swift, H.H. **(1953)** Quantitative aspects of nuclear nucleoproteins. Intern Rev Cytol 2:1-69.

Takeyama, N., Y. Itoh, Y. Kitazawa, and T. Tanaka. **(1990)** Altered hepatic mitochondrial fatty acid oxidation and ketogenesis in endotoxic rats. Am J Physiol 259:E498-E505.

Teplitz, C. **(1988)** The pathology and ultrastructrue of cellular injury and inflammation in the progression and out come of trauma, sepsis and shock. In: Clowes, G.H.A., Jr. (ed.). Trauma, sepsis and shock. Marcel Dekker, New York, pp71-122.

Thal, A.P., R.G. Robinson, T. Nagamine, R. Pruett, and A.V. Wegst. **(1976)** The critical relationship in intravascular blood volume and vascular capacitance in sepsis. Surg Gynecol Obstet 143:17-22.

Thomson, R.Y., F.C. Neagy, W.C. Hutchinson, and J.N. Davidson. **(1953)** DNA content of the rat cell nucleus and its use in expressing the results of tissue analysis; with particular reference to the composition of liver tissue. Biochem J 53:460-474.

Tian, S et **Baracos**, V.E. **(1989)** Prostaglandin-dependent muscle wasting during infection in the broiler chick (Gallus domesticus) and the laboratory rat (Rattus norvegicus). Biochem J 263:485-490.

Tracey, K.J., B.Beutler, S.F. Lowry, J. Merryweather, S.Wolpe, I.W. Milsark, R.J. Hariri, T.J. Fahey III, A. Zentella, J.D. Albert, G.T. Shires, and A. Cerami. **(1986)** Sock and tissue injury induced by recombinant human cachectin. Science 234:470-474.

Tracey, K.J., Y.Fong, D.G. Hesse, K.R. Manogue, A.T. Lee, G.C. Kuo, S.F. Lowry, and A. Cerami. **(1987)** Anti-cachectin/TNF monoclonal antibodies prevnt septic shock

during lethal bacteraemia. Nature 330:663-664.

Tracey, K.J., S.F. Lowry, and A. Cerami. **(1988)** Cachectin/TNF mediates the pathophysiological effects of bacterial endotoxin/lipopolysaccharide (LPS). In: Levin, J., H.R. Buller, J.W. ten Cate, S.J.H. van Deventer, and A. Sturk (eds.). Bacterial endotoxins. Pathophysiological effects, clinical significance, and pharmacological control. Alan R. Liss, New York, pp77-88.

Tracey, K.J., H. Vlassara, and A. Cerami. **(1989)** Pepatide regulatory factors. Cachectin/tumour necrosis factor. Lancet 8647:1122-1125.

Trump, B.F., I.K. Berezesky, and R.A. Cowley. **(1982)** The cellular and subcellular characteristics of acute and chronic injury with emphasis on the role of clcium. In: Cowley, E.R. et Trump, B.F. (eds.). Pathaphysiology of Shock: Anoxia and ischemia. Willsons and Wikens, Baltimore, pp85-95.

Ulevitck, R.J. **(1978)** The preparation and characterization of a radioiodinated bacterial lipopolysaccharide. Immunochemistry 15:157-164.

Vary, T.C., J.H. Siegel, T. Nakatani, T.Sato, and H. Aoyama. **(1986)** A biochemical basis for depressed ketogenesis in sepsis. J Trauma 26:419-425.

Vary, T.C., J.H. Siegel, B.D. Tall, G. Morris, and J.A. Smith. **(1988a)** Metabolic effects of partial reversal of pyruvate dehydrogenase activity by dichloroacetate in sepsis. Circ Shock 24:3-18.

Vary, T.C., J.H. Siegel, B.D. TAll, G. Morris, and J.A. Smith. **(1988b)** Inhibition of skeletal muscle protein synthesis in septic intra-abdominal abscess. J Trauma 28:981-988.

Vary, T.C. et **Kimball**, S.R. **(1992)** Regulation of epatic protein synthesis in chronic inflammation and sepsis. Am J Physiol 262:C445-C452.

Vilcek, Jan et **Lee** Tae H. **(1991)** Tumor necrosis Factor New insights into the molecular mechanisms of its multiple actions. J Biol Chem 266:7313-7316.

Vom Dahl, S., C. Hallbrucker, F. Lang, W. Gerok, and D. Häussinger. **(1991)** Regulation of liver cell volume and

proteolysis by glucagon and insulin. Biochem J 278:771-778.

Waisbren, B.A. **(1964)** Gram-negative shock and endotoxin shock. Am J Med 36:819-824.

Wannemancher, R.W., Jr., M.C. Powanda, R.S. Pekarek, and W.R. Beisel. **(1971)** Tissue amino acid flux after exposure of rats to Diplococcus pneumoniae. Infect Immun 4:556-562.

Wannemancher, R.W., Jr., R.S. Pekarek, P.J. Bartelloni, R.T. Vollmer, and W.R. Beisel. **(1972)** Changes in individual plasma amino acids following experimentally induced sand fly fever virus infection. Metabolism 21:67-76.

Wannemacher, R.W., Jr., M.C. Powanda, and R.E. Dinterman. **(1974)** Amino acid flux and protein synthesis after exposure of rats to either Diplococcus pneumoniae or Salmonella typhimurium. Infect Immun 10:60-65.

Wannemacher, R.W., Jr., R.E. Dinterman, R.S. Pekarek, P.J. Bartelloni, and W.R. Beisel. **(1975a)** Urinary amino acid excretion during experimentally induced sand fly fever in man. Am J Clin Nutr 28:110-118.

Wannemacher, R.W. Jr., R.E. Dinterman, and M.C. Powanda. **(1975b)** Phenylalanine metabolism in the infected rat. Federation Proc 4:900 (No.3854).

Wannemacher, R.W. Jr., H.A. Neufeld, and P.G. Ganonico. **(1976)** Hepatic gluconeogenic capacity and rate during pneumococcal infection in rats. Federation Proc 35:343 (No.771).

Wannemacher, R.W., Jr., J.G. Pace, F.A. Beall. **(1979)** Role of the liver in regulation of ketone body production during sepsis. J Clin INvest 64:1565-1572.

Warren, R.S., D.B. Donner, H.F. Starnes, Jr., and M.F. Brennan. **(1987)** Modulation of endogenous hormone action by recombinant human tumor necrosis factor. Proc Natl Acad Sci USA 84:8619-8622.

Warren, R.S., H.F. Starnes, Jr., N. Alcock, S. Calvano, and M.F. Brennan. **(1988)** Hormonal and metabolic response to recombinant human tumour necrosis factor in rat: in vivo and in vitro. Am J Physiol 255:E206-E212.

Watters, J.M. et **Wilmore**, D.W. **(1989)** The metabolic responses to trauma and sepsis. In: DeGroot, L.J. (ed.)

Endocrinology, Vol.iii (2nd ed.). Saunders, Philadelphia, pp2367-2393.

Waynforth, H.B. **(1979)** Special surgical techniques. In: Experimental and surgical technique in the rat. Academic Press, London, pp. 136-142.

Weibel, E.R., W. Stäubli, H. R. Gnägi and F. Hess. **(1969)** Correlated morphometric and biochemical studies on the liver cell: I. Morphometric model, stereologic methods, and normal morphometric data for rat liver. J Cell Biol 42:68-91.

Wernerman, J. et **Vinnars**, E. **(1987)** The effect of trauma and surgery on inter-organ fluxes of amino acids in man. Clin Sci 73:129-133.

Westphal, O., O. Lüderitz, F. Bister. **(1952)** Uber die extraktion von bakterien mit phenolwasser. Z Naturforsch 7B:148-155.

Wichterman, K.A., A.E. Baue, and I.H. Chaudry. **(1980)** Sepsis and septic shock - A review of laboratory models. J Surg Res 29:189-201.

Williamson, D.H. **(1974)** D-(-)-3-hydroxybutyrate. In: Bergmeyer, H.U> (ed.) Methods of enzymatic analysis, Vol. IV. Academic Press, New York, pp. 1836-1837.

Wilmore, D.W. **(1976)** Hormonal responses and their effect on metabolism. Symposium on response to infection and injury. II. Surg Clin N Am 56:999-1043.

Windmueller, H.G. et **Spaeth**, A.F. **(1974)** Uptake and metabolism of plasma glutamine by the small intestine. J Biol Chem 249:5070-5079.

Wolfe, R.R., D. Elahi, and J.J. Spitzer. **(1977)** Glucwse and lactate kinetics after endotoxin administration in dogs. Am J Physiol 232:E180-E185.

Wu, Guoyao, J.R. Thompson and V.E. Baracos. **(1991)** Glutamine metabolism in skeletal muscles from the broiler chick (Gallus domesticus) and the laboratory rat (Rattus norvegicus). Biochem J 274:769-774.

Wusteman, M., D.G.D. Wight, and M. Elia. **(1990)** Protein metabolism after injury with turpentine: a rat model for clinical trauma. Am J Physiol 259:E763-E769.

Zar, J.H. (1984) Multiple comparisons. In: Biostatistical analysis. Prentice-Hall, Inc., Englewood Cliffs, NJ, pp. 186-205.